

1. Wing Aerodynamic Design

1.1 Introduction

When designing a new aeroplane wing, the designer has a large number of parameters that can be varied to reach the final product. Some of them need to be fixed early in the design process because they address performance requirements for the wing/aeroplane. Others are finalised later in order to improve the flying qualities and the aerodynamic efficiency of the wing (and in many cases to solve problems introduced by the first set of decisions).

The main parameters that can be decided upon performance requirements are:

- Wing Area (or Wing Loading, W/S)
- Aspect Ratio $AR=b^2/S$ (or Span Loading, W/b)
- Wing Sweep

The decision is based on basic wing theory and empirical correlations. **Section 1.2** will briefly review the impact of the aircraft specification on these parameters.

The next step involves optimising the aerodynamic efficiency of the wing (for example elliptic lift distribution), altering local flows, addressing specific aerodynamic or stability related problems due to some of the above design parameters as well as off-design behaviour. Stall characteristics will be optimised during this process.

Parameters that fall into this category are:

- Taper Ratio
- Twist
- Spanwise Camber
- Thickness distribution
- Wing/Fuselage integration

and will be discussed in **Section 1.3**.

Even after all this process of ‘aerodynamic optimisation’ (at least on paper), rarely does the final product behave acceptably throughout the flight envelope. Therefore, a number of ‘fixes’ need to be employed to alleviate local flow problems. Fixes like vortex generators, fences, strakes as well as wing tip designs (including the all important winglet) will be discussed in **Section 1.4**.

Almost all the basic design parameters of the wing will have been covered by that point with the exception of probably the most important: the aerofoil. **Section 1.5** will focus on aerofoils, from conventional NACA series aerofoils to modern supercritical sections as well as methods for the design of custom aerofoils.

Finally, **Section 1.6** will provide a brief presentation of the design process for the final product, the 3D wing: from direct methods using 2D approach to fully automated entirely 3D methods utilising CFD and numerical optimisation algorithms, and even Multi Disciplinary Optimisation.

Some Useful References

- <http://adg.stanford.edu/aa241> - “Aircraft Design: Synthesis and Analysis” notes from Stanford University
- http://www.aoe.vt.edu/~mason/Mason_f/ConfigAero.html - “Configuration Aerodynamics” from Virginia Tech
- <http://www.esdu.com> - Engineering Sciences Data Unit (*UoB has a subscription*)
- ESDU 97017 ‘Guide to Wing Aerodynamic Design’, August 1997
 - ESDU 90008 ‘Introduction to Transonic Aerodynamics of Aerofoils & Wings’, April 1990
 - ESDU 98013 ‘Aerodynamic Principles of Winglets’, June 1998
 - ESDU 93024 ‘Vortex Generators For Control Of Shock-Induced Separation’, Feb 1995
- <http://www.ae.uiuc.edu/m-selig/ads.html> - “UUIC Airfoil Data Site”
- Abbott, I.H. and von Doenhoff, A.E., *Theory of Wing Sections*, Dover 1959
- Hoerner, *Fluid Dynamic Lift and Fluid Dynamic Drag*
- Küchemann, D., *The Aerodynamic Design of Aircraft*, Pergamon, 1978
- McCormick, B.W., *Aerodynamics, Aeronautics and Flight Mechanics*
- Raymer, D. P., *Aircraft Design: A Conceptual Approach*, AIAA 1999
- Roskam, J., *Airplane Design*, Parts 1-8, Roskam Aviation and Engineering Corporation, 1986
- Shevell, R., *Fundamentals of Flight*, Prentice-Hall Int., 1983
- Stinton, D., *Anatomy of the Airplane and Design of the Airplane*
- Torenbeek, E., *Synthesis of Subsonic Airplane Design*, Delft University Press, 1976
- Whitford, R., *Design for Air Combat*, Jane’s Publishing, 1987

1.2 Wing sizing for performance

The three wing design parameters that are directly related to the performance of the wing are the Wing Area, the Aspect Ratio and the Wing Sweep. The effect of these parameters on the wing performance and flying characteristics, as well as the main reasons driving the final choice of their values will be presented.

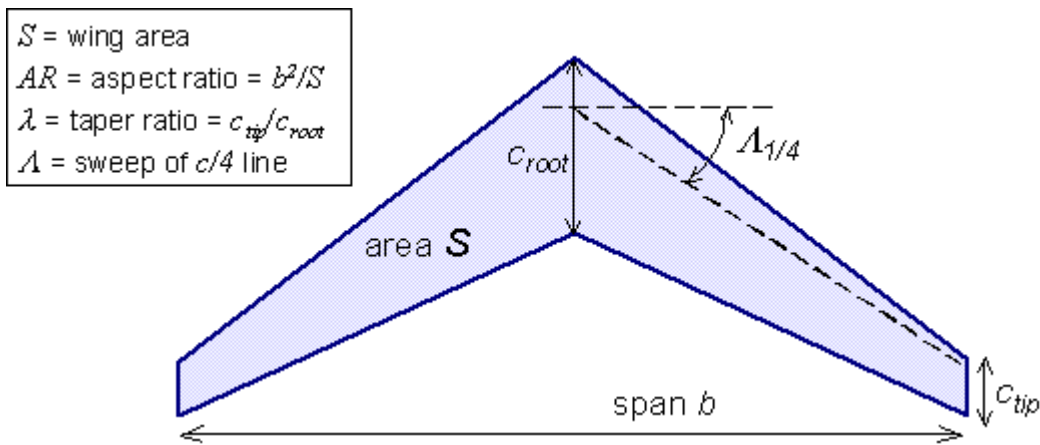


Figure 1: Basic wing design parameters

1.2.1 Wing Area

The wing area S (or more usually during the design phase Wing Loading W/S) defines the available lift, the exterior wing surface area (wetted area) and the physical size of the wing. Through these, it affects the following aspects of the aerodynamic performance of the wing:

- Available lift: stalling speed (landing and take-off), instantaneous manoeuvre, cruise buffet, gust response, operational ceiling
- Wetted area: cruise drag
- Physical wing size: fuel volume, wing weight, wing span (also in relation to AR)

Out of these parameters, cruise drag and stall speed are the two main ones used for choosing the wing area. For modern airliners cruise is the most important part of their flight envelope so it takes first place in the designer's considerations, as long as a suitable high lift device system can be used to provide the necessary minimum stall speed. Otherwise, stall speed may be the main concern.

Wetted area

Drag is divided in profile drag and induced drag. However, with the latter being proportional to the square of the lift coefficient, the result is that during cruise conditions (high speed therefore low C_L) the induced drag is significantly less than the profile drag (Anderson mentions 25% of the total). Note that high speed is required for maximising

range; from the Breguet equation¹ maximum range is obtained for maximum ML/D (and not simply L/D). The result of increasing the wing area is to increase the wetted area and therefore the profile drag. Low wing area (high wing loading) is preferred for jet airliners.

However, if we accept (as a first approximation) that the fuselage wetted area remains constant (independent of the wing area), then increasing the wing area will reduce the contribution of the fuselage to the total skin friction drag and therefore the total skin friction drag coefficient (for the simple reason that the drag coefficient is based on the wing area):

$$C_{D0} = C_{D_p \text{ wing}} + C_{D_p \text{ fuselage}} \frac{S_{\text{fuselage}}}{S_{\text{wing}}}$$

The result is a reduction in C_{D0} which translates² in an increase in the maximum L/D ratio and a reduction in the C_L at which it is achieved, both beneficial for high endurance aeroplanes or for flight at extreme altitudes (high L/D required).

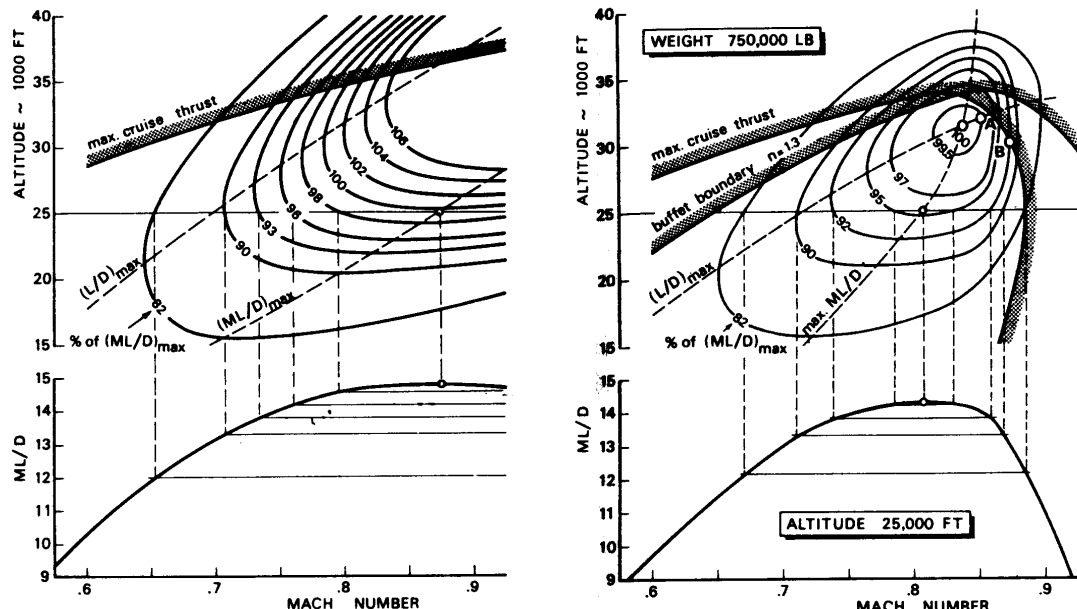


Figure 2: Effect of compressibility on optimum cruise conditions

Note that when sizing wing area on the basis of cruise drag it is also essential to take into account:

- drag rise at high (transonic) Mach number, and
- engine performance (thrust or power) fall-off with Mach Number and altitude

Although the basic (simplified) Breguet range equation for jet aircraft gives optimum range when $C_D/C_L^{1/2}$ is a minimum ($C_L = \sqrt[4]{C_{D0}/3K}$), the combined effect of these two

¹ $R = \frac{V}{fg} \frac{C_L}{C_D} \ln\left(\frac{W_1}{W_2}\right) = \frac{a_0}{fg} \left[M \frac{L}{D} \right] \ln\left(\frac{W_1}{W_2}\right)$

² $\left(\frac{L}{D}\right)_{\max} = \frac{1}{2\sqrt{C_{D0}K}}$ and $C_{L,\min\text{drag}} = \sqrt{\frac{C_{D0}}{K}}$

Mach Number effects can drive the optimum cruise point to close to maximum L/D (ie minimum C_D/C_L) – corresponding to a rather higher optimum cruise C_L ($= \sqrt{C_{D0}/K}$) and hence a higher wing loading.

Available lift

The effect of the wing area on the available lift is quite straight forward. ($L=C_LqS$). Maximum lift will dictate the minimum speed (**stall speed**) and this has to be below a critical value (for safety reasons). In a similar fashion, maximum **instantaneous turn rate** is governed by the maximum available lift³. In both cases, additional high lift devices may be employed, especially for take-off and landing (during dogfights do not expect to see massive flaps extending; only some small devices can practically be used).

The effect of the wing size on the **operational ceiling** is also very simple to understand if you remember that the dynamic pressure at high altitude will be significantly less than at sea level. The reason is twofold: The density of air at high altitude is significantly lower and so is the temperature, which translates in a lower value for the speed of sound i.e. a lower velocity for the aeroplane (in order not to exceed a given Mach number). In other words, aeroplanes designed for high altitudes really need a lot more “contribution” from their C_L and S to obtain their necessary lift.

Buffet onset during transonic cruise (due to shock-induced separation) can also limit the maximum useable lift (see Fig. 3) which may necessitate a larger wing area. However, this issue can also be tackled with appropriate aerofoil design.

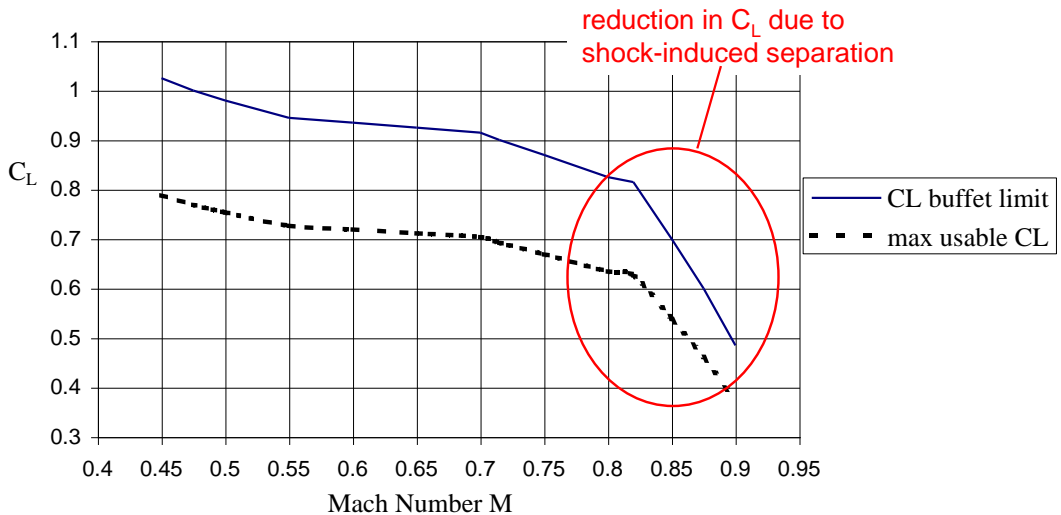


Figure 3: Transonic buffet limit on cruise C_L

Gust response is also linked to wing loading, and may become a limiting factor for low-level high-speed cruise (eg TSR-2 strike mission). For a given speed and weight, the

³ Maximum sustained turn rate, is the turn rate at which the aeroplane does not lose altitude or speed, therefore its thrust equals the total drag. Maximum instantaneous turn rate is of course higher because there is no requirement for not losing either altitude or thrust; it merely depends on the maximum lift the wing can generate (and load it can structurally withstand).

higher the wing loading the higher the C_L and hence the higher the angle of attack α . For a given gust velocity the *relative* change in incidence and hence in load factor will then be lower.

Since change in incidence $\Delta\alpha$ for a vertical gust v is v/V , the corresponding change in load factor n is

$$\Delta n = \frac{\Delta L}{W} = \frac{\frac{1}{2}\rho V^2 S \Delta \alpha C_{L\alpha}}{W} = \frac{\frac{1}{2}\rho V v C_{L\alpha}}{W/S}$$

The higher the wing loading (and the lower the lift curve slope) the more comfortable the ride in turbulent conditions.

Gust response considerations also limit maximum useable C_L in cruise to rather less than the buffet limit (see Fig. 3) in order to prevent buffet entry due to a gust (improves ride quality and structural fatigue).



Physical size

The effect of the physical size of the wing on the **fuel volume**, **wing weight** and **span** is even more straightforward. The larger the wing, the heavier it will be and (assuming a constant AR) the bigger the span (again increasing the weight). On the other hand, a larger wing will provide plenty of internal volume for fuel, in some cases necessitating a minimum wing size.

1.2.2 Aspect Ratio

Aspect ratio defines mainly the induced drag but also affects the lift curve slope and of course the physical size of the wing. Through these, it affects the following aspects of the aerodynamic performance of the wing:

- Induced drag: endurance, climb, sustained manoeuvre, operational ceiling, noise
- Lift curve slope: gust response, fuselage attitude
- Physical wing size: fuel volume, wing weight, span limits, flutter

Based on the previous discussion regarding the importance of induced drag during cruise, we can safely say that the choice of aspect ratio will not be based on cruise performance when it comes to high speed airliners. On the other hand, if we were to design a sailplane (so much lower speed and more importantly very high L/D required) then the aspect ratio would be at the top of the list. Endurance and high altitude aeroplanes will also require a high aspect ratio. However, in practise aspect ratio is chosen based on the required performance during demanding low speed high induced drag phases of the flight envelope; mainly take-off with an engine failure and climb.

Keep in mind that although we refer to aspect ratio, if the wing area has already been defined (and it usually has by the time AR is dealt with) in the end what we are about to choose is the span of the wing.

Induced drag

The effect of aspect ratio on induced drag is well known from basic aerodynamic theory:

$$C_{Di} = \frac{k}{\pi AR} C_L^2$$

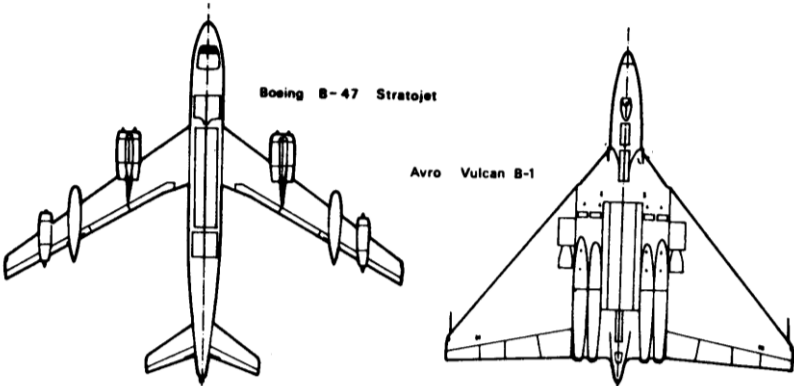
and obviously is important when the lift coefficient is high. Therefore, a high AR is beneficial for **endurance** (aeroplane flying at max L/D i.e. min Drag), for **climb** (low speed), **sustained turn rate** (low speed AND at the same time low drag required so as not to overcome the available thrust) and **operational ceiling** (where aeroplane flies at high C_L). It will also have a positive effect on **noise** at low speeds due to reduced engine thrust requirements (engine noise) and tip vortex strength (airframe noise).

An alternative parameter to aspect ratio often used in civil aircraft design is the span loading W/b , since

$$\begin{aligned} D &= C_{D_0} \frac{1}{2} \rho V^2 S + K C_L^2 \frac{1}{2} \rho V^2 S \\ &= C_{D_0} qS + \frac{K W^2}{qS} = C_{D_0} qS + \frac{k W^2}{\pi A R q S} \\ &= C_{D_0} qS + \frac{k}{\pi q} \left(\frac{W}{b} \right)^2 \end{aligned}$$

In other words, for a given weight W and dynamic pressure q the induced drag is inversely proportional to the span b squared, not the aspect ratio as such.

The most well known example of the above finding is the comparison of the B-47 Stratojet and the Avro Vulcan. Both aircraft were designed for similar roles but are apparently completely different; nevertheless, they have roughly the same wetted area –



hence the same profile drag – and the same span loading – hence the same induced drag at cruise (despite aspect ratios of 9.4 and 2.8 respectively). The differences come down to cruise C_L and structural weight. Max L/D for the Vulcan occurs at a C_L of 0.235 compared with 0.68 for the B-47; when cruising at high altitude the Vulcan had a greater margin for manoeuvring without risking serious buffeting.

Lift curve slope

Again going back to basic wing theory, we know that the aspect ratio affects the wing lift curve slope:

$$a = \frac{a_0}{1 + a_0 / \pi AR}$$

An increase in the aspect ratio increases the wing lift curve slope going towards the 2-D aerofoil value. On the other hand, when a low AR is chosen, **gust response** is more benign (beneficial for both passenger aeroplanes as well as low level attack aircraft). However, this reduction in the lift curve slope means the aeroplane's angle of attack will have to vary considerably to produce a change in C_L .



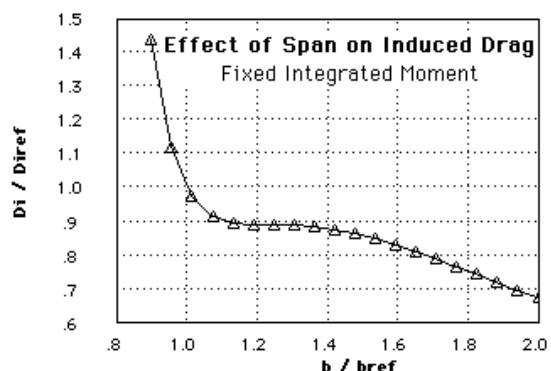
This results in a very wide range of angles of attack for the **fuselage** between low speed (take-off and especially landing) and cruise conditions. The result is usually an aeroplane that has to take-off and land at a very high angle of attack, which can lead to problems like a long undercarriage (so that the tail does not strike the ground) and visibility issues for the pilot (both supersonic passenger airliners – Concord and Tu-144 – had drooped noses for the landing phase).

Physical size

The choice of aspect ratio (or wing span, since the area has been defined) will impact on other design features as well. **Wing weight** depends on aspect ratio but can be surprisingly nonlinear – in design studies for the F-16 combat weight increased only slightly when AR was increased from 3 to 3.5, but trebled when AR increased from 3.5 to 4! A long (slender) wing reduces the **volume available for fuel**, and can lead to problems with structural stability due to wing bending (ie divergence and **flutter**). It also may become more difficult to locate the landing gear at the root of the wing. There are also operational constraints on the maximum **span size** like physical limits imposed by airports⁴ or aircraft carriers.

[NB At high (supersonic) speeds drag is dominated by wave drag, which can be alleviated by using a low aspect ratio – helps to achieve good area ruling

As aspect ratio is reduced the spanwise lift distribution shifts further away from the ideal elliptical form so the lift efficiency factor k becomes



⁴ The best example is the A380: its span had to be limited to 80m but at the same time the majority of airports had to undergo some upgrades to be able to accommodate it.

$>> 1$ – this can be alleviated using taper, sweep or twist to shift the loading outboard. In the limit, the loading for *slender* wings – ie low aspect ratio/high sweep – becomes elliptical again.

If wing structural weight is taken into account when selecting the aspect ratio for minimum induced drag – for example by varying wing area (and hence wing loading) to maintain a constant root bending moment – then the optimum is quite flat and may require a very large span coupled with high wing loading, so that other practical constraints may take precedence.

High AR leads to low drag during landing which flattens the approach glide and makes judgement of landing point more difficult. Also leads to floating after touch down. Plus too much damping for roll manoeuvres combined usually with small chord ailerons. Therefore, moderate AR of 7 to 9 is usually preferable for general aviation aircraft.]

1.2.3 Wing Sweep

Sweep is introduced to the wing design to reduce the adverse effects of compressibility (transonic and supersonic flows). Usually, sweep is chosen for high subsonic speed aeroplanes on the basis of transonic performance (increase critical Mach number). In the case of supersonic flight, sweep would be advantageous by positioning the entire wing within the Mach cone thus ensuring subsonic flow over the entire wing; however this is not always the case as it will be discussed later on.

Sweep however, is not necessary for low speed flight (aeroplanes that fly up to M0.6 usually are designed with no sweep); in fact, sweep can introduce a number of problems during low speed flight especially on stability and during high lift phases of the flight. Therefore, the final choice of sweep will have to take into account a number of factors affected by the sweep angle:

- high subsonic cruise: critical Mach Number
- supersonic dash: subsonic or supersonic leading edges
- low-speed performance: lift distribution, lift curve slope, maximum lift
- low-speed stability: pitch-up, dihedral effect, cg location
- radar cross-section: edge alignment
- structural constraints: wing bending, wing spar, engine and undercarriage location

High subsonic cruise

For high subsonic cruise, the **critical Mach number** corresponds to the initial appearance of supersonic flow over the wing (in the high velocity region near the leading edge), closely followed by a rapid rise in drag as the upper surface shock leads to boundary layer growth and possibly separation.

For a 2D aerofoil the onset Mach Number and magnitude of the drag rise is governed primarily by the aerofoil thickness t/c and lift C_L since both of these affect peak upper surface velocities. Drag rise Mach Number (not to mention onset of buffet at cruise C_L ,

reduction in $C_{L_{max}}$ and transonic trim changes) can be alleviated to a certain extent by reducing aerofoil thickness and/or by appropriate section design (ie supercritical aerofoils), but by far the most effective solution is sweeping the wing (forward or rearwards).

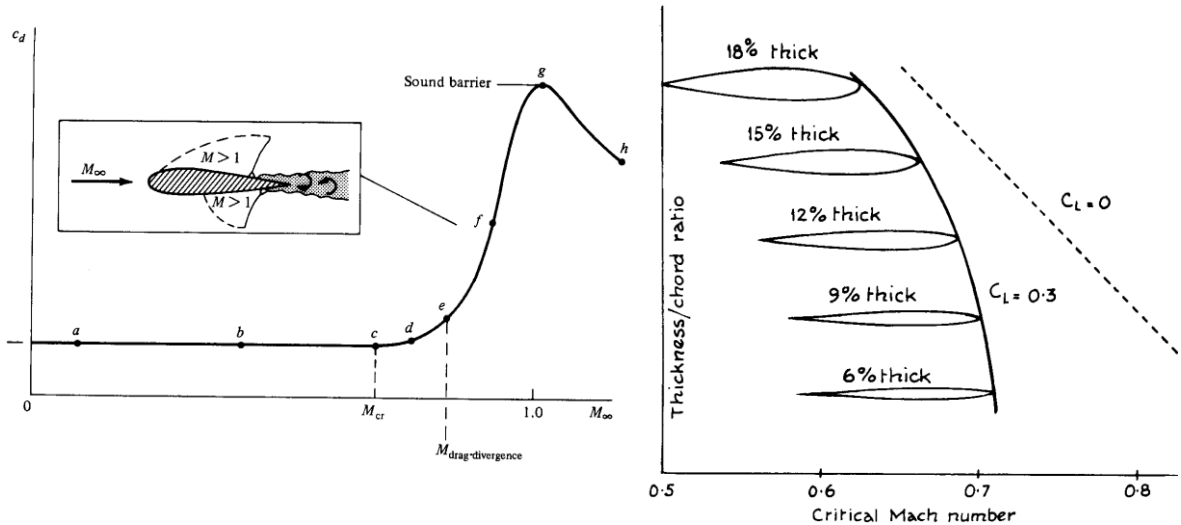


Figure 4: Transonic drag rise for a 2D aerofoil

The theory behind wing sweep is based on the fact that only the component of velocity normal to the leading edge is important in defining the critical conditions. This is because when we assume an infinite wing, there would be no pressure gradient parallel to the leading edge, so only the velocity component normal to the leading edge will vary over the aerofoil section. Reducing the normal Mach number by sweeping the wing therefore delays the onset of local transonic flow and hence transonic drag rise.

[NB However, set against this favourable effect are two adverse consequences of sweep:
(i) an increase in the equivalent pressure and lift coefficients – same pressure perturbation, but reduced effective freestream velocity – and (ii) an increase in the equivalent section thickness – same thickness, but reduced effective chord. The reduced normal Mach number predominates, so the overall effect of sweep is beneficial]

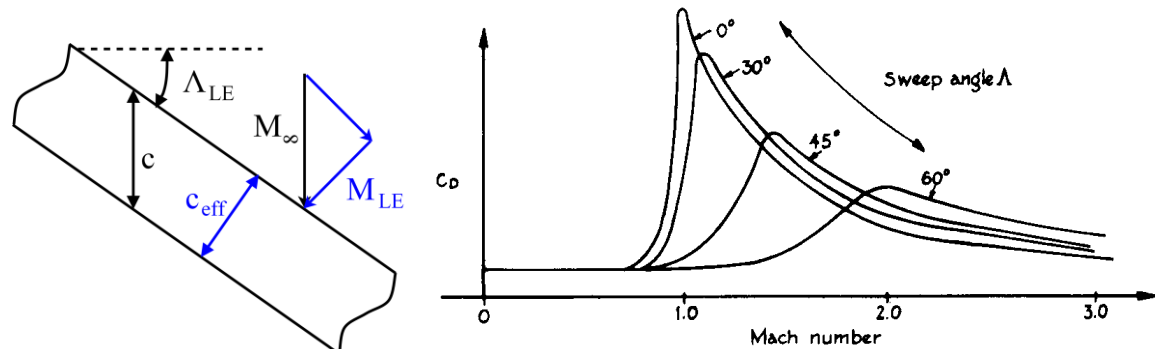


Figure 5: Effect of wing sweep on transonic drag rise

Wing sweep can therefore be used to either increase the cruise speed (modern airliners), or to increase the permissible wing thickness for a given cruise speed (F-86, Victor – improved wing structure and airframe packaging).

Supersonic dash

At supersonic cruise/dash conditions the effect of wing sweep is a little more complex. To obtain minimum wave drag in supersonic flight it is necessary to sweep the wing so that the leading edge lies within the Mach cone emanating from the wing root – giving what is known as a **subsonic leading edge** (since $M_{LE} \leq 1$).

Basic geometry gives the corresponding sweep angle as $\Lambda_{LE} \geq \cos^{-1}(1/M)$, but optimum sweep angles are of the order of 6° greater than the critical value. Historical data from Raymer indicates that this is achievable for design Mach Numbers below about 1.3. Above this value, the required sweep angle becomes structurally impracticable (very few aircraft have leading edge sweeps exceeding 60°).

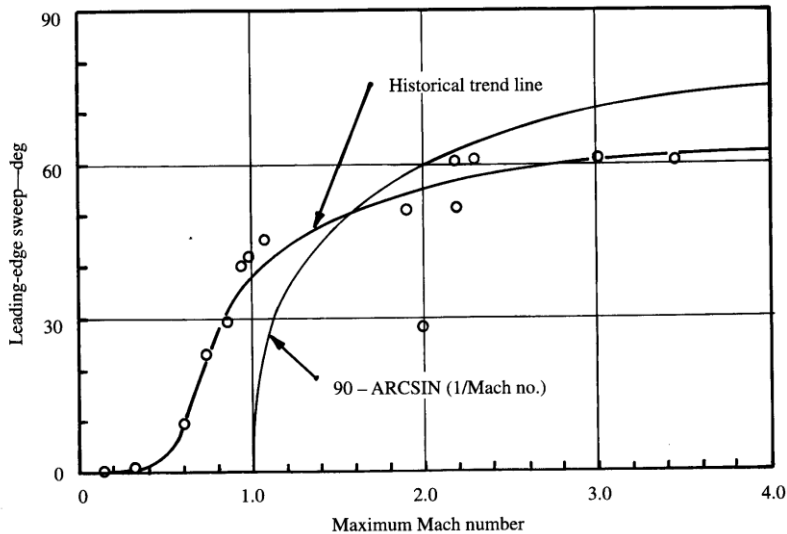


Figure 6: Wing sweep historical trend (from Raymer)

At very high cruise Mach Number, if a subsonic leading edge cannot be achieved, then reducing sweep angle can actually give lower wave drag as the flow becomes almost wholly supersonic over the wing (see Fig. 5 – high Mach numbers). The F-104 is a classic example of this approach, using a 30° sweep for Mach 2 performance – but needing an extremely thin (3.4%) and sharp aerofoil section to offset the poor transonic performance.

Low speed performance

The impact of wing sweep on low-speed performance is generally adverse. Increasing aft sweep alters the **lift distribution** by shifting the spanwise loading outboard, leading to an increase in induced drag factor as the loading departs further from the elliptical (forward sweep shifts loading inboard but still increases induced drag). Higher peak local C_L then gives a **lower overall maximum lift** as the outboard (or inboard) wing stalls early. Sweep also gives a very significant reduction in **lift curve slope**.

However, taper and twist can be used to alleviate some of these impacts – or alternatively use a variable-sweep wing to match low- and high-speed performance requirements.

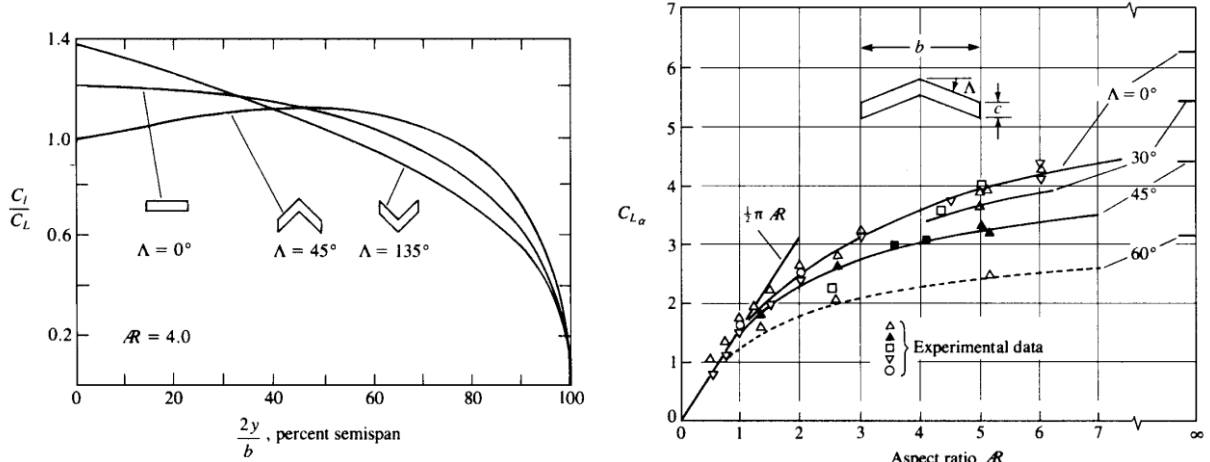


Figure 7: Effect of sweep on spanwise loading and lift-curve slope

A combination of high sweep and low aspect ratio gives the delta wing planform, which at high incidence generates additional lift from the formation of streamwise vortices from flow separating at the swept leading edges. These are an important feature of the low-speed (landing & manoeuvre) performance of many military aircraft.

[NB Reduced lift-curve slope will improve gust response, which may be an advantage for military aircraft operating at high-speed at low-level (TSR2, Tornado).]

High trailing edge sweep can also reduce the effectiveness of wing controls and trailing edge flaps.]

Low speed stability

The effect of sweep on stability is most marked at low-speed. The aft sweep shifts the wing aerodynamic centre aft, changing the longitudinal trim and stability balance (a particular problem for variable-sweep aircraft which must cope with a shift in aerodynamic centre in flight). The **wing cg** also shifts aft, which may lead to an overall destabilising effect. [For example, the small amount of sweep on the Me262 twin-jet fighter was in fact a means of sorting out a cg problem.]

For flying wings (eg the Horten wings), sweep angle is a means of providing enough moment arm for pitch stability and control.

At high-lift, the high tip loading on an aft swept wing leads to a tip-stall – and since the tips are well aft of the cg the local loss of lift can lead to a dangerous **pitch-up**. Since the spanwise loading is also affected by the aspect ratio (with low aspect ratio shifting the loading inboard), tip-stall is most likely on wings combining high aspect ratio and high aft sweep (not a problem with forward sweep). Tip stall may also lead to loss of roll control (and roll damping) as flow separates over the ailerons.

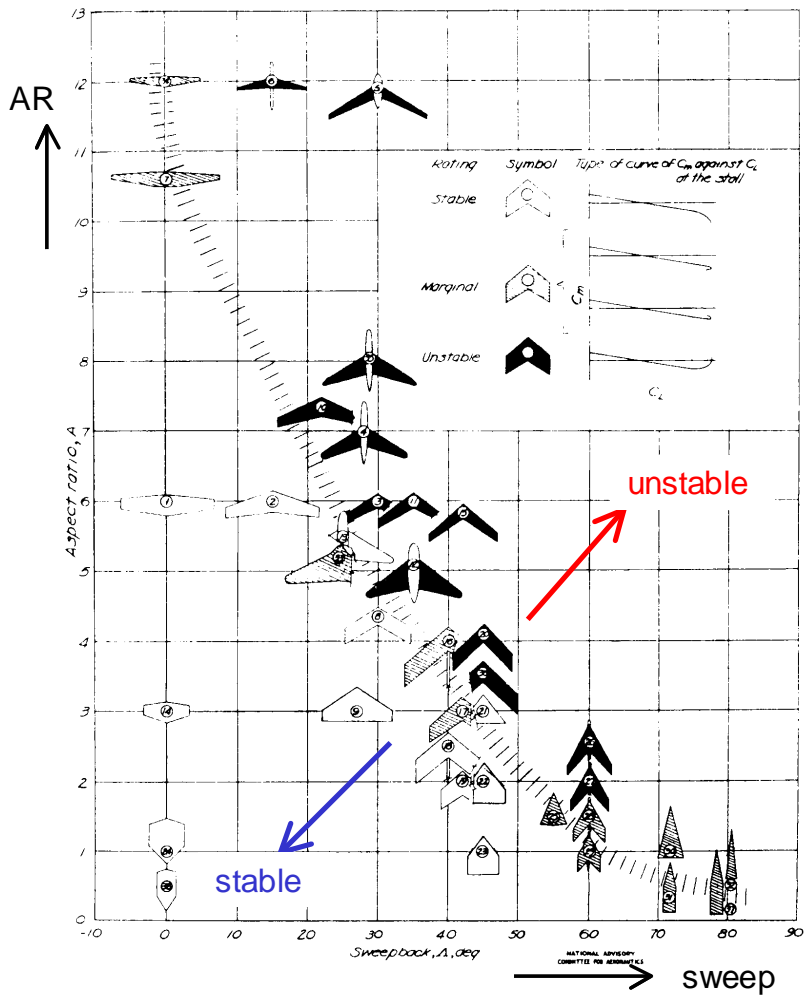
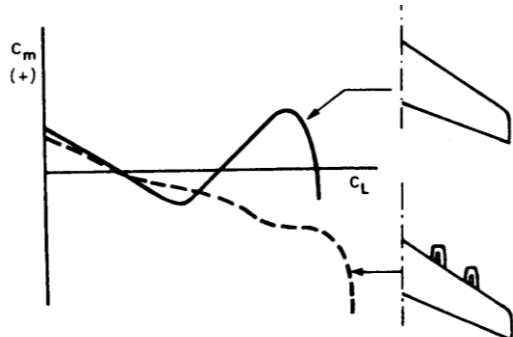


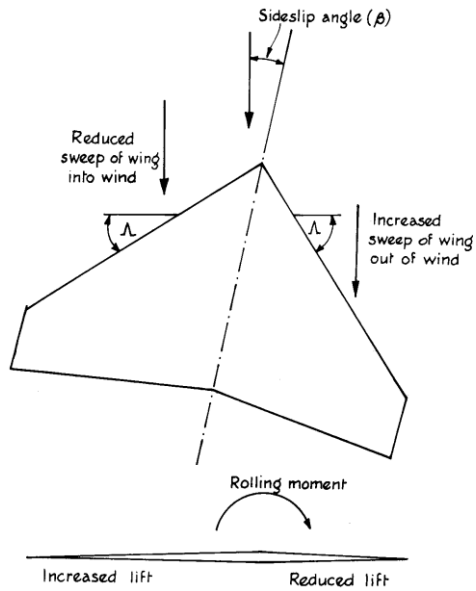
Figure 8: Empirical correlation of effect of sweep and aspect ratio on pitch-up

As a viscous flow phenomenon, pitch-up is difficult to predict theoretically, hence recourse is usually had to empirical correlations (eg Fig. 8). The one shown here is for the tail-off low-speed case – similar plots are available for tailed configurations and for high-speed stall (eg NASA TN-1093).



Interestingly enough, wing-mounted engines can have significant effect on the pitch break – the interaction of engine pylons with the wing flow at high incidence can counteract pitch-up. [Presented as one of the arguments in favour of the wing mounted engines against engines buried inside the wing/fuselage.]

Wing sweep has a major impact on lateral stability – increased sweep increases roll moment due to sideslip $C_{l\beta}$ – the so-called ‘**effective dihedral**’ derivative. If the aircraft is sideslipping the ‘windward’ wing has a lower effective sweep than the ‘leeward’ wing, hence it generates more lift (increased lift curve slope) – giving a rolling moment ‘away’ from the sideslip. The effect is more marked at high lift. The resulting (negative) $C_{l\beta}$ contribution is stabilising, tending to roll the aircraft to oppose the sideslipping motion. However, for highly swept aircraft at high lift the increase in stability can be excessive, leading to problems in cross-wind landings (B-52 tandem undercarriage) and with dutch-roll oscillations. The high wing position on many military aircraft may further exacerbate these difficulties (due to the additional dihedral effect).



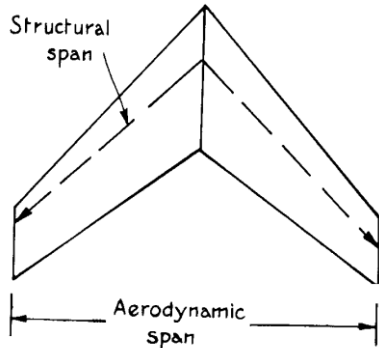
Radar Cross Section

Radar Cross Section (RCS) is a relatively modern concept (although there have been aeroplanes with a minimal RCS even during WWII like the Mosquito) and impacts on aircraft design in many ways (rarely to the benefit of the aerodynamicist). From the point of view of wing design RCS requirements can affect aerofoil section (leading edge shaping, prismatic surfaces), control surface design (no gaps) and aerodynamic fixes (no add-on bits) – but the most critical impact is on sweep angle. A major contribution to RCS is reflection/scattering from edges (leading and trailing edges, control surface gaps, access panels etc), producing ‘spikes’ in the radar signature in particular directions. Since **edges** are unavoidable, they are instead **aligned** so that the spikes are oriented in a known direction which can be pointed away from threat radars (assuming the position of the enemy radar is known, which in most cases will be directly ahead of the aircraft). The leading edge is the main contributor, so for modern combat aircraft RCS requirements can dominate choice of sweep angle – usually by setting a minimum sweep. The actual value will depend on the mission and level of Radar Absorbent Material (RAM) treatment applied, but typical values for newer stealth aircraft are of the order of 40° (cf 1st generation stealth aircraft the F-117 with a much higher sweep angle). This sweep angle is in the transition region between low (airliners) and high-sweep (delta wings) flow regimes and is particularly poor aerodynamically. [Significant amount of research is being carried out at the moment because of the popularity of such wing planforms for modern UCAVs.] Aligning trailing edges and wing tips imposes severe constraints and in the limit leads to diamond or lambda wing planforms (eg B2). Considerable local shaping is then required to overcome



the basic poor aerodynamics of these configurations (particularly in the trailing edge crank region on the lambda wing).

Structural constraints



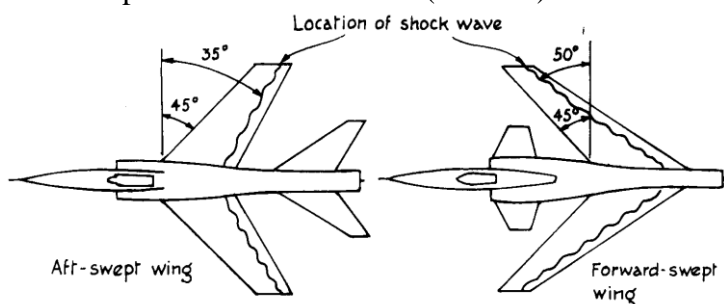
Significant sweep leads to some severe structural constraints. The ‘structural span’ is increased since for the same area and aspect ratio (= same span) the **wing spar** increases with increasing sweep. This in turn increases wing weight, particularly when combined with increased tip loading and the fact that sweep (aft) shifts the lift distribution outboard (both result in increased **wing root bending**). The increased torsional loads at the root due to sweep also increase wing weight.

For aft sweep, the position of the wing torsional axis in relation to the centre of pressure leads to a tendency to twist nose-down at the tip under load – giving a structure that is statically stable – although the flight stability may be adversely affected as the centre of pressure moves forward and inboard. (Stability of flexible aircraft is rather more complex than stability of rigid aircraft...) Dynamically (aeroelastically), however, the aft inertia axis means that flutter can be a problem.

Sweep angle also affects load paths from the wing to the fuselage. Too much sweep can make it difficult to **accommodate the main undercarriage** in the wing or near the main spar.

Unconventional sweep

The conventional choice of the designer is to sweep the wing aft. The wing can also be swept forward with the same effect on the flow for the infinite wing case. However, in the 3-D case the flow will differ and will present some aerodynamic advantages. The spanwise loading shifts inboard, leading to a safer stall pitch break and retention of roll control and roll damping at high incidence. Excessive effective dihedral is also avoided. At high subsonic speed the shock sweep is higher, leading to reduced shock strength and hence reduced transonic drag rise – a lower leading edge sweep can therefore be used, increasing lift-curve slope, reducing induced drag and potentially reducing wing area. A disadvantage of the last effect is the increased sweep of the trailing edge which reduces the effectiveness of the flaps and control surfaces (ailerons).



A variation on the theme is to sweep one wing forward and one aft – to give an oblique wing. This has lower wave drag due to (a) improved volume distribution and (b)

avoidance of ‘unsweeping’ the flow near the wing apex. Induced drag is also improved over the basic swept wing. The asymmetry of the aircraft poses remarkably few control problems, with a manned demonstrator (the AD-1) having been test flown by NASA. Variable sweep is straightforward to implement (only one pivot, although this single pivot will have to be able to withstand very high loads thus will increase the wing weight), so oblique wings are beginning to appear as deployable surfaces on missiles. If the fuselage is removed, the concept leads naturally to an oblique flying wing.



Figure 9: Oblique wing aircraft projects

Structurally, forward sweep is also at a disadvantage compared to aft sweep. Instead of the statically stable tip (under load), the tip twists nose-up under load leading to structural divergence. This can be countered using a tailored composite structure (eg X-29) to prevent the wing twist. Alternatively the German Ju-287 wartime project used aft mounted podded engines to provide dynamic balancing of the wing structure.

Forward sweep has also been chosen for reasons not directly related to its aerodynamic performance. The HFB 320 Hansa Jet had a small amount of forward sweep in order to enable a carry-through wing box structure that did not run through the cabin pressure vessel.

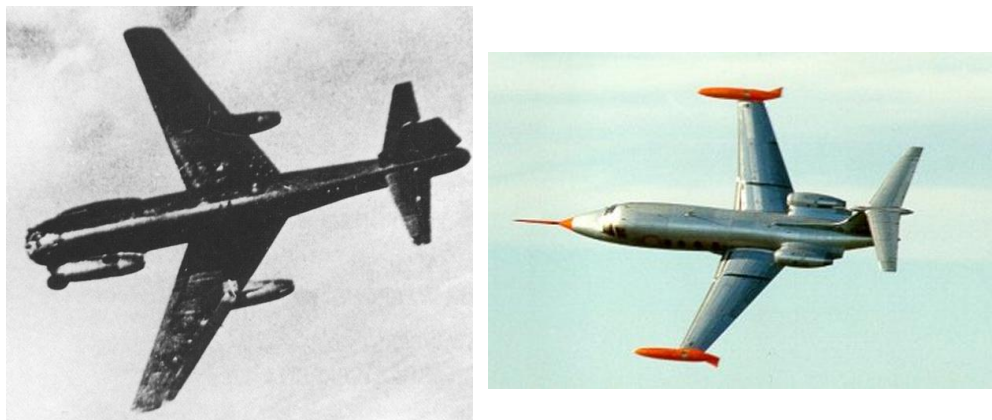
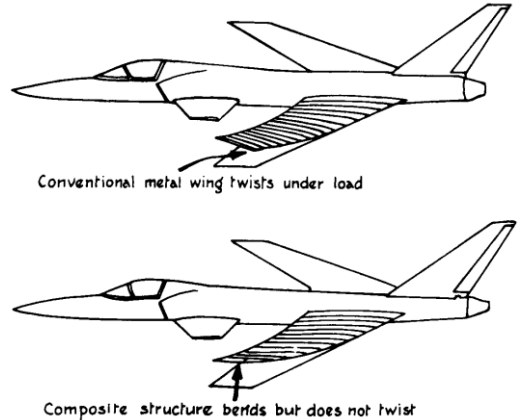


Figure 10: Ju-287 and HFB 320 forward swept aircraft projects

Effect of sweep on performance (range)

An interesting simplified analysis due to Küchemann gives some further insight into the effect of sweep angle on cruise performance.

For a family of conventional swept-wing aircraft with the same wing area S , and fuselage and tail-plane size the wing sweep Λ is varied according to the cruise speed to maintain the same Mach Number normal to the leading edge. From geometry, the cruise Mach Number and wing aspect ratio for each aircraft are then

$$M_{cruise} = \frac{M_0}{\cos \Lambda} \quad \text{and} \quad AR = AR_0 \cos^2 \Lambda$$

where the subscript 0 denotes the unswept member of the family. To a first order the wing structure may be taken to be the same for each aircraft, so that the overall weight W and wing loading W/S remain constant.

If each aircraft cruises at the same proportion n of its maximum lift/drag ratio (see *Section 1.2.1*) then

$$\left(\frac{L}{D} \right)_{cruise} = n \left(\frac{L}{D} \right)_{max} = n \frac{1}{2\sqrt{C_{D0}K}} = \frac{n}{2} \sqrt{\frac{\pi AR}{k C_{D0}}}$$

Assuming that each aircraft is designed to the same aerodynamic standard, the induced drag factor k and the zero-lift drag coefficient C_{D0} also remain constant. Cruise L/D is therefore proportional to \sqrt{AR} , so that

$$\frac{L}{D} = \left(\frac{L}{D} \right)_0 \sqrt{\frac{AR}{AR_0}} = \left(\frac{L}{D} \right)_0 \cos \Lambda = \left(\frac{L}{D} \right)_0 \frac{M_0}{M}$$

and hence

$$M \frac{L}{D} = \text{constant}$$

Since we are considering a family of aircraft with constant weight, and hence constant lift, then it follows that M/D is also constant – so that drag (and hence required thrust) only increases linearly with design Mach Number (rather than quadratically as would be the case for an individual member of the family). Although a simplistic analysis, Fig. 11 shows that this captures the variation in cruise L/D of a realistic family of aircraft rather well.

The next step is to look at the effect on cruise performance – specifically on range. Recall the basic Breguet range equation:

$$R = \frac{V}{fg} \frac{C_L}{C_D} \ln \left(\frac{W_1}{W_2} \right) = \frac{a_0}{fg} \left[M \frac{L}{D} \right] \ln \left(\frac{W_1}{W_2} \right)$$

For cruise above the tropopause (ie a height of 11km and above) temperature T and hence speed of sound a_0 are constant. Further, for turbojet engines the specific fuel consumption f at the design point is roughly constant, while the weight breakdown and hence start/finish weight ratio W_1/W_2 for the family of aircraft is also constant. The Breguet range R is then simply proportional to ML/D , and from the above analysis therefore constant for the family of aircraft considered.

In other words, the range of a family of aircraft is (to a first order) independent of sweep angle.

Sweep can therefore be considered primarily as a way of increasing cruise speed and hence reducing block time for a given range.

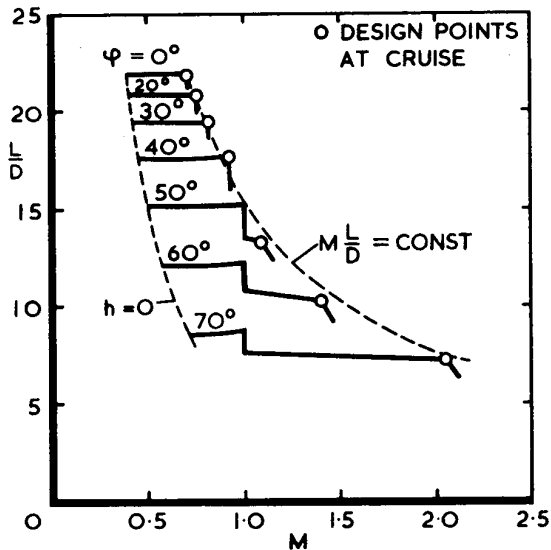


Figure 11: Lift/drag ratios for a family of swept-wing 150-seat transatlantic aircraft
($\varphi \equiv \Lambda$)

1.2.4 Summary

	Aspect Ratio AR		Wing Area S		Sweep Λ	
	lift curve slope $C_{L\alpha}$	induced drag K	profile drag C_{D0}	wing loading W/S	critical Mach Number M	pitch up at stall
Take-Off		✓			✓	
Climb		✓				
Cruise			✓		✓	
Loiter		✓				
Instantaneous Turn				✓		✓
Sustained Turn		✓				
Gust Response	✓			✓		
Landing				✓		✓
Fuel Volume		✓		✓		

Table 1: Performance requirements affecting basic wing planform parameters

1.3 Wing design parameters affecting flying qualities

1.3.1 Taper ratio (planform)

For a given sweep angle and aspect ratio determined as discussed above, the taper ratio is generally then chosen (in conjunction with wing twist) to:

- maximise aerodynamic efficiency – essentially to keep the spanwise loading as close to elliptical as possible, and to
- minimise wing weight – driving towards as small a taper ratio as possible.

When choosing taper ratio it is important to take into consideration a number of factors:

- The chosen shape does not lead to a lift distribution so far from the elliptical that the required twist for low cruise drag will result in large off-design penalties
- The lift coefficient distribution under cruise conditions (varies with the load and the chord distributions) leads to lift coefficients compatible with the performance of the aerofoil at each station. In other words, avoid high local C_L which could lead to drag rise or buffet or separation.
- The lift coefficient distribution under cruise conditions (varies with the load and the chord distributions) leads to lift coefficients compatible with the high lift abilities of the aerofoil and with the desired stalling characteristics. Again, avoid high local C_L especially at the tip which can lead to early tip stall followed by a wing drop (very poor stalling behaviour for an aeroplane).
- The tip chord is not too small as the low resultant Reynolds numbers can lead to early stall.

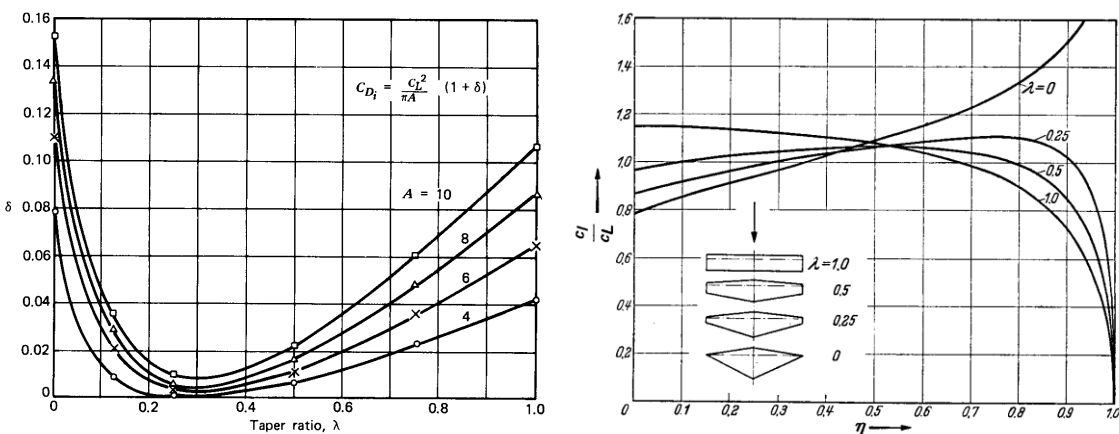


Figure 12: Effect of taper on induced drag and lift coefficient distribution

Aerodynamically, an untwisted wing with an elliptical planform would be ideal, since this gives an elliptical lift distribution and constant local lift coefficient $C_L(y)$ along the span (see 2nd year Aerodynamics notes). In practice, this is difficult to manufacture and can suffer from poor lateral stability at the stall (unpredictable wing drop tendency) – a simple straight taper wing is almost as effective, with a taper ratio of ~ 0.4 on a straight wing giving a induced drag only 1-2% greater than the elliptical optimum. Although a slightly lower taper ratio would apparently give even less induced drag, the spanwise position for maximum local C_L (and hence stall initiation) would move dangerously outboard (from 0.6s to 0.8s), greatly increasing the chances of tip-stall.

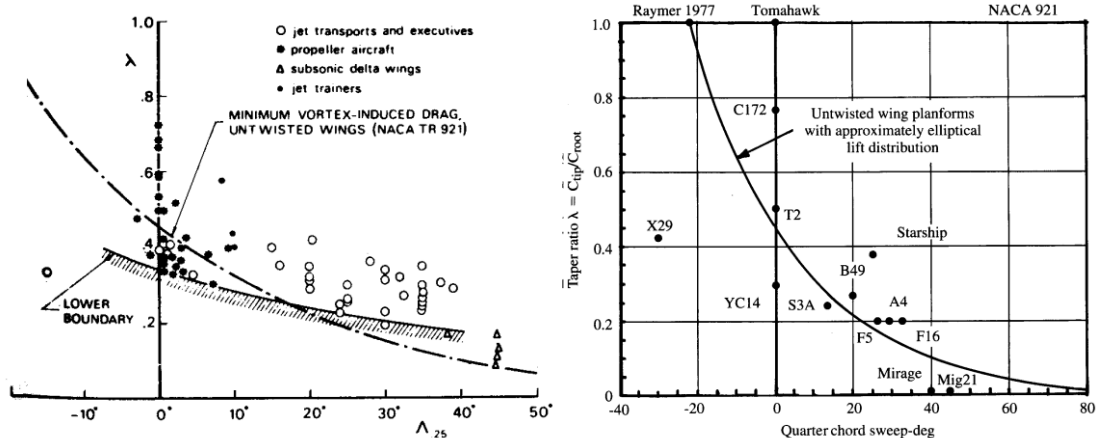


Figure 13: Effect of sweep on taper ratio – civil & military

[NB The famous Spitfire elliptical planform actually resulted from a packaging problem – how to fit eight machine guns into the wing! Many later models had cropped tips to improve manoeuvrability.]

For high speed aircraft, a small taper ratio permits a high leading edge sweep (good transonic/supersonic performance) to be combined with a low trailing edge sweep (improved flap & aileron effectiveness). The longer root chords associated with low taper ratio also make it possible to increase the wing root thickness, giving reduced weight (stiffer section), increased fuel volume as well as stowing provision for the undercarriage. A tapered wing also has high torsional rigidity, a desirable feature for high-speed aircraft as it minimises aeroelastic problems.



On the other hand, a low speed low cost aeroplane can be designed with no taper (and use twist to improve cruise performance) which will result in a much cheaper construction and also have the advantage of constant chord flaps extending from tip to tip (very effective flaps). Such wings are also designed with a rather small AR to minimise wing weight.

Although it seems unrealistic, inverse taper has also been applied in an attempt to overcome tip stall & pitch-up characteristics associated with swept wings. The XF-91 only remained as a prototype though (not necessarily due to problems with the inverse taper; still, nobody went down that route again).

1.3.2 Wing twist

Wing twist is chosen to:

- maximise aerodynamic efficiency at *cruise conditions* – by compensating for the effects of planform (taper ratio and sweep). Twist can also be used to delay transonic drag rise (on swept wings) by adjusting effective sweep angle of the flow itself.
- improve stall characteristics – *washout* (increasing nose-down twist towards the tips) shifts the loading inboard and helps prevent tip-stall – common on both highly-swept wings (high-speed aircraft) and rectangular wings⁵ (low-speed light aircraft).

Twist can also be used to reduce wing weight by shifting centre of pressure inboard and hence reducing wing root bending moment. Whether this is a good idea or not depends on the trade-off between reduced weight and increased drag due to a non-elliptical lift distribution.

The main difference between twist and taper as a means to increase wing efficiency is that a fixed twist distribution can only minimise induced drag at one condition – off-design the drag may be increased. That is why large amounts of twist are avoided (anything more than 5° washout).

The reason for this is clearer if you consider how twist affects the *relative* change in lift at a given spanwise position, since this is proportional to the ratio between the untwisted angle of attack and the new one. However, the increment in incidence is fixed, so the ratio will depend on the original angle of attack. In turn, the change in the shape of the lift distribution will depend on the original wing angle of attack. Since for an untwisted wing the lift distribution is independent of angle of attack, twist optimisation can only be done at a single incidence.

The overall effect of twist on drag is similar to that of camber, with a shift in the parabolic drag polar.

$$C_D = C_{Dmin} + \frac{k}{\pi AR} \left(C_L - C_{Lmin\ drag} \right)^2$$

The ‘design’ lift coefficient $C_{Lmin\ drag}$ for minimum drag is generally positive for negative twist (wash-out), and vice versa for positive twist (wash-in), while the minimum drag C_{Dmin} is increased over the basic (untwisted) zero-lift drag C_{D0} . For an *optimum* twist (or camber) distribution, the overall drag is lower than an untwisted wing, provided that the lift coefficient C_L is greater than half the design lift $C_{Lmin\ drag}$.

Twist can be:

- *geometric* – in which case the physical aerofoil incidence angle varies from root to tip
- *aerodynamic* – in which case the local zero-lift angle of attack varies from root to tip. This is achieved by varying the aerofoil section from root to tip [usually the camber is modified, but more subtle changes in thickness and section type are possible]

⁵ Twist will also unload the tips of the rectangular wing thus improve the lift distribution.

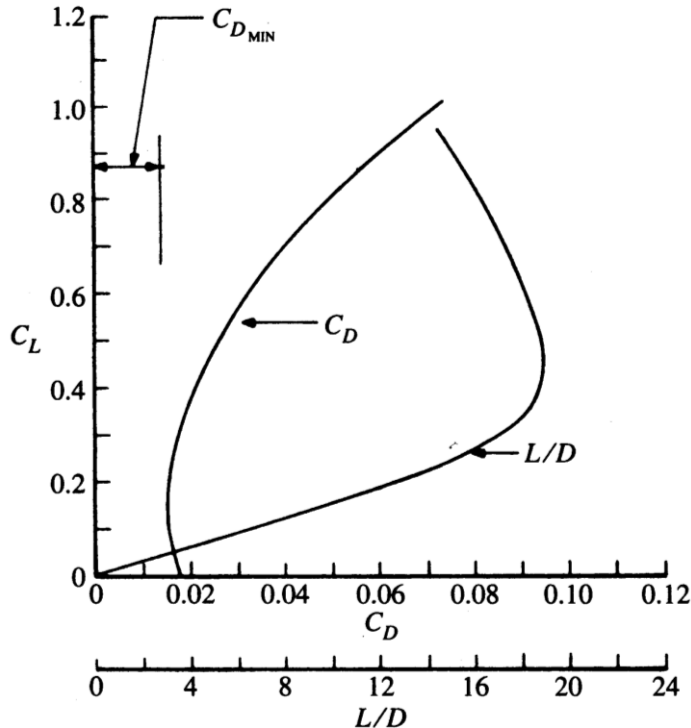


Figure 14: Drag polar for a twisted/cambered wing

Twist also changes the structural weight by modifying the moment distribution over the wing, while twist on swept-back wings also produces a positive pitching moment which has a small effect on trimmed drag. This positive moment can be used to offset the excessive nose-down pitching moments of some supercritical aerofoils (eg AV-8B).

The selection of wing twist is therefore accomplished by examining the trades between cruise drag, drag in second segment climb, and the wing structural weight. The selected washout is then just a bit higher to improve stall.

Swept wings tend to twist naturally under load (increasing washout for aft sweep and vice versa for forward sweep – as much as 10° at high-g combat conditions), so the built-in twist at 1g has to be carefully matched to the high-g deformation. For accurate wind tunnel measurements of cruise drag it is often necessary to build models with the correct wing deformation (in bending and torsion) – complicated by the deformation of the model itself under load.

As a final note, an example of a non-optimum twist distribution is given by the deflection of a part-span flap⁶. Here, a 15° flap deflection on a rectangular wing drops the span efficiency factor e from 0.96 to 0.84. The rapid changes in circulation at the flap boundaries are manifested as flap-edge vortices in the wake.

⁶ The deflected flap in effect increases the camber of the aerofoil sections along its span resulting in aerodynamic twist.

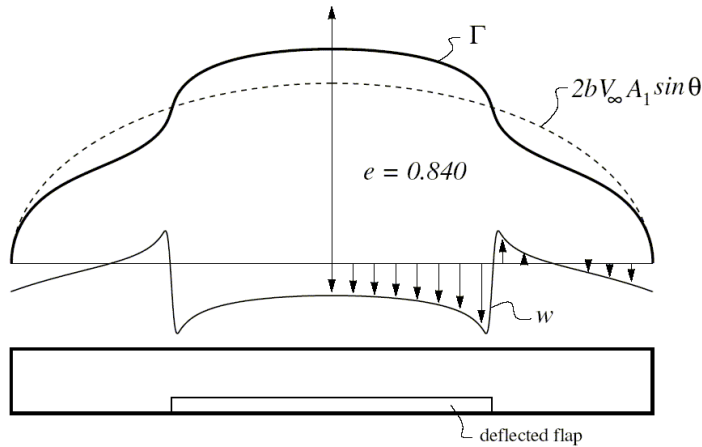


Figure 15: Effect of flap deflection on lift distribution and induced drag

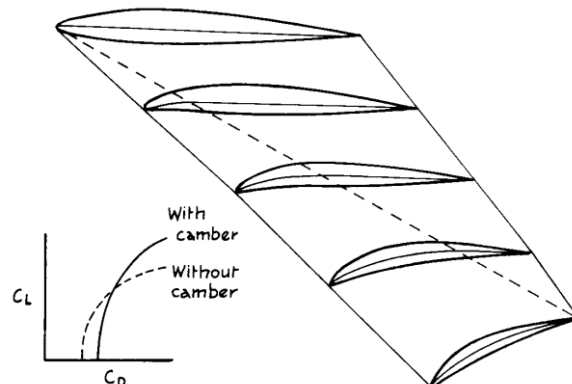
1.3.3 Spanwise camber variation

For a 2D aerofoil, camber has several effects:

- an increase in lift at a given incidence, giving a negative shift in zero-lift incidence,
- an increase in maximum lift (delayed stall) due to the leading edge droop,
- an increase in form drag, and
- a reduction in critical (ie drag rise) Mach number.

The first effect is equivalent to a nose-up pitch (or twist) so is relatively straightforward to deal with.

The increase in local maximum lift is rather desirable (so many aircraft employ increasing camber towards the tip), but comes with a drag/buffet penalty. Variable camber is one solution, using scheduled leading and trailing edge flaps to optimise camber for manoeuvre. Alternatively, many older fighter aircraft (F-106, F-15) use *conical camber* – where the wing is cambered progressively from root to tip ahead of an imaginary line starting at the wing apex (and ending, for example, at the tip trailing edge⁷) – to improve the off-design performance of wings designed for supersonic flight. This camber variation is referred to as conical because the wing geometry is straight along rays through the wing apex (the surface ahead of the imaginary line is part of the surface of a cone). Conical camber counteracts (to some extent) the loss of (attained) leading edge suction on highly swept wings, reducing induced drag – but at the cost of an increase in zero-lift drag.



Although less aerodynamically efficient than variable camber, conical camber is lighter, cheaper and simpler.

⁷ Obviously a different imaginary line is required for delta wing aircraft (the line will end somewhere at the trailing edge).

Note that a spanwise variation in camber applies an effective aerodynamic twist to the wing, with the same difficulties with off-design performance as geometric twist.

Overall, the difference between twist and camber is that for a given planform:

- *twist is used to set the desired basic spanwise load distribution (fix lift on each section), while*
- *camber is used to adjust the pressure distribution in particular, the isobar sweep (fix pressure distribution on each section while “maintaining”⁸ the section lift)*

1.3.4 Thickness distribution

Wing thickness distribution is chosen to:

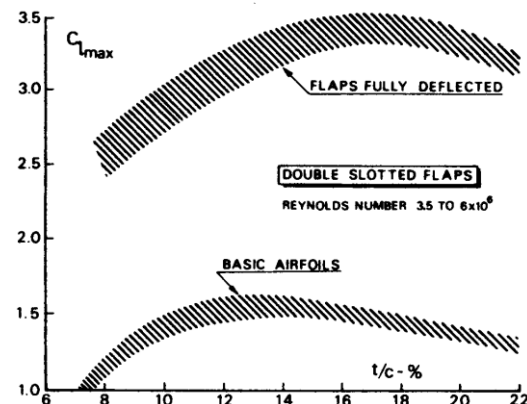
- minimise wing structural weight – increased thickness gives a stiffer section and hence permits a lighter wing (plus greater internal fuel volume)
- minimise drag penalty – increased thickness gives small increase in form drag at low speed (increased boundary layer growth) plus a large increase in wave drag (reduced critical Mach number) at high speed.

A simple parameter showing the impact of thickness on weight is the cantilever ratio

$$\frac{\rho/2 \cos \Lambda_{1/2}}{t_{root}}$$

(or variations upon this

theme), since historically wing weight fraction has been found to be directly proportional to this ratio. Increasing aspect ratio tends therefore to drive up thickness ratio.



Increased root thickness may also aid undercarriage design and permit a ‘buried’ engine configuration (Vulcan, Victor).

Greater thickness does also tend to increase C_{Lmax} up to a point, depending on the high lift system, but gains above about 12% are small (if any). Most of this effect comes from the change in nose shape (ie leading edge radius).

Mitigating against thick aerofoils are the earlier onset of transonic drag rise, and increased form drag at low speed. The profile drag rise only becomes significant at rather high thickness/chord ratio, hence a choice between 15-20% at the root is usually best (also maximum C_{Lmax} with high lift devices). Anything more than 20% at the root is very rarely used because of increased profile drag and low C_L during cruise (look at the basic airfoils curve of the graph). This in effect limits the maximum aspect ratio to values around 13. High speed aircraft will usually have smaller thickness ratio, even down to 4%.

⁸ Since twist and camber actually affect each other this difference between their effects on a planform is oversimplified; especially true for the “maintaining” part.

Thickness ratio does not have to be kept constant along the span. In fact, by reducing the thickness at the tip we can obtain both aerodynamic (higher C_{Lmax} for 12-15% thickness⁹) and structural (lower weight) advantages. The variation of thickness ratio along the span is usually non-linear due to the linear lofting used between the root and tip sections.

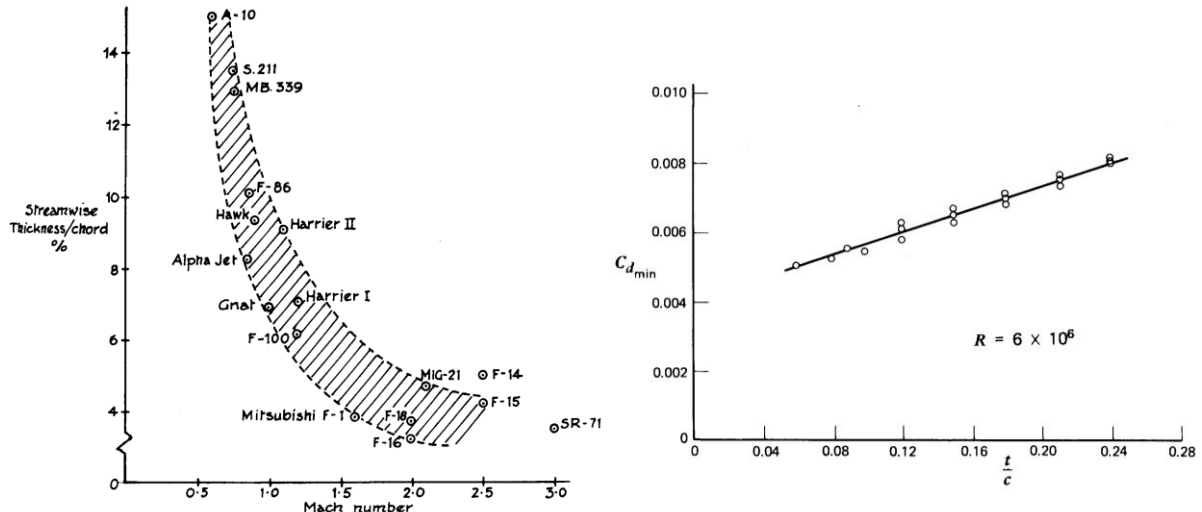


Figure 16: High-speed and low-speed consequences of thickness

2.3.5 Wing/fuselage integration

Wing/fuselage integration has both structural and aerodynamic implications. Elements we will consider include:

- wing vertical location: high, mid or low wing
- wing inclination: dihedral or anhedral
- wing incidence setting
- wing root shaping: fillets, local camber variations and area rule

Wing vertical location

The wing vertical location (relative to the fuselage) is largely chosen on configuration grounds. A high or low wing offer the structural advantage of not having to pass the wing box through the fuselage, which requires stiffening the fuselage (more weight) and splits its internal volume (not at all practical for passenger or cargo planes). On the other hand, the wing box being above or below the fuselage will require some fairing and will add frontal area.

A high wing (common on military cargo planes) puts the fuselage very close to the ground thus making loading and unloading easy even in rudimentary airstrips. Additionally, the engines placed below the wings have good clearance from the runway, which will be quite rough and full of debris in many cases. On the negative side, the undercarriage will have to be attached to the fuselage, which will require significant structural stiffening to carry the landing loads. On top of that, the undercarriage will in most cases be stored in external

⁹ Refers to subsonic aeroplanes

blisters that add drag. A high wing on light aeroplanes can obscure pilot's vision; a number of aeroplanes have been made with transparent panels to avoid this problem.

A low wing provides the ideal mounting point for undercarriage; the already very strong wing box. In addition there is plenty of space in the wing root for stowing the undercarriage. The engines will be closer to the ground, thus easier to inspect and maintain. The undercarriage will have to be longer to provide the necessary clearance but this will place the fuselage far from the ground level necessitating additional equipment to load the aeroplane. None of this is a problem though in modern airports and the majority of airliners are of the low wing design.

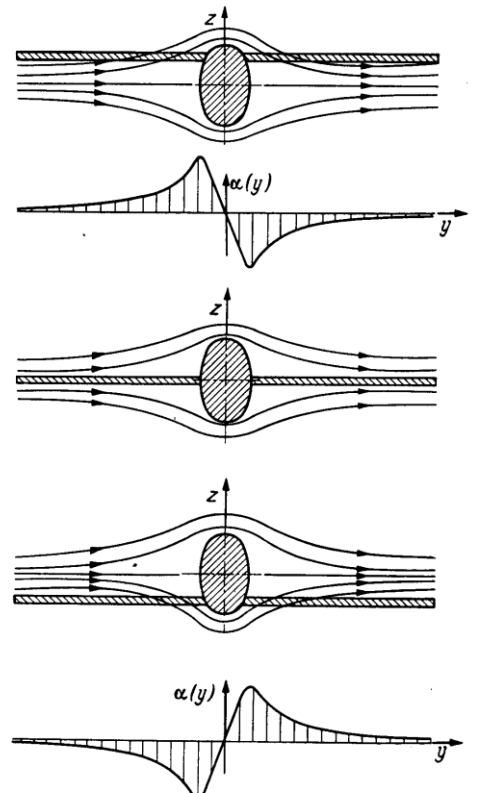
Aerodynamic issues that need to be taken into account when considering the wing vertical location include:

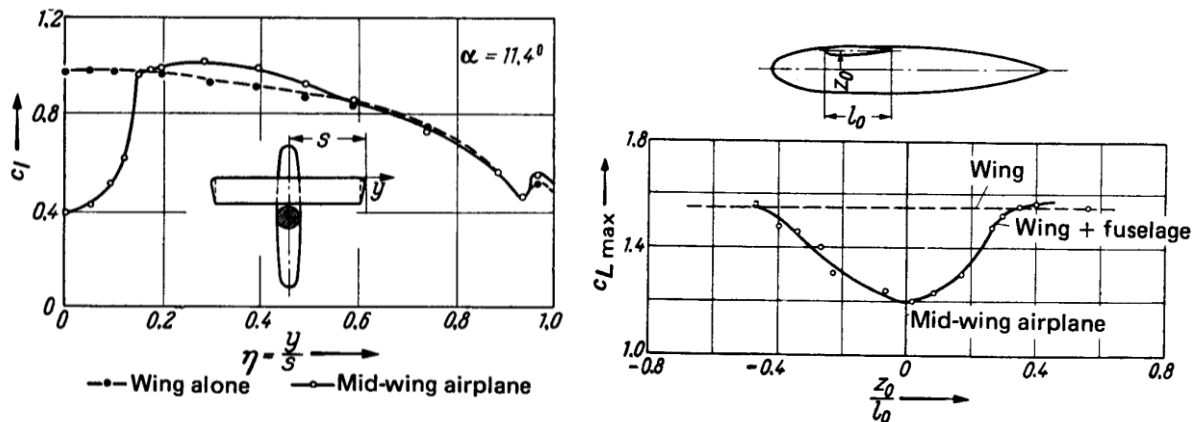
- dihedral effect: rolling moment due to sideslip.
- lift loss/carry-over on portion of wing blanketed by the fuselage.
- wing wake/tail interaction: reduction in dynamic pressure at the tail, plus possibility of tail blanketing/tail buffet at high incidences.
- interference drag at wing/fuselage junction.
- wing/fuselage interaction: induced flow on fuselage gives pitching moment (and hence shift in aerodynamic centre).

Dihedral effect due to wing vertical location results from the flow around the fuselage in sideslipping motion. For a high position the windward wing sees an upwash around the fuselage and the leeward wing a downwash, giving a stabilising rolling moment 'away' from the sideslip (ie a negative $C_{l\beta}$). The opposite occurs for a low wing position, which therefore tends to reduce roll stability.

The vertical position of the cg is largely irrelevant because no significant sideforce is generated ... it is the wing/fuselage flow in sideslip that causes a *rolling moment*. In other words there is no such thing as 'pendulum stability'!

The **lift loss** over the 'blanketed' part of the wing appears to be significant – but it is (largely) compensated for by an increase in fuselage lift due to the upwash and downwash induced on it by the wing. The overall lift is then almost the same.



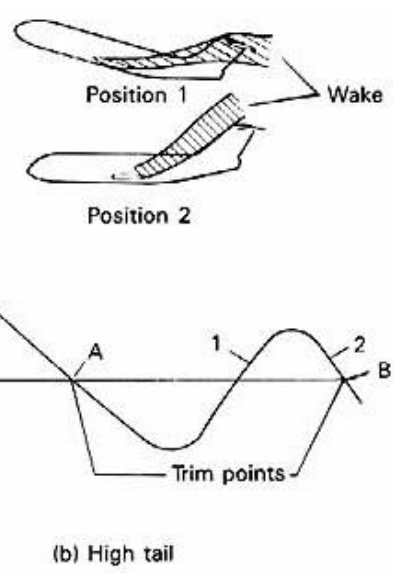


However, the *maximum* lift level is rather dependent on wing vertical and longitudinal position on the fuselage, since the fuselage is a poor lifting surface at high incidence – the greatest loss occurs for a mid wing set more than a chord's length back from the fuselage nose.

Wing wake/tail interactions depend on the relative heights of wing and tail, and the angle of attack. If the wing wake comes close to the tail than we will see a reduction in dynamic pressure q and a corresponding loss in tail effectiveness. The reduction is directly related to the wing profile drag (= energy loss to the wake) - so will be larger for (a) poor wing design, or (b) at high angles of attack with wing flow separation.

The latter case is by far the most significant, but may not necessarily be a problem. For low wing aircraft with stall beginning in towards the wing root, the wake interaction gives a natural warning of ‘incipient’ stall. The unsteady turbulent wake from the stalled inboard region *buffets* the tailplane, giving a physical indication (through either airframe or stick vibrations) to the pilot that the aircraft is on the verge of a full stall¹⁰. The Beagle Bulldog until recently operated by the University Air Squadrions was a good example: a max-rate turn was achieved by banking and ‘pulling to the edge of buffet’. In the absence of this physical indication of stall onset artificial means have been used – eg stall warning devices actuated by leading edge suction (Cessna 172), stick pushers (Jetstream) or inboard stall strips on the wing leading edge (Hawk).

A more serious interaction can occur with a high T-tail – if the wing is fully stalled the very low energy wake can blanket the tail, resulting in a loss of tail effectiveness, and hence any means of recovering from the stall. A well known example was the BAC1-11, with at least one aircraft lost to ‘deep stall’ during flight test at Bristol. Deep stall recovery is possible – by using aileron and rudder to convert the stall into a spin (apparently done on the Gloster Javelin delta wing fighter which is also a T-

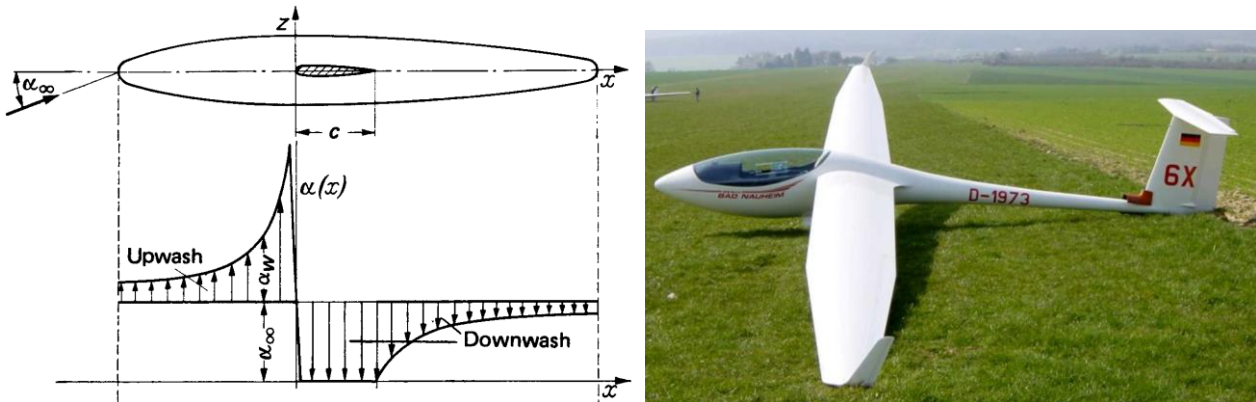


¹⁰ This technique is not used in large airliners because the buffeting can well be too much for both the pilot and the structural integrity of the tail.

tail aircraft) ... not terribly useful since stall tends to happen near the ground! The basic fix for this problem is not to put the tail in the wing wake path ... failing that, civil T-tail aircraft use a stick pusher or other artificial limiter to prevent the pilot stalling the aircraft in the first place.

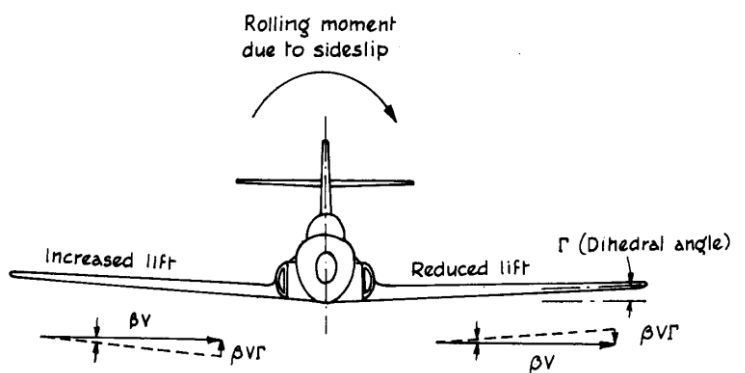
Interference drag at the wing/fuselage junction comes from a number of sources which will be considered later. Alleviation of the interference effects requires shaping of the junction region – which is considerably more straightforward for mid wing rather than high/low wing configurations – particularly for high-speed aircraft.

The upwash and downwash distribution **induced on the fuselage by the wing flow** clearly depends on the wing position – although longitudinal rather vertical is the most critical. As mentioned above, the induced incidence variation produces lift (which counteracts the loss in wing lift) plus pitching moment (which moves the aerodynamic centre – generally forward). In addition, by effectively adding negative camber the induced flow increases fuselage drag (profile plus induced drag – if the fuselage is lifting). This can be counteracted by physically cambering the fuselage to keep it aligned with the local flow (but only at one incidence – since the induced velocity varies with wing lift). A cambered fuselage is a distinctive feature of many high-performance gliders.



Wing Inclination

Wing inclination – dihedral for tips higher than the root and anhedral for tips lower than the root – is primarily chosen based on lateral stability. With dihedral, any sideslipping motion gives a (small) increase in incidence on the windward wing and vice versa on the leeward wing, giving a stabilising rolling moment ‘away’ from the sideslip (ie a negative $C_{l\beta}$). The opposite occurs for anhedral, which therefore tends to reduce roll stability.



The penalty for dihedral is a slight loss in aerodynamic efficiency due to the inboard inclination of the lift vector.

Anhedral is often used to counteract excessive levels of effective dihedral on aircraft with high-mounted swept wings (the Harrier is the classic example). Excessive lateral stability can lead to problems with roll control in crosswind landing, dutch roll oscillations, roll response to lateral gusts and variations in roll manoeuvre performance with incidence.

Dihedral/anhedral can also impact on other layout issues – giving for example increased ground clearance for engines or underwing stores for low wing aircraft (bank angle limit on landing), or reduction in length of wing-mounted undercarriage (Harrier outriggers).

Some aircraft employ dihedral on the outer wing panels only (Jodel and Robin). An aerodynamic argument for this layout is that since dihedral is needed to generate rolling moment due to sideslip, then it is the outboard wing that is most effective (maximum moment arm). For the same $C_{l\beta}$ then, a large dihedral angle on the outboard wing may give a smaller penalty in lift than a smaller dihedral angle over the entire span. In fact, outboard dihedral is claimed to achieve a closer approximation to an elliptical lift distribution for a rectangular wing planform by shifting the loading inboard, and so reducing induced drag. Unlike twist/washout, this adjustment should be effective at any incidence, since it is proportional to the local lift (whereas twist gives a constant change in lift). The Robin and its precursor the Jodel certainly have a good reputation for efficiency and low-speed stability – but there must be a weight penalty for introducing a break in the wing spar structure?



In the limit, this argument would lead to a curved wing, which is approximated by the ‘polyhedral’ sometimes seen on model aircraft (apparently from a consideration of bird wings). This curved wing (non-planar) will produce a non-planar wake and is expected to be even more efficient than the elliptical ‘optimum’.

Wing incidence setting

Wing incidence setting is relatively straightforward – the ‘rigging angle’ of the wing sets the fuselage inclination in horizontal flight. For civil aircraft we require the fuselage floor

to be close to horizontal ($\pm 2^\circ$) in flight. For other aircraft it may be more important to ensure minimum fuselage drag, or adequate forward view on approach. Some aircraft (eg Vought F-8) have had variable wing incidence to optimise fuselage attitude for low- & high-speed cruise and for landing.

[NB Wing (or tail) incidence setting has no relevance to stability – despite the widespread use of ‘longitudinal dihedral’ to explain pitch stability.]

Wing root shaping

The most complex aspect of wing/fuselage integration is the shaping of the junction region.

This may be split into two issues:

- straight wings at low speed
- swept wings at high speed

At **low speeds** the wing/body junction gives problems with boundary layer growth and separation. In the simplest case of a non-lifting round-nosed wing intersecting the wall of a fuselage, the adverse pressure gradient ahead of the wing causes flow separation on the fuselage ahead of the wing. In extreme cases this may lead to the formation of a horseshoe vortex around the wing root. In either case we can expect a significant increase in drag (unwanted vortices = lost energy), and possibly an unsteady loading on the tailplane.

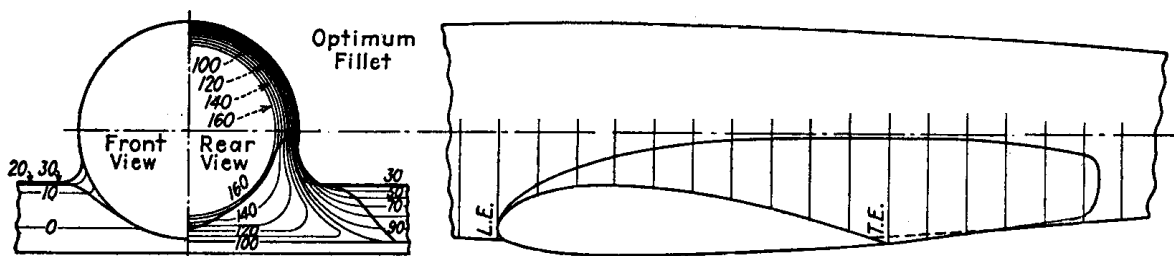
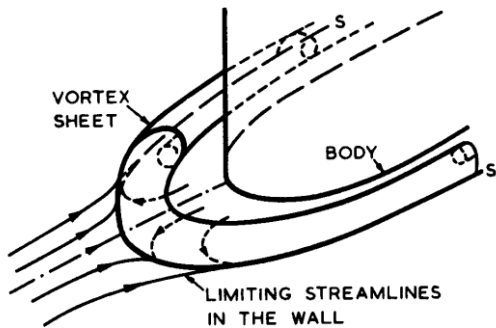


Figure 17: Example of pre-war ‘optimum’ fillet design for low wing monoplane

The solution to this problem is to fair in the junction with a fillet – which can be a simple filling-in of the corner or a complex change in local thickness, chord and camber. Fillet design is not straightforward (it is possible to make matters worse rather than better) – since local changes to the wing root affect lift distribution, and hence both induced drag and downwash at the tail (performance and trim).

Fillet design tends to be most straightforward on mid-wing aircraft (little more than a radius of the junction, particularly if the fuselage side is flat – ie a 90° included angle), and most complex on low wing aircraft (where a large fillet at the trailing edge may be needed).

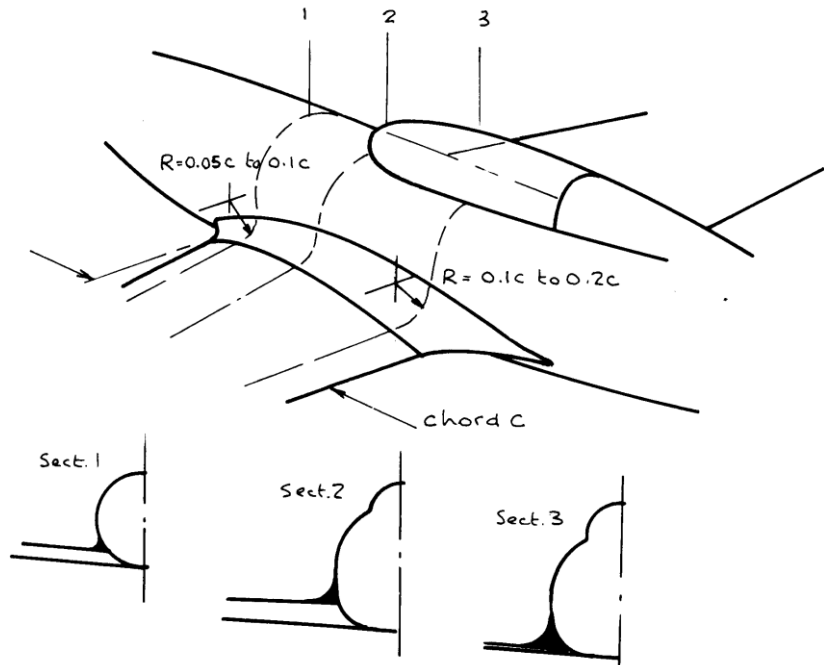


Figure 18: Typical low-speed fillet geometry (from Stinton)



Figure 19: Spifire & He-111 wing root fairings

A low-speed fillet needs to address four aspects of the junction flow:

- the effect of the adverse pressure gradient on the fuselage ahead of the wing root due to the wing blockage – alleviated by sweeping the leading edge forward and reducing local nose radius.
- 3D boundary layer growth in the corner between the wing surface and the fuselage (particularly where the wing/body joint is not perpendicular) – alleviated by filling in the corner with a (small) radius
- the effect of the adverse pressure gradient (pressure recovery) on the aft portion of the wing upper surface at the root (the diffuser effect) – alleviated by increasing the fillet radius, sweeping the trailing edge aft and reducing local camber

- local variations in spanwise lift distribution (due to the introduction of the fillet¹¹) affecting induced drag and downwash at the tail alleviated by a marked negative camber at the root trailing edge (Spitfire fillet)

Note that if too large a fillet radius is used then drag can be increased rather than reduced.

Wing/fuselage junction shaping for **swept wings at higher speeds** is aimed primarily at controlling local regions of supersonic flow caused by the constraint the fuselage places on the cross-flow on the wing.

To see the reason for this we first of all look at the inviscid flow over an infinite sheared (swept) wing (ie no tip or root). Because there is no change in surface slope parallel to the leading edge, there can be no pressure gradient in this direction and hence no change in the corresponding velocity component parallel to the leading edge. This is why it is the Mach number perpendicular to the leading edge that is critical.

As the flow decelerates ahead of the wing, accelerates over the front portion then decelerates over the aft portion geometrical considerations alone indicate that a typical streamline viewed from above will change direction in a rather complex manner – firstly curving ‘outboard’ to run parallel to the leading edge (corresponding to the forward stagnation point in 2D flow, but with a spanwise velocity $v' = V_\infty \sin A_{LE}$), then curving inboard as the velocity component perpendicular to the leading edge increases to a maximum, then straightening up in the pressure recovery region. Overall the streamlines over the wing are displaced ‘inboard’.

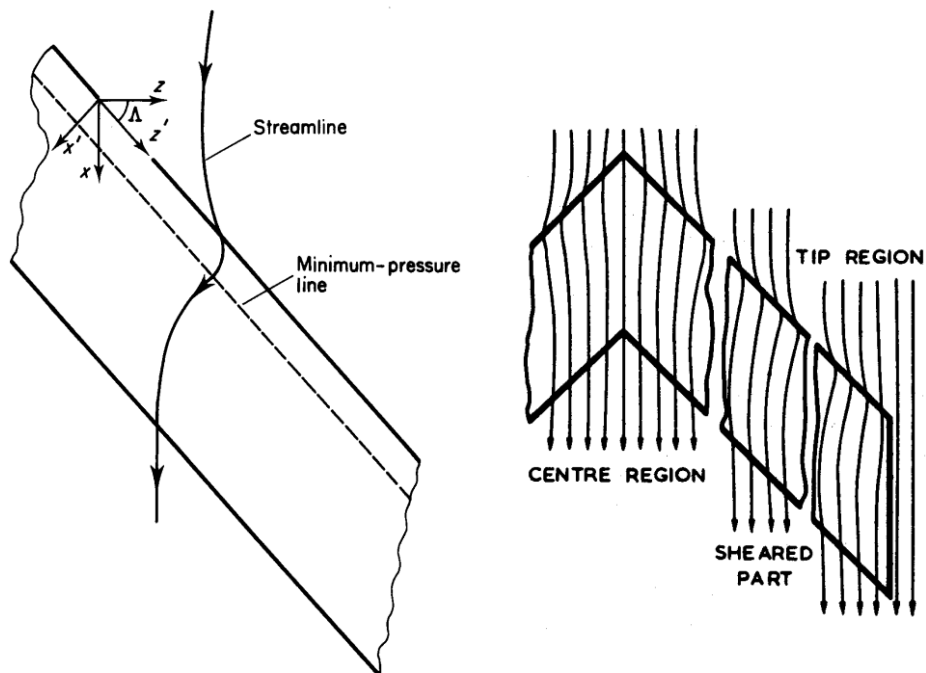


Figure 20: Cross-flow on infinite and finite sheared wings at zero incidence

¹¹ A fillet with a large radius at the trailing edge will in the end increase the root chord and thus the generated lift.

This is fine for an infinite wing, but in the case of a finite swept wing the flow departs from the 2D (infinite wing) sheared pattern at both the tips and at the root (one of the reasons why a lifting line type wing theory is inaccurate for swept wings):

- the constraint presented by the reflection plane on the centreline (or equivalently the fuselage side) straightens up the local flow here – the local suction peak is reduced and shifted rearward
- at zero lift (the case sketched in most text-books) the flow in the tip region must also straighten up to follow the freestream direction – the local suction peak increases slightly and moves forward
- as incidence increases the tip flow is dominated by the usual 3D effects of tip vortex formation – inflow on the upper surface, outflow on the lower surface

For **inviscid, incompressible flow** the results of this can readily be calculated using lifting surface theory. For a straight wing, tip effects shift the local neutral point forward of the 2D quarter-chord point. For a swept wing the local neutral point is shifted forward at the tips and aft at the root, with the overall aerodynamic centre shifted aft of that given by assuming 2D characteristics. The lift distribution is also affected, with a lifting surface calculation ('3a') showing a significant lift loss on the centreline compared with quasi-2D lifting line ('1') theory – exacerbating the outboard loading shift associated with wing sweep.

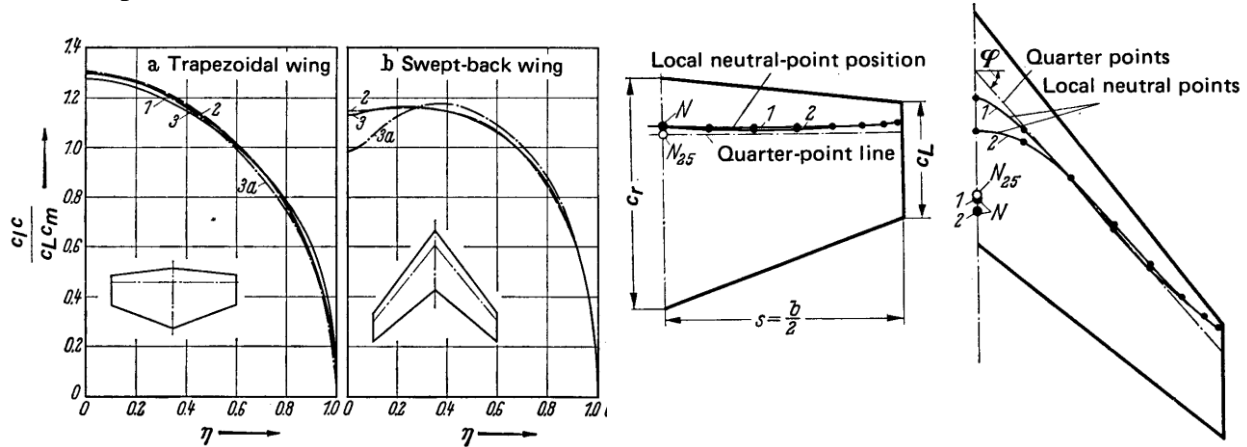
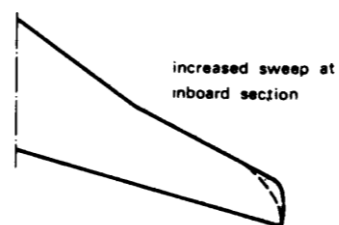


Figure 21: 'Centre effect' on swept wing lift distribution

Note that the effect of 3D flow on spanwise loading is relatively small at the tips – it is the root section where the most lift is lost. One solution is to twist the wing – or to change the planform by increasing chord (and hence leading edge sweep) at the root (a feature seen on many transport aircraft planforms).



Alternatively, one can do away with the root region by using an asymmetric oblique wing.

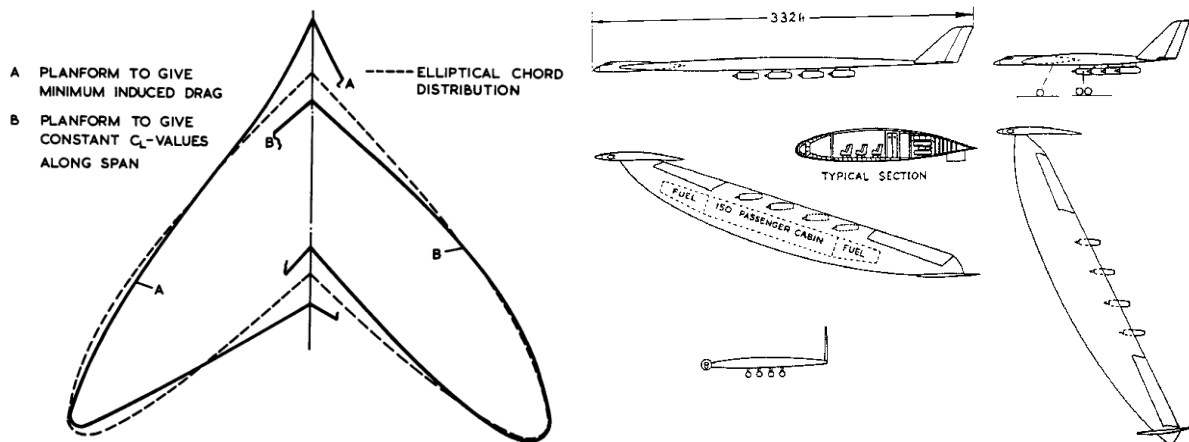


Figure 22: Combating the centre effect – planform shaping vs oblique wing

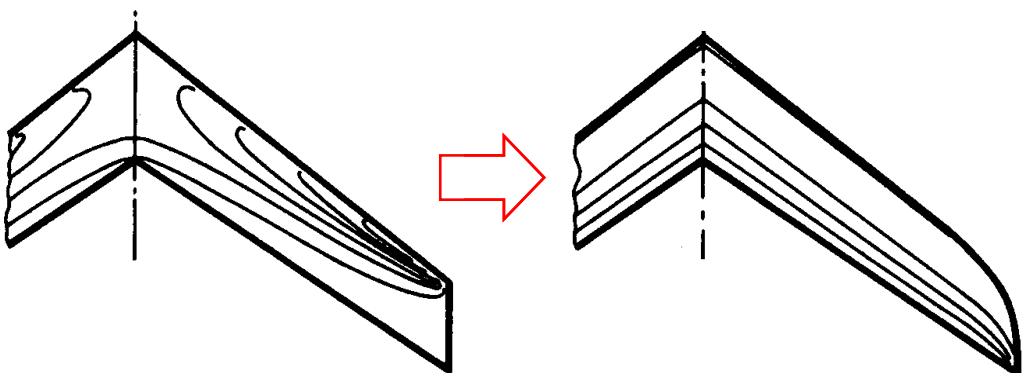


Figure 23: Wing design for straight isobars

For **compressible flow** the situation becomes rather more complex. For high subsonic flows the effects are often described using plots of isobars on the upper surface. For an ‘untreated’ wing the root and tip effects at low incidence effectively ‘unsweep’ the local flow – counteracting the effect of leading edge sweep on critical Mach Number. As a result, a complex 3D shock system will form and M_{crit} is reduced. The outboard region is relatively easy to deal with – using twist, camber and tip planform shaping (eg the Kuchemann tip) to maintain straight isobars almost to the tip.

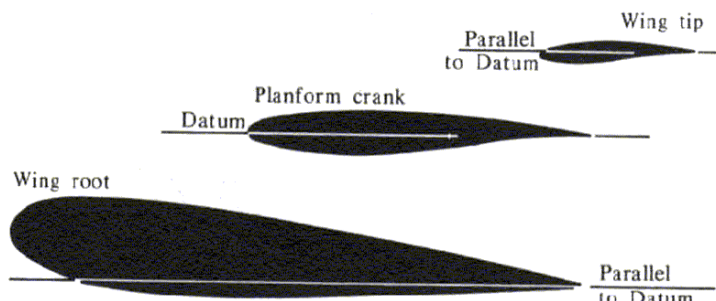


Figure 24: Example of twist, camber and thickness variation designed to give a uniform section pressure distribution across the span

Theoretically, a similar procedure could be undertaken for the root region, but in practice the required twist/camber/thickness changes required are often too large to be fully achievable. In terms of *wing shaping*, the two approaches most often seen are to:

- increase wing sweep near the fuselage, blending the wing in a smooth fashion into the forebody of the fuselage (B-1B)
- adjust the wing root isobars using an aerofoil designed to have its pressure peak very near the nose – resulting in a thick root section having a large nose radius, a fairly flat top and negative camber (!). The loss of local lift due to the negative camber then necessitates a large nose-up twist to maintain a good spanwise lift distribution. (commonly used on large airliners – Fig. 24)

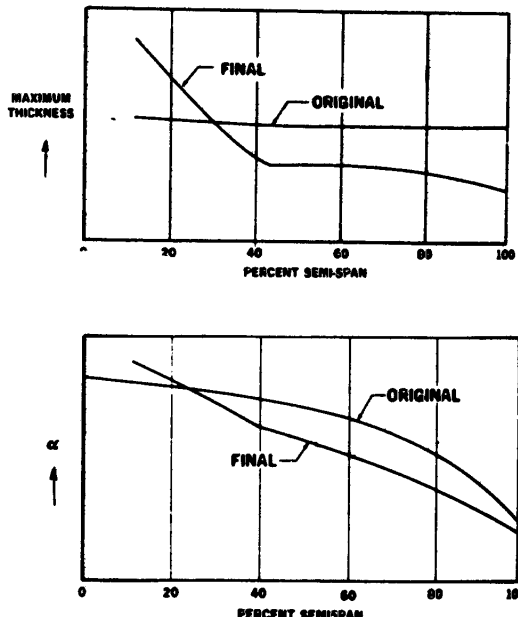


Figure 25: Examples of thickness and twist modifications used to improve centre-section flows (from Torenbeek)

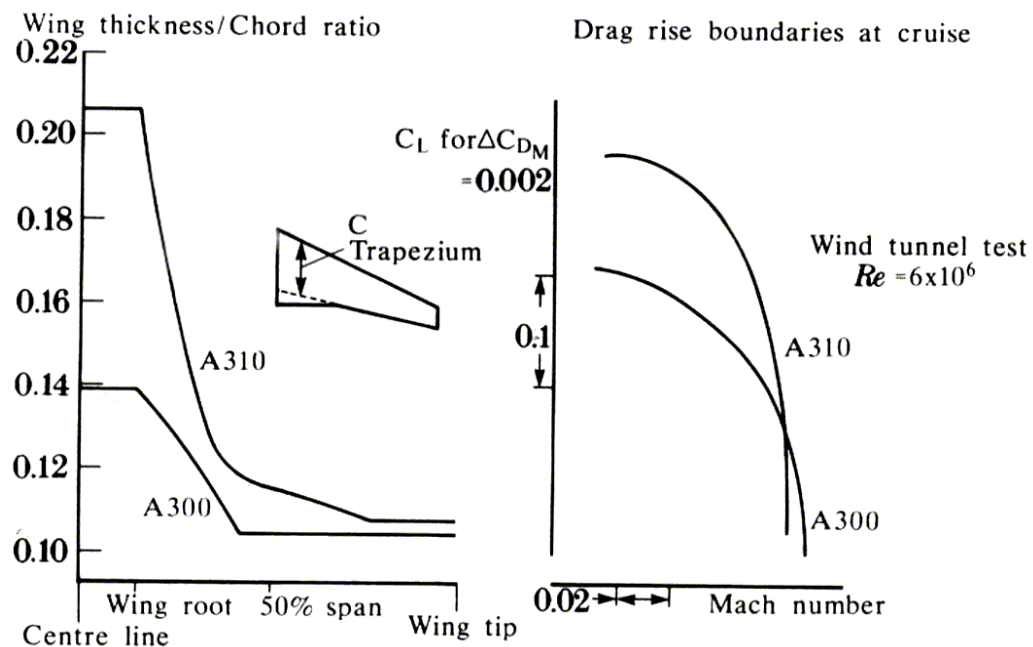


Figure 26: A310 (1980s) wing compared with A300B (1960s) showing increased thickness and improved drag standard at high Mach Number

Figure 25 illustrates a rather old wing design – but Fig. 26 shows how improvements in computational capabilities have enabled an increase in wing thickness (particularly at the root) coupled with an improvement in high-speed drag (or rather the drag-rise lift coefficient).

For ***supersonic aircraft***, more drastic action is called for, with more attention to be paid to the fuselage effects. Initial work on this problem looked at the ‘near-field’ flow details – to be followed later by the ‘far-field’ area rule technique with the end results looking pretty much the same.

In supercritical conditions the centreline constraint results in a deceleration of the supersonic flow (streamlines turned ‘into’ the flow \equiv compression wedge). The compression-wave system required to achieve this propagates across the span and may coalesce into a rear tip shock – increasing the wave drag.

Conceptually the solution is obvious – to ‘waist’ the fuselage to reduce the level of compression by returning the local flow to the infinite sheared wing case. In practice this ‘near-field’ design process is rather complex, requiring 3D shaping of the fuselage to maintain a straight fully swept isobar pattern.

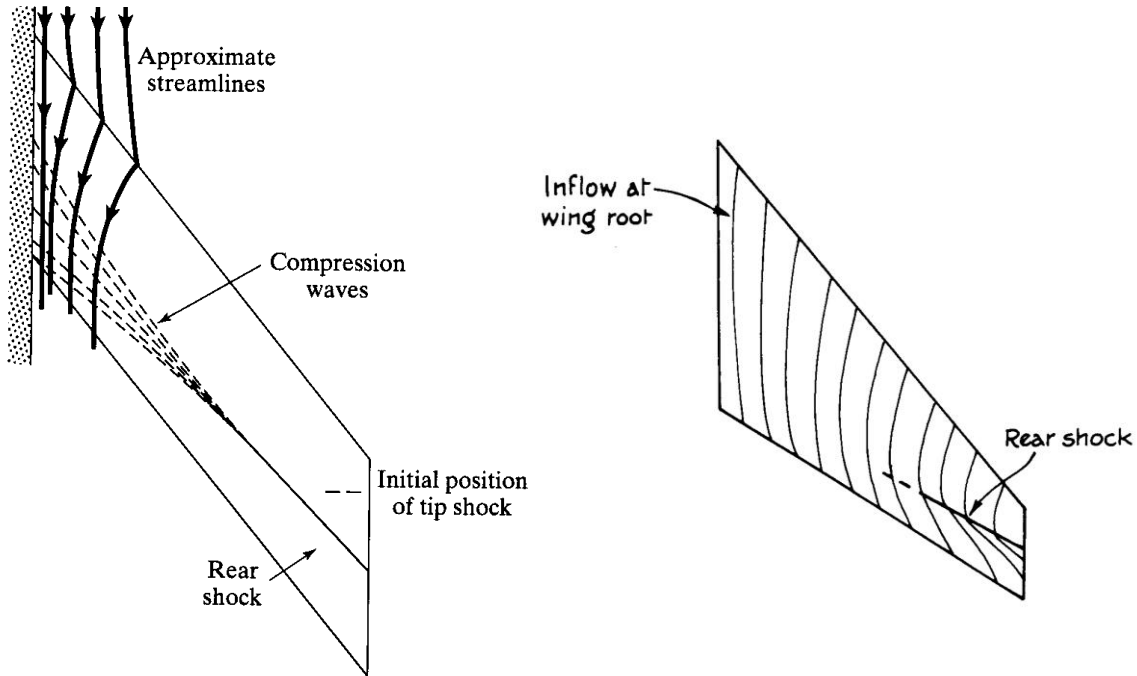


Figure 27: Outboard effect of flow constraint at wing root

A simpler approach developed by Whitcomb at NASA is the ‘Area Rule’. Put simply, for ***sonic Mach numbers*** (ie $M \approx 1.0$) the longitudinal distribution of the cross-sectional area of the complete aircraft (fuselage + wing + cockpit + stores + etc) should approximate to the minimum-drag Sears-Haack body (or at least vary smoothly). The resulting shapes are similar to the near-field approach, and give similar large increases in critical Mach number, and large reductions in transonic drag levels.

If not done carefully, though, area ruling can be overdone – since if the fuselage is contoured too severely the resulting adverse pressure gradients can lead to rapid compressions and shock waves in the plane of the wing.

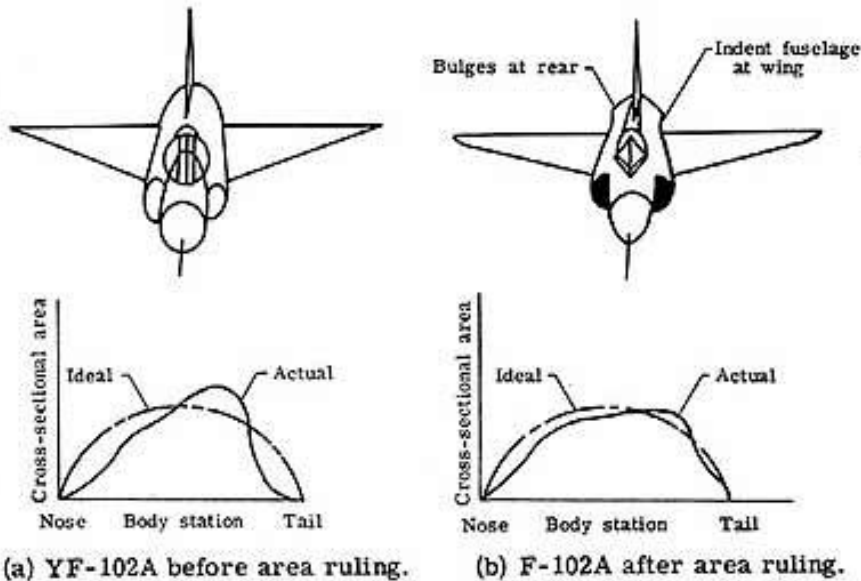


Figure 28: Application of area rule to F-102 (which initially ‘refused’ to go supersonic even though according to the design it was supposed to be able to do so!)

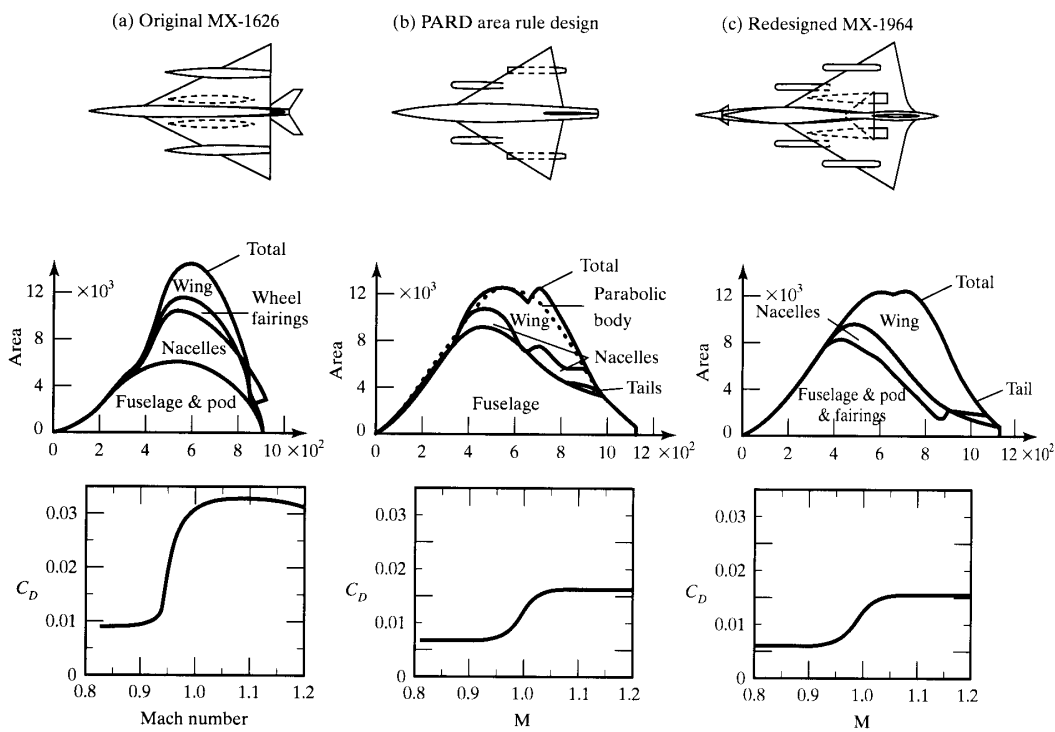


Figure 29: B-58 area ruling

Area ruling for **supersonic speed** is rather more complex – rather than taking the cross-sectional area in a perpendicular plane, cuts are taken tangent to the Mach cone and projected onto a plane normal to the aircraft axis. Since the area depends on the roll angle

at which the cut is taken there is no longer a single equivalent body – instead an integrated average is taken.

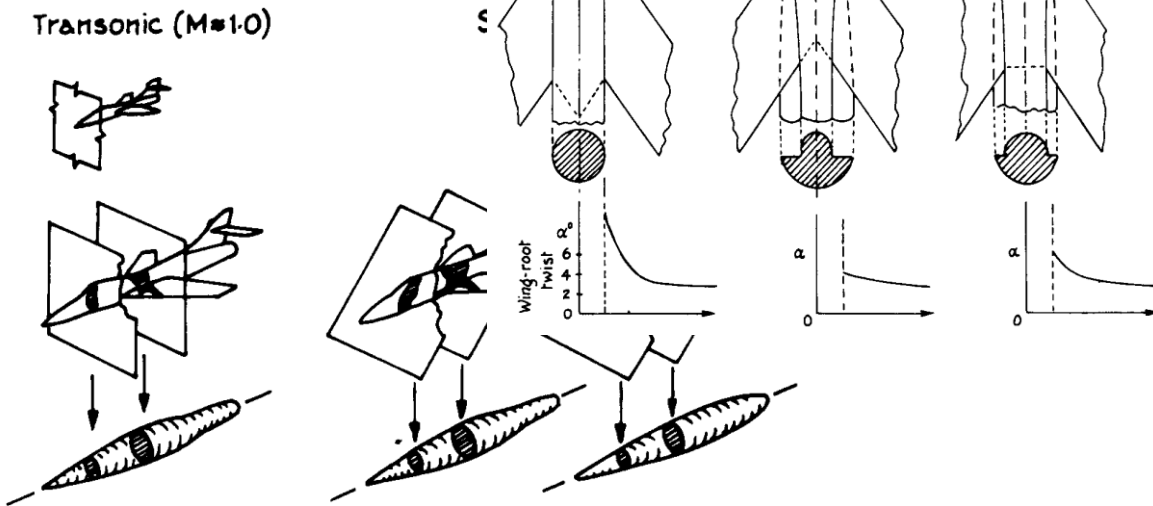


Figure 30: Area ruling – equivalent bodies at sonic and supersonic speeds

The basic area rule is aimed at minimising zero-lift wave drag due to volume. For *cruise* (ie non-zero) lift conditions, it is necessary to go back to the ‘near-field’ approach. In this case, designing for an ‘infinite sheared flow’ results in different body shaping above and below the wing (since the lateral displacement of the streamlines will differ above and below). In general, more waisting is needed above the wing than below – leading to an increase in wing lift from the pressure differential. The degree of waisting depends on the balance between local twist and fuselage shaping used to achieve the desired isobar pattern – at one extreme, differential body waisting can lead to the formation of distinct shelves on the fuselage sides.

Area ruling is not confined to wing/body junctions – the F-5 for example has area ruled tip tanks to improve transonic buffet & pitch up but also to reduce drag. Many early UK jet aircraft made extensive use of area ruled bodies to alleviate local transonic flow problems. The Buccaneer had a very obviously area-ruled fuselage but also a body at the fin/tail junction to sort out a buffet problem.

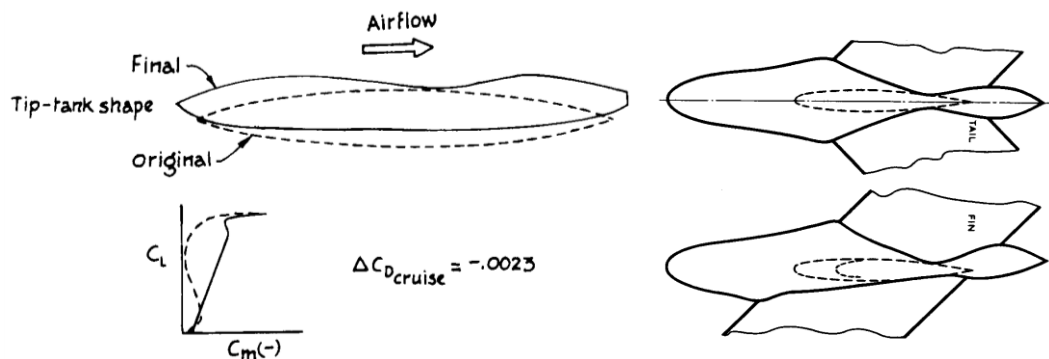
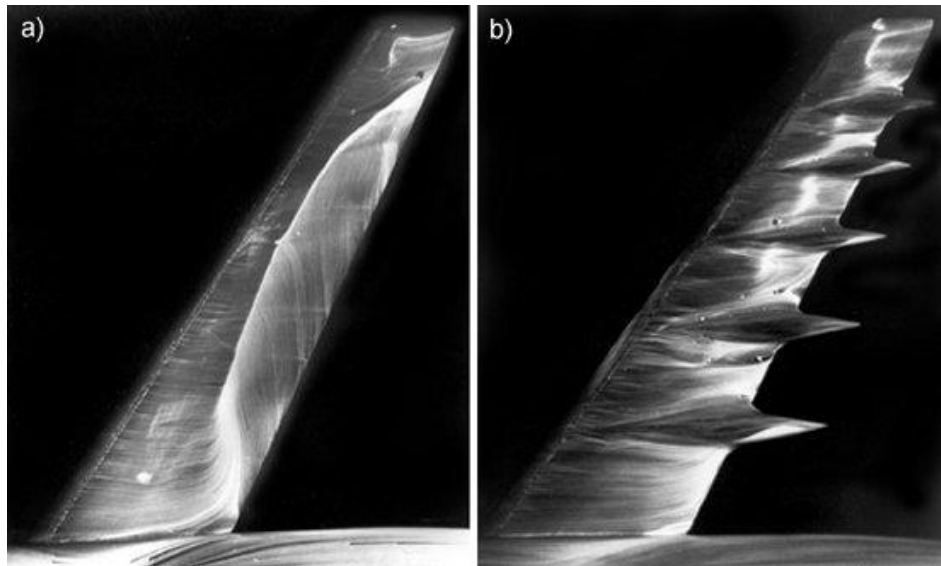


Figure 31: Area-ruled bodies

The Victor has two trailing edge bodies on the wings – referred to as ‘Kuchemann carrots’ or ‘Whitcomb bodies’ which improve overall area-ruling by sorting out a local flow

problem. These bodies break up the rear shock directly on the wing, rather than by addressing the wing/fuselage interference that causes it to form in the first place. The benefit of multiple bodies is shown in an experimental study (Fig. 32). In practice, fewer bodies were actually used; for example the Victor had only two bodies presumably reflecting a better wing/body design combined with local shock formation at the point where the crescent wing sweep changes. The modified F-102 had similar bodies positioned on the rear fuselage. More sophisticated wing/fuselage design has largely done away with the need for such ‘fixes’.



*Figure 32: a) Large region of shock-induced flow separation on a swept wing
b) virtually eliminated by trailing edge bodies*



Figure 33: Kuchemann carrots and fin bullets on the Victor

1.4 Aerodynamic Fixes

One seemingly inevitable feature of applied aerodynamics is that no matter how well a flow is ‘designed’, there will be some aspect of it that is (at best) unsatisfactory – generally through some unanticipated viscous flow effect. If detected early enough in the design process then we can re-design – but life being what it is, problems often do not become apparent until flight test. At this stage all that is left is to apply some form of aerodynamic ‘fix’ – vortex generators, strakes etc.

Two difficulties with describing implementations of fixes are that (a) having a problem with your design is rather embarrassing, so is very rarely reported outside the company, and (b) that fixes are applied in a hurry, so that their configurations are developed empirically, and again not reported upon. Within an aircraft company there will be (or was) a (proprietary) knowledge base on how to fix problems – getting hold of this knowledge is difficult and there is remarkably little in the way of design guidelines out there in the open literature!

Swept wings in particular are prone to viscous flow problems – ranging from 3D boundary layer growth and outboard ‘drift’ to tip separations at high incidence to complex 3D shock formation. Shock/boundary layer interactions leading to loss of aileron effectiveness are a particular problem, and are the major driver for vortex generator installations on large airliners. The majority of fixes will be found on the outboard sections of swept wings – but the fuselage and tail regions are not neglected, particularly on smaller commercial aircraft.

1.4.1 Wing fences

Wing **fences** are rare now, but were almost universal on early swept wing aircraft. Typical fences extend over the front portion of the upper surface, around the leading edge and a short distance under the lower surface. Fence heights are typically much larger than local boundary layer depth. Fences are most commonly found at around two-thirds of span.

Fence design and positioning is largely empirical – being generally based on a large number of wind tunnel tests – and their mode of operation is not straightforward. Their most obvious function is to act as a physical barrier to spanwise (outboard) boundary flow at low incidence, and to inboard spread of flow separation at high incidence.

[*NB* although the usual picture of the flow direction over a lifting wing shows inboard flow on the upper surface and vice versa on the lower surface, this is only strictly speaking applicable to a straight wing with elliptical lift distribution. For a swept tapered wing the peak suctions are out towards the tip and hence much of the wing flow on the upper surface is directed outboard rather than inboard.]

More important, however, is the vortex shed by the fence. The large fence protrudes forward out of the wing boundary layer into the freestream – the spanwise cross-flow separates off the edge of the fence to form a large vortex over the outboard wing (rotating in the opposite direction to the adjacent tip vortex) – which in turn generates additional lift. Note that in this case the vortex is large and rather far off the surface and so is not ‘re-energising’ the boundary layer (see section on vortex generators), but is acting in a similar

way to a delta wing vortex by inducing an increased suction on the upper surface. It also presents a ‘boundary’ between the inboard and outboard flows.

The effect on aerodynamic behaviour at higher incidences is large, but (surprisingly) there appears to be little or no lift or drag penalty from single-fence installations. The way in which the fence vortex interacts with the outer wing flow is complex, and depends strongly on whether or not tip separation is present. In general maximum lift is increased and pitching moment behaviour at the stall improved. Fences can also act to maintain flow symmetry on an aircraft, preventing wing drop at the stall or roll unsteadiness at high incidence.

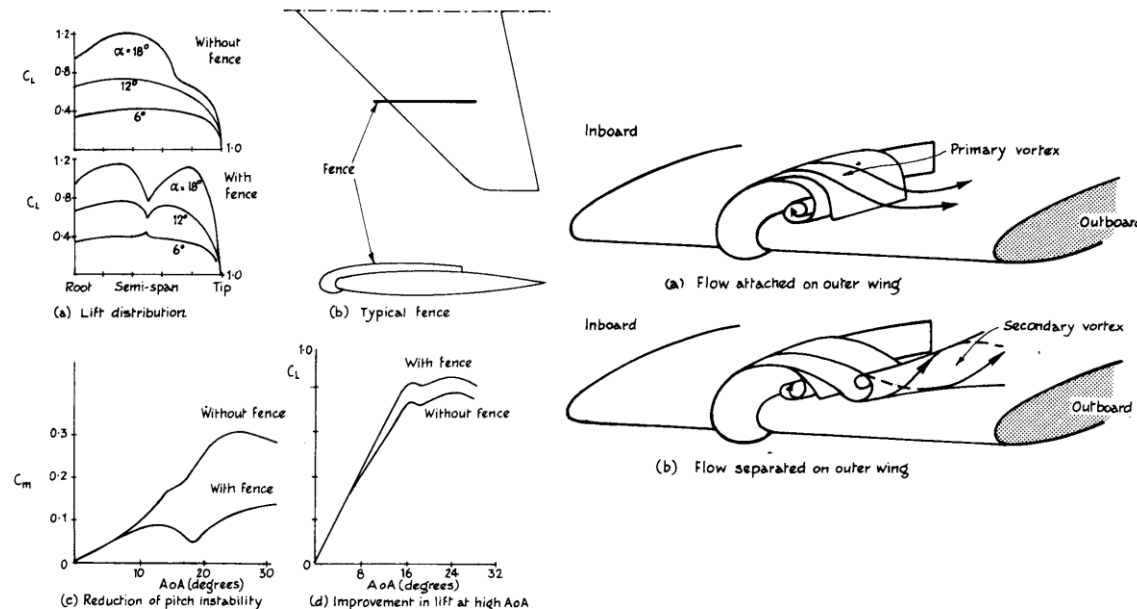


Figure 34: Wing fence operation on Hawk (from Whitford)

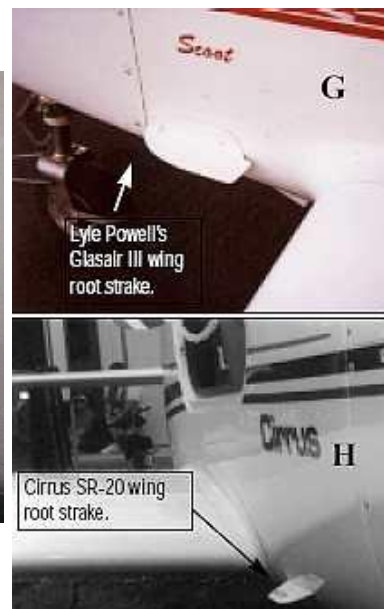


A typical swept wing installation has the fence at around two-thirds of the span, but other positions are seen. At the two extremes, the VC-10 has a very large fence at the wing root and the Embraer RJ-135 a small fence at the wing tip. I have no information on the reasons for these configurations – presumably the VC-10 fence is acting to suppress a separation over the root fillet, while the RJ-135 fence will act as a sort of winglet. It

should be pointed out that the RJ-135 tip also has a set of vortilons at the leading edge and a row of vortex generators, suggesting that Embraer had some real problems with the flow there!

The **vortilon** is a variation on the wing fence, consisting of a small streamwise forward swept surface placed just below the leading edge looking rather like an engine pylon¹² with no engine. At high angles of attack the local flow under the leading edge is outboard, meeting the vortilon at an angle and generating a large vortex which in turn wraps over the top of the wing. Since it interacts with the lower rather than the upper surface flow, the drag penalty of a vortilon at low (cruise) incidences is potentially less than that of an equivalent fence.

A surprising number of light aircraft are fitted with fuselage fences just ahead of the wing root –sometimes referred to as strakes.



A larger wing root fence can be found on the A-10, coupled with a fixed inboard slat to sort out an adverse interaction with the twin fins and aft fuselage-mounted engines.



¹² The engine pylon has the same effect on the flow as the vortilon

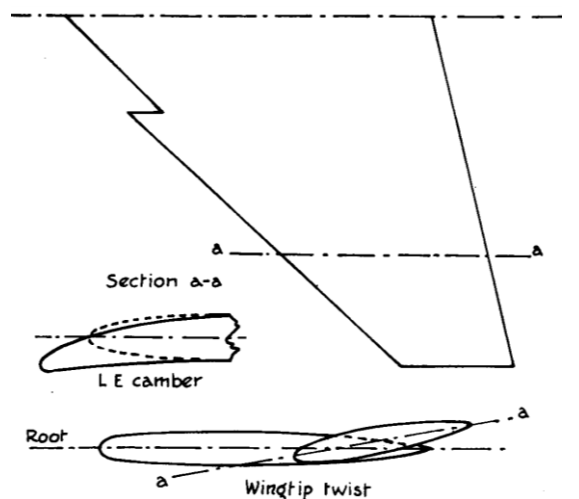
1.4.2 Leading edge discontinuities

Fences are a rather crude way of generating streamwise vortices. An alternative way is to introduce a discontinuity (step) into the spanwise lift (vorticity) distribution, since this will then manifest as a vortex (see your 2nd year Aerodynamics notes).

There are two ways of doing this:

- saw-tooth leading edge (also known as a dog-tooth, or a leading edge snag)
- leading edge notch

The **saw-tooth** essentially consists of a chord extension outboard of the point at which the vortex is required. The increased lift outboard results in a step (up) in the lift distribution, giving a counter-rotating vortex which then acts in a similar manner to a fence vortex. The leading edge extension reduces the local aerofoil thickness for reduced drag, and is often used to introduce an element of leading edge droop (= camber) to the outboard wing panel for improved stall behaviour.



Saw-teeth were common on many 2nd generation jet fighters – often introduced to address stability problems. For example, the Viggen saw-tooth compensates for pitch instability introduced by large underwing stores. Some light aircraft also use a cambered outboard leading edge extension to improve stall performance.

Alternatively, a local indentation, cut or '**notch**' in the leading-edge can be used to generate a pair of counter-rotating vortices. The strength of the vortices generated is less than for a saw-tooth, unless the outboard camber is changed to increase the lift discontinuity.

For highly swept delta wings both saw-teeth and notches can be considered as a means of sub-dividing a single leading edge vortex into two, with a new vortex system forming outboard of the discontinuity. Even a small break (such as gaps in a leading edge flap system) can partition a leading edge vortex in this way¹³. Remarkably, there is little effect on the magnitude of the vortex lift, but a considerable improvement in longitudinal and lateral stability.

It would seem obvious that leading edge breaks are not acceptable for stealth aircraft due to the apparent discontinuity. However, depending on the conditions, the opposite may actually be true. The F-22 has chamfered edges for its control surfaces (flaps, ailerons, LE flaps) which are designed in a way to scatter radiation at the 'sensitive' edge. Although the primary reason has to be RCS reduction¹⁴, there is a possibility that the front notch also proves beneficial aerodynamically. The new F-35 also has similarly designed control surfaces.

¹³ cf recent F-106 in-flight flow visualisation testing

¹⁴ Otherwise they wouldn't be at the trailing edge as well.



On the other hand, it is possible to incorporate a leading edge notch for aerodynamic reasons and address the RCS implications by using a porous surface – which can be made electrically continuous but still allow air to pass through it. A major wing drop problem on the ‘new’ F-18E/F was fixed in this manner, using a notch in the leading edge at the wing fold position.

A crude form of leading edge fix is the ‘**stall breaker**’ or ‘**stall strip**’ – a triangular cross-section strip applied along the inboard leading edge to force a root stall and therefore maintain lateral control at high incidence. These were applied to the original RAF Hawk T1, but in view of their significant drag penalty were later replaced by a multiple fence configuration. Some Mooney aircraft are also fitted with stall strips.



One unusual form of leading edge discontinuity is the very large well strake for want of a better name fitted to the Turbo Bonanza, apparently to improve aileron performance at high altitude and high incidence.



Figure 35: Leading edge ‘strake’ (?) on the Beech Turbo Bonanza

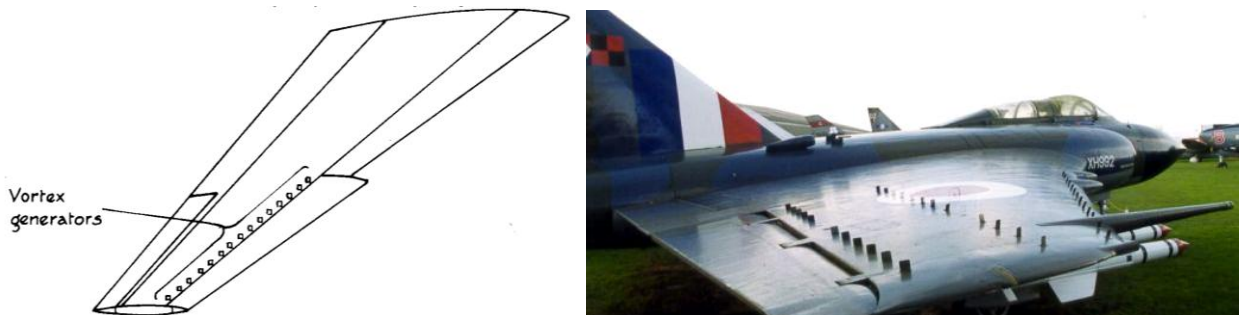
1.4.3 Boundary layer control

Boundary layer control takes a wide variety of forms – far too many to cover in detail here. All essentially aim to re-energise the low energy flow close to the surface in order to prevent separation. The modes of operation can be divided into:

- *boundary layer tripping* – forcing early transition from laminar to turbulent using surface roughness of one form or another near the leading edge (close to the point of maximum velocity to avoid re-laminarisation)
- *pneumatic* – injection of high energy air or extraction of low energy using slots or porous surfaces. Installation and maintenance a real problem, but can be made to work (cf Buccaneer)
- *streamwise vortex generation* – entraining high-energy air into the boundary layer
- *enhanced mixing* – *changing the boundary layer profile* using sub-boundary layer vortex generators or by exciting 3D instabilities using distributed roughness elements (DREs)

Commonest form of boundary layer control are **vortex generators** (VGs) – which are most often seen on the rear of swept wings (particularly in front of the ailerons) where they are intended to improve transonic flow characteristics, or on the aft fuselages of large aircraft (eg Boeing 737) where they are intended to alleviate separation over the tail (boat-tail) fairing.

VG design and positioning remains a black art, although ESDU 93024 provides a detailed description of their use in the control of shock-induced separation.

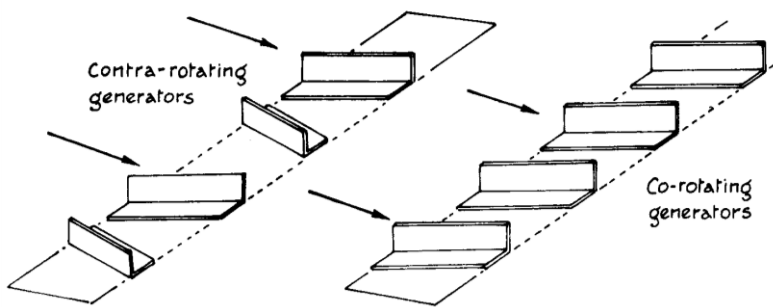


However, any situation where unwanted boundary layer separation occurs (or is predicted to occur), in the flow over an actual or project aircraft, is potentially a candidate for treatment by the application of vortex generators.

- extending the flight envelope boundary (in the C_L, M plane) imposed by unacceptable buffeting resulting from boundary layer separation of the wing flow
- removing, or reducing, wing-drop tendency resulting from boundary layer separation occurring asymmetrically over outboard parts of the wing
- alleviating pitch up tendency at high lift as a result of either (a) wing pitching moment characteristics being affected by boundary layer separation, or (b) wing boundary layer separation influencing the tailplane
- alleviating a reduction in control effectiveness resulting from flow separation occurring either upstream of or over the control (applied to wing, fin and tails)

- regulating the development of wing boundary layer separation to produce a steady stall progression
- increasing $C_{L_{max}}$ with flaps deflected (on thicker wing or horizontal tailplane sections) by delaying boundary layer separation
- reducing local flow separations which produce nuisance effects (eg local vibrations/noise or small drag increments)
- drag reduction (eg upswept rear fuselages)
- wind tunnel models, in order to remove or control a boundary layer separation which occurs at the test Re but not at flight Re
- controlling boundary layer separation in wide angle diffusers

The commonest form of VGs are vane devices, consisting of arrays of angled vanes set to produce either contra-rotating or co-rotating vortices (usually contra-rotating). These vanes are effectively low aspect-ratio slender wings set at a high angle of attack, and have either rectangular or triangular (delta wing) planforms. If the vane angle is too high the vortices will break down too early and dissipate – vane settings are therefore a fine balance between vortex strength and vortex stability.



As devices intended to re-energise the boundary layer, vane VG heights are typically of the order of the local boundary layer depth. One supplier of VGs for light aircraft states that VGs sized to be $\sim 80\%$ of the boundary layer depth avoid problems with icing. Hoerner suggests that vane-type VGs applied to the upper surface of an aerofoil have the following properties: a height/chord ratio h/c of 0.01, a length/height ratio l/h of 2, a lateral spacing/height ratio y/h of 6, and be angled at 15° to the flow.

VGs exact a drag penalty which will be largely independent of lift – vortex drag at low speed, and wave drag in supersonic flow. For high-subsonic cruise this is more than offset by the improvement in transonic drag rise (due to reduced boundary layer growth aft of the rear shock) – elsewhere the drag penalty is prohibitive, hence the relative paucity of wing VGs on supersonic fighters. Drag effects at subsonic cruise speeds will depend on the basic efficiency of the wing design – a good aerofoil will not need them!

VGs have however become rather popular as ‘add-ons’ on many light aircraft, because of the improvements in stall speed/behaviour and (when fitted on fins) engine-out performance. These installations can easily end up being rather over the top (as with most add-on modifications), with a row of VGs spanning the entire wing. Being aimed at delaying (trailing edge) stall on relatively thick wings, these VGs tended to be mounted well forward on the wing.



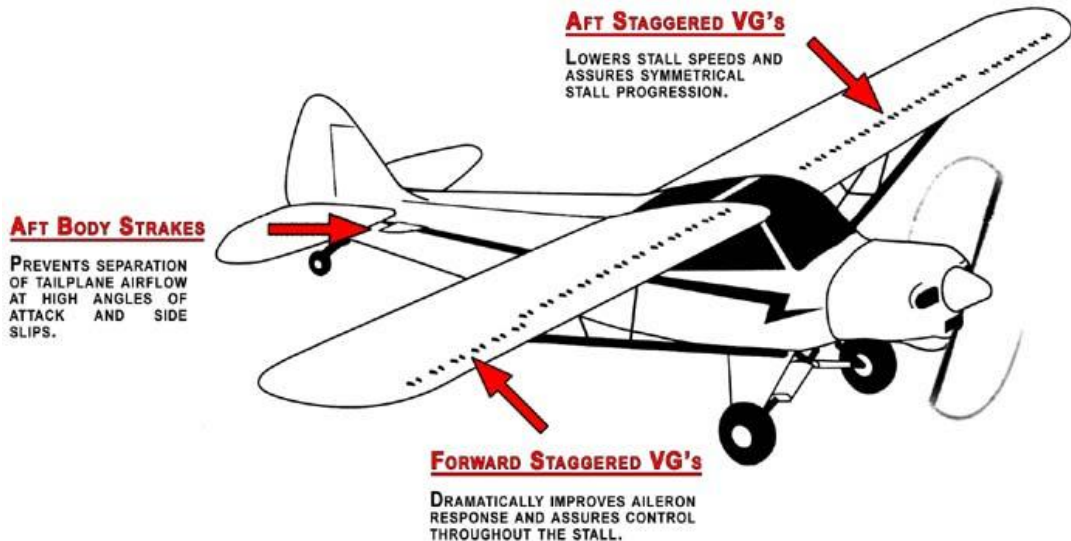


Figure 36: Example of VG + strake modifications for 'STOL Super Cub'

Recently, **sub-boundary layer VGs** have been developed, consisting of surface-mounted angled wires of a similar height to the laminar sub-layer – acting to modify the profile rather than entrain flow. Although aerodynamically less effective the high-speed drag penalty is greatly reduced, and the devices are sufficiently small to be actuated using MEMS technology.

One of the more unusual VG installations can be found on the A4 Skyhawk – which has a conventional set of VGs on the outboard wing combined with VGs (and small fences) on the leading edge slats.



Figure 37: Slats, VGs and fences on the A4 Skyhawk

Variations on the vane VG theme are air-jet vortex generators (AJVGs) and ramp VGs. AJVGs direct an air-jet perpendicular to the surface, which forces the boundary layer flow upstream to separate and form a horseshoe vortex around the jet. Angling the jet can force the vortex to roll-up into the jet and increase its effectiveness as a boundary layer control device. The advantage of AJVGs are that they can be controlled – switched off when not needed – so drag penalty can be minimised. Intermittent (pulsed) operation had been found to further increase their effectiveness.

AJVGs are the subject of significant current research effort in the UK for application to helicopter rotors and highly-curved (ie stealthy) engine intakes. However, as with all pneumatic devices air supply and control is a problem. One possibility is the synthetic jet¹⁵ (zero mass flux jet), which can generate a jet flow with no external piping.

Ramp VGs are small delta-wing-like triangular ramps which shed counter-rotating vortices from their angled edges. The ramps can be mounted in either direction – sharp end forward or backward – and can be solid, or cut from sheet and bent upwards. A similar effect can be achieved with a notch cut into the surface of a similar form to the well-known NACA inlet. Ramp VGs offer the possibility of MEMS actuation for active flow control.

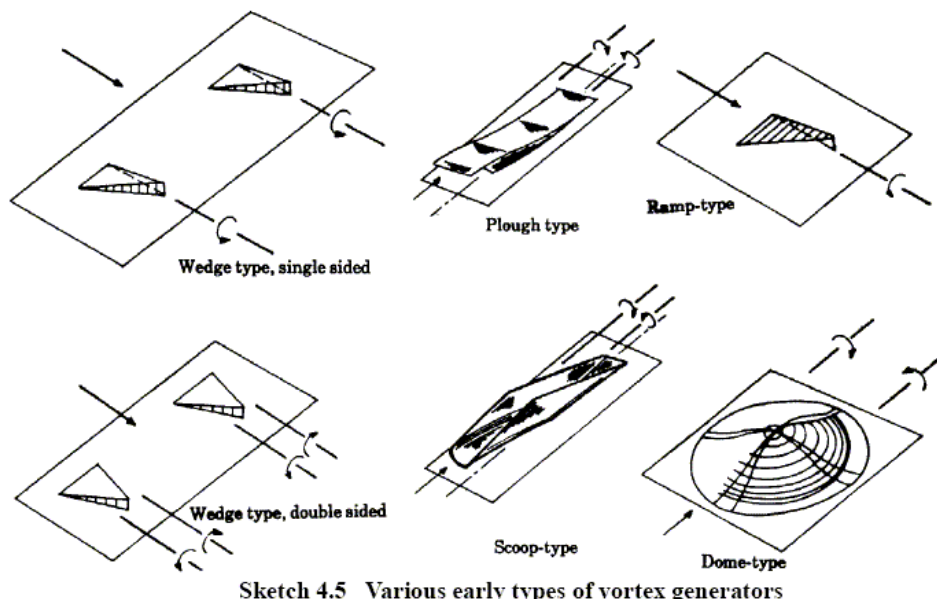


Figure 38: Some alternative VG types (from ESDU 93024)

1.4.4 Strakes

Strakes are additional (slender) lifting surfaces attached to a body (fuselage or engine nacelle). Strakes have two modes of operation:

- a) generation of lift/sideforce at the strake itself – eg forebody strake on Concorde
- b) generation of vortex to interact with downstream flow – eg engine nacelle strake on DC-10

(or a combination of the two – eg leading edge root extension on F-18)

Strakes intended to act as a stand-alone lifting surface are usually there to solve a stability problem – either pitch trim (Concorde, Eurofighter) or more commonly directional (weathercock) stability. Tail strakes perform two functions: firstly they increase basic

¹⁵ The synthetic jet uses the forced oscillation of a cavity behind a sharp orifice to generate a stream of ring vortices which in turn entrain air from the surroundings to form a jet directed away from the surface.

fin/tail area, and secondly as slender/swept surfaces they have a very high stall angle and so can maintain some fin/tail effectiveness up to high angles of sideslip/attack.



Strakes as vortex generators act in a similar manner to fences, except that they are not attached to the surface whose flow they are intended to control. For example, the strakes found on many engine nacelles form a vortex at high incidence which comes up over the wing leading edge and interacts with the wing and flaps (and/or the horizontal tail) to improve maximum lift – often counteracting a problem caused by poor design of the nacelle and pylon in the first place. Cockpit strakes on stretch versions of the DC-9 were actually intended to cure a flow problem over the fin at moderate sideslip – some 30m downstream!



‘Combined action’ strakes (also known as *leading edge root extensions* or forebody chines) are a common feature of current fighter aircraft – and are not a ‘fix’ as such since they are part of the basic aerodynamic design of the aircraft. For example, the LEX on the F-18 is an integral part of the wing – acting as a lifting surface in its own right, but also generating a vortex system which interacts with the main wing flow to greatly improve its high-lift performance. Unfortunately, the LEX vortex system also interacts with the twin tail to give a real problem with fin buffeting at high incidence. The interaction was deliberate – to improve fin effectiveness in manoeuvre – but the buffet was unexpected. The fix found (accidentally?) for this consists of a small vertical strake (or large VG) on the upper surface of the LEX which (somehow) modifies the energy/frequency content of the LEX vortex. Just as an example of how ‘fixes’ work, the fins were also strengthened

by... adding three L-shaped brackets at the roots (it was the cheapest and easiest solution!).



Figure 39: F-18 LEX (operation and solution to problem)

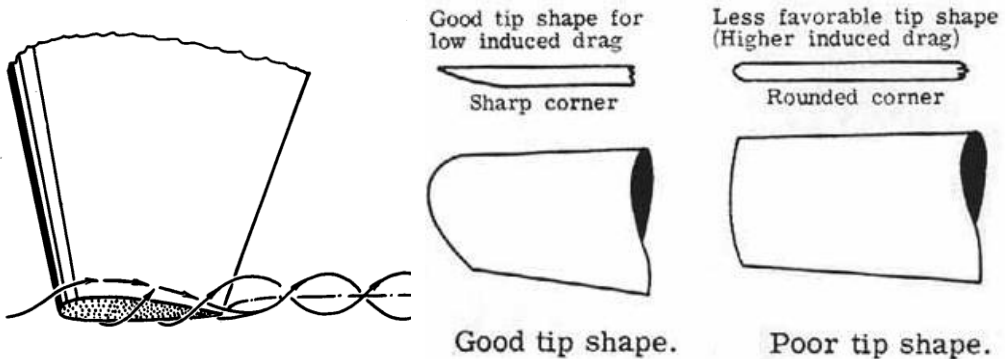
1.4.5 Wing tip shaping

Tip vortices are responsible for induced drag – so it has seemed a natural approach to drag reduction to attempt to modify the tip flow. In practice this has not been straightforward since once the wing lift distribution is close to elliptical there is not in fact much you can do ... you can't get something for nothing, and ingenious devices such as tip turbines end up generating more drag than they save.

There are two exceptions:

- devices that do improve the spanwise lift distribution – particularly on swept wings with outboard loading, and
- non-planar devices (ie winglets) – which offer the possibility of a drag improvement over the planar elliptical ‘optimum’.

Tip **planform shaping** to improve drag at low speed is almost as old as wing design – with early aircraft displaying a wide variety of tip planforms. (Although it appears that in fact relatively little can be done to improve over the basic squared-off tip). In general, tips with sharp edges perform better than rounded edges. These tips are often described as increasing the ‘effective span’ of the wing. Note that in ideal wing theory the tip vortices



form from the wake roll-up downstream of the wing – however in practice the vortex formation begins at the tip leading edge as the cross-flow separates and rolls around the tip. The resulting vortex flow over the tip region induces a local lift increment (and therefore a departure from the near-elliptical distribution predicted by lifting line theory). Low-speed tip shaping therefore appears to be largely aimed at keeping this vortex off of over the wing. In addition, by increasing the lateral distance between the tip vortices, their induced downwash is reduced.

Planforms that claim to achieve this include elliptical tips (vortex roll-up downstream), forward-swept tip (vortex roll-up outboard) and aft-swept or raked tips (vortex tracks close to tip edge). Raked tips also have a structural benefit, helping to avoid aeroelastic problems (flutter) at high speed.



Tip Shape (calculated from Ref 4.8)	Oswald efficiency ϵ percent	$K : K' = 1/\epsilon$ Eqs (4-9) and (4-9b)
'Hoerner' tip sharp rear corners	80	1.25
rounded (1) (2)	(1) 75 + (2) 75 -	about 1.33 with (1) slightly more efficient than (2)
square with sharp edges	81	1.23
A sharp rear corners Rake angle A = 0° for A = ∞ 28° for A = 6 25° for A = 1 to 5	82	1.22

} (Refs 4.10, 4.21)

Figure 40: Effect of tip planform shaping (from Hoerner via Stinton)

Tip shapes are also modified at in the vertical plane, with many light aircraft tips having an upward chamfer to further shift the vortex outboard (sometimes referred to as a Hoerner tip). More recently, both up-swept and down-swept tips have become popular for high-performance light aircraft – the choice between the two being possibly aesthetic rather than aerodynamic.



Figure 41: A-10 (downswept), Katana DV20 (upswept) and PA28 (Hoerner) tips

At high speeds a curved swept tip (the Kuchemann tip) on a swept wing can assist in maintaining an infinite sheared flow (constant isobar sweep). This configuration was very common on UK jet aircraft.

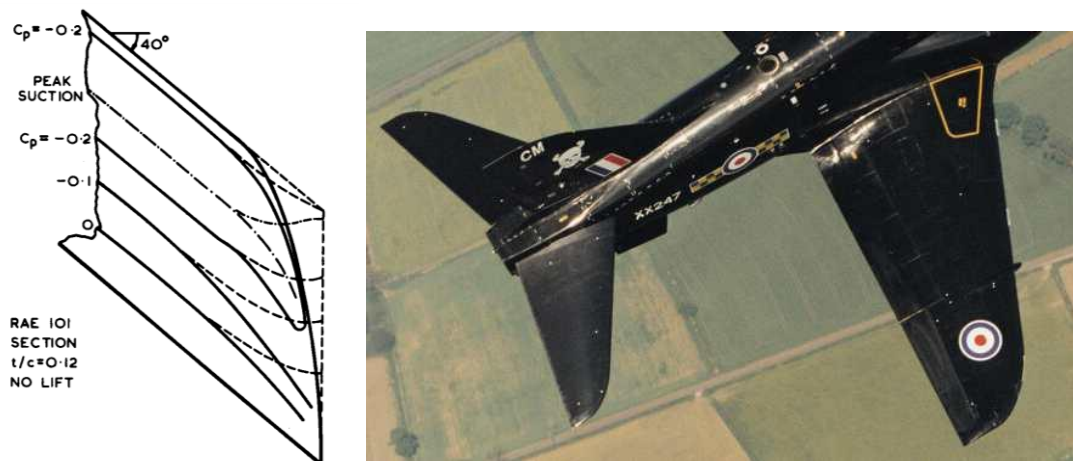


Figure 42: Kuchemann tips on Hawk wing, tail and fin

Non-planar concepts – winglets and tip-sails – operate in a more complex manner. It is often said that the local flow at the angled surfaces is such that their lift vector is angled forward – thus producing a thrust component and hence reducing drag. What is actually happening is that at their design point the net ‘sidewash’ at the winglet is zero, so that the winglet thrust associated with the wing flow is cancelled out by the winglet’s own self-induced drag. What is left is the effect of the winglet flow on the wing – with optimum design the winglet flow reduces the average downwash on the wing for a given lift level. It is this effect that reduces the overall lift-dependent drag.

An equivalent way of looking at their performance is that the winglet vortex system is partially cancelling out the main wing vortex.

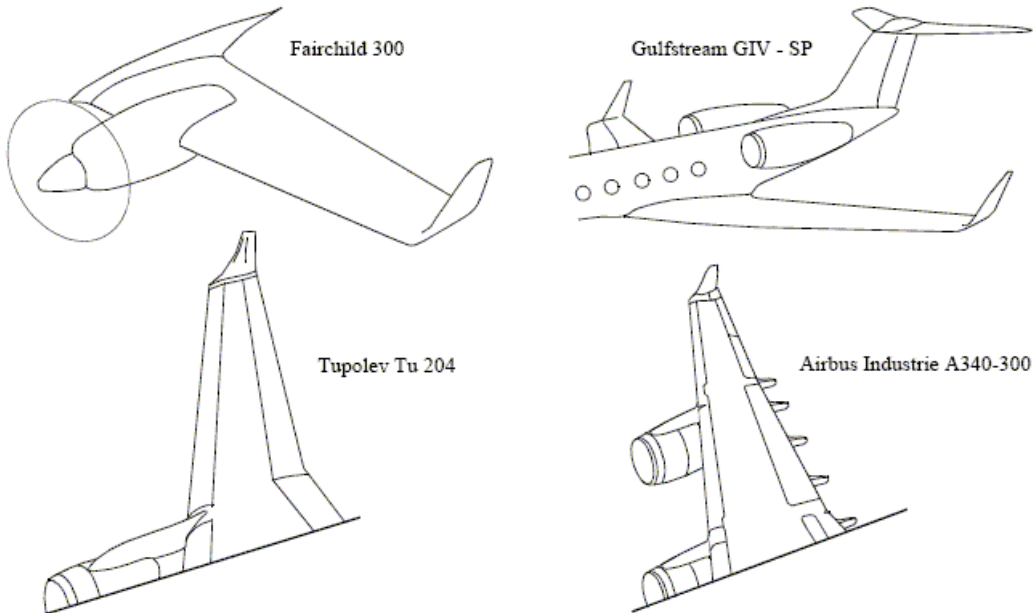


Figure 43: Upper surface winglets (from ESDU 98013)

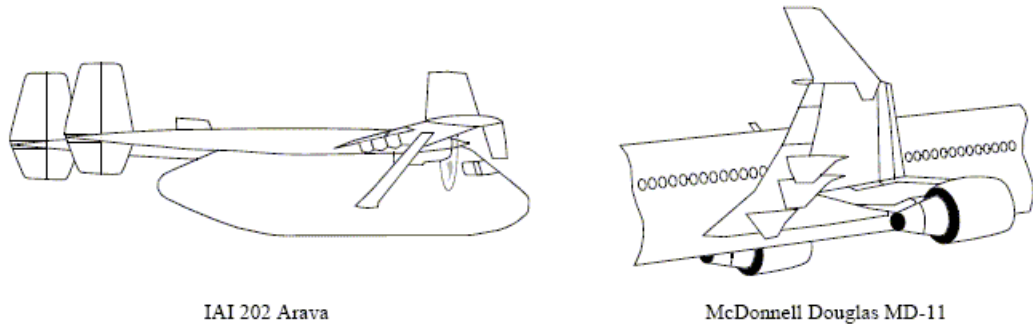


Figure 44: Lower surface winglets (from ESDU 98013)

The lift distribution on a wing designed with winglets for optimum (minimum) induced drag is no longer elliptical – however, if the tip loading is added in, the distribution does look sort of elliptical!

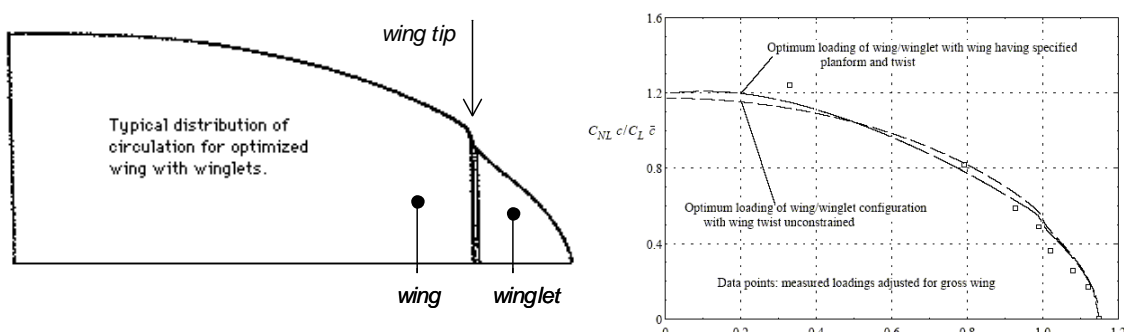


Figure 45: Loading distributions for 'optimum' winglets – theory & experiment

Two factors mitigate against widespread use of winglets: firstly, they must be properly designed (size, sweep, twist and camber) to interact with a given wing flow (get it wrong and you'll just add drag and weight), and secondly, they are only about half as effective as increasing the span by the same distance (Fig. 46).

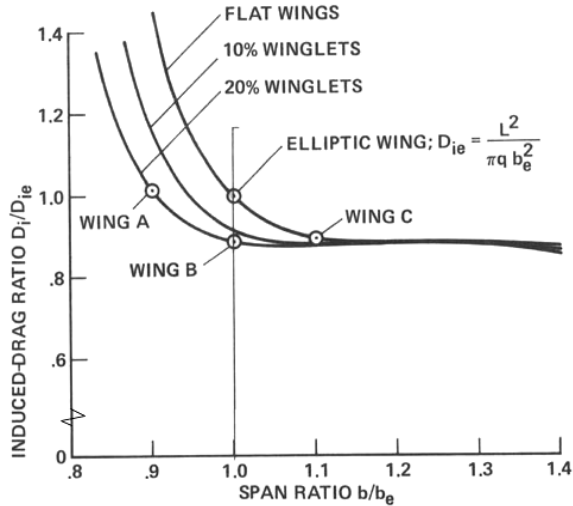


Figure 46: Winglets vs tip extensions with root bending moment constraint

Winglets only really come into their own if there is a constraint on wing span. If span itself is limited (for example by airport terminal restrictions) then winglets can improve performance significantly. If wing root bending moment is limited, then winglets (having a smaller mass & aerodynamic load moment arm) become competitive with simple tip extensions.

However, the potential improvement is small (of the order of a percent or so), and can only be achieved if the wing is designed aerodynamically and structurally with the winglet in place (cf Airbus 380). The aerodynamic/structural interactions then become rather complex, and often counter-intuitive.

For example, Fig. 47 shows the variation of induced drag and wing root bending moment with increasing winglet loading (eg due to increasing winglet toe-in) for three winglets of increasing height. As loading is increased a minimum drag point is seen, indicated by the locus A-B for the three winglets. However, the true optimum locus is line C-D, which minimises drag for a given root bending moment. In other words, for a given winglet height with loading optimised for minimum drag, there is always a more lightly loaded but taller winglet which will give lower drag for the same bending moment.

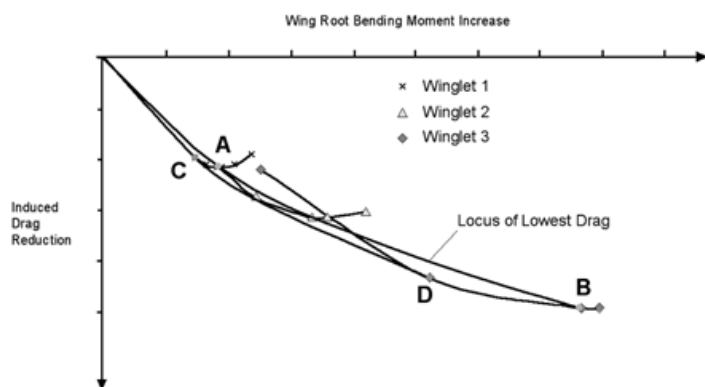


Figure 47: Winglet optimisation for various heights (Airbus)

Structural flexibility must also be taken into account, particularly for high aspect ratio swept wings. For an aft-swept wing, increasing aerodynamic loading at the tip gives increased washout as the wing bends upwards, giving the drag characteristic A-B (winglet off) in Fig. 48a. Adding a winglet reduces the induced drag, but also increases the outboard loading and hence wing washout. For a lightly loaded wing (A), both effects contribute to a drag reduction (A'). For a heavier aircraft (B) it is possible for the drag increase as the wing twists away from its optimum shape to be of a similar magnitude to the static winglet reduction, so that the improvement may disappear (B').

Wing bending in the spanwise direction will also affect the contribution of a winglet to the wing root bending moment. Figure 48b illustrates how a winglet canted outward on the ground can be raised to a vertical position in 1g cruise conditions (A), giving an increase in wing root bending moment. However, at 2.5g manoeuvre conditions (B) the combination of wing and winglet bending can be such that the wing root bending moment is actually reduced (although bending moments in the outboard sections still remain elevated).

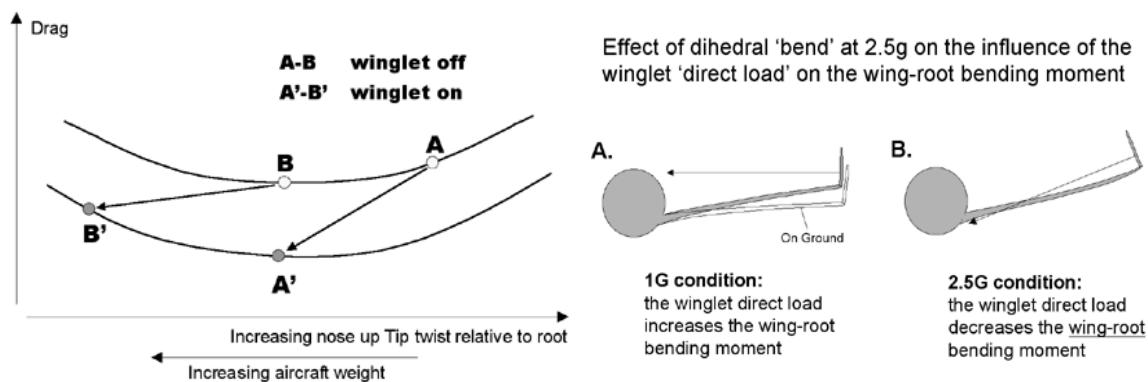
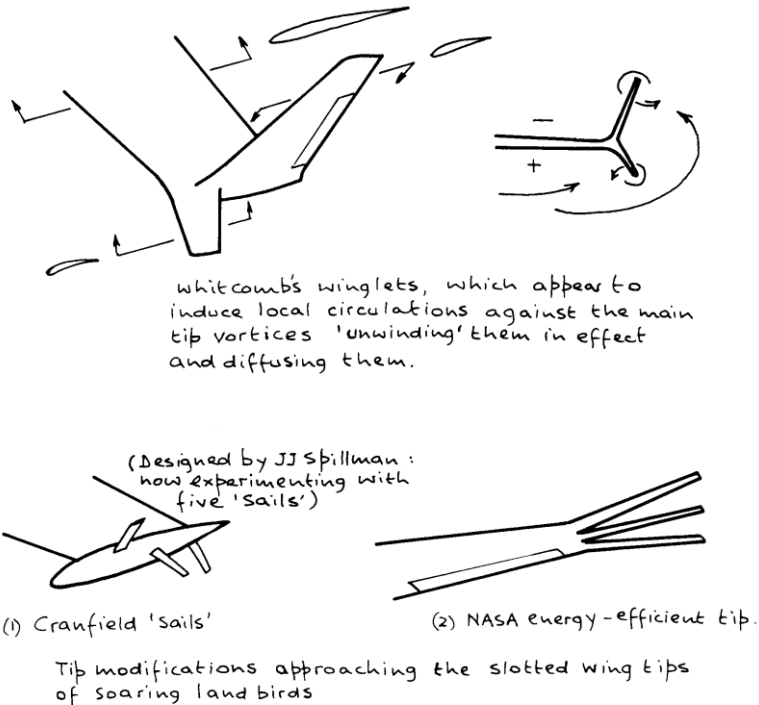


Figure 48: Effect of wing flexibility on winglet performance (Airbus)

Winglets as optional add-ons are even more controversial. While some claim not to have seen any increase in aerodynamic efficiency (Boeing claimed not to have been able to measure any difference in drag on the 737), others publish reductions in fuel consumption up to 6% (Aviation Partners on a Boeing 737!). Styling wise and from a marketing point of view they have become almost mandatory on new aircraft. Having said that, a number of airlines retrofitted their aeroplanes with winglets during the last year or so, due to increasing fuel costs.

[NB winglets also provide additional fin area, so are common on flying wing aircraft (eg BWB), and aircraft with limited tail arms (eg VariEze).]



Tip modifications are constrained by many practical considerations – in particular wing root bending moment. Any mass added to the tip will have an adverse impact on structural loads – as a result many devices can only achieve their full benefit when designed into the wing from the start. Streamwise tips are desirable on combat aircraft as a place to mount light air-to-air missiles.

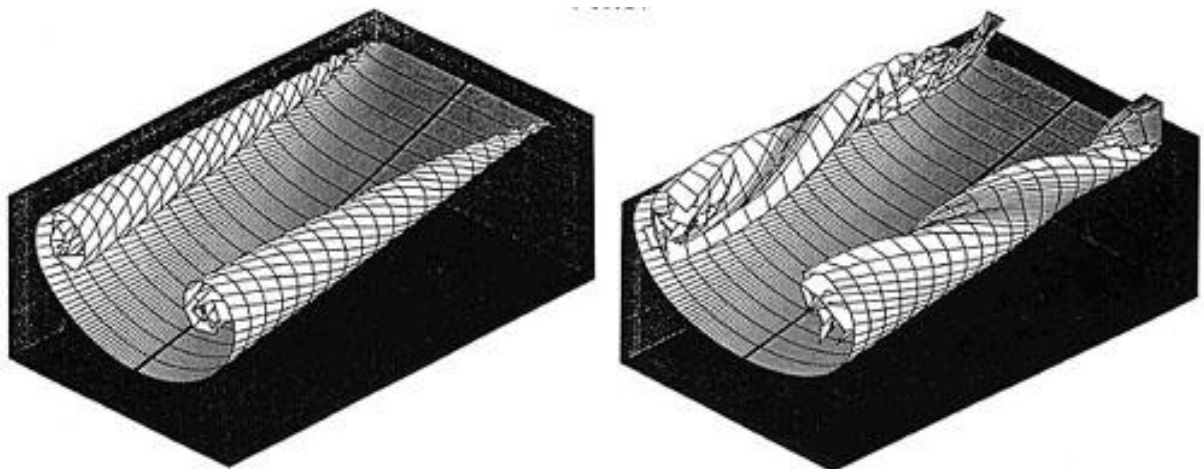


Figure 49: Planar wing wake roll-up compared with C-wing wake

Note that there may be other reasons for modifying tip vortices – wake vortex hazard for large aircraft, and environmental concerns regarding vapour trail formation increasing cloud cover for example. By altering the velocity distribution in the tip vortices it may be possible to accelerate viscous dissipation of the downstream wake. Alternatively, introducing a time-varying element into the spanwise lift distribution (ie Boeing's oscillating aileron/flap concept) can excite natural instabilities in the vortex wake system far downstream.

1.4.6 Trailing edge modifications

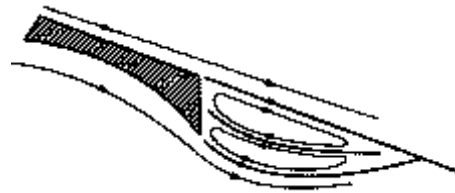
It is the Kutta condition at the trailing edge that sets the amount of lift on an aerofoil, so fixes applied in this region can have a remarkably large effect.

Most trailing edge modifications address trailing edge thickness. Many modern aerofoil design methods result in rather sharp trailing edges – which as well as the obvious structural difficulties can have an adverse aerodynamic effect. In viscous flow, the upper and lower surface boundary layers at the trailing edge can be rather deep, with the potential for local flow separation – giving (a) increased profile drag, and (b) a ‘dead-band’ in the response of the lift/pitching moment to control surface deflection.

The cure for both these is to blunt the trailing edge (and to avoid a concave profile in this region) – the adverse pressure gradient at the rear of upper surface is reduced (particularly in transonic flow as the upper and lower surface pressures are decoupled) and profile drag is reduced (by a significant margin over the corresponding increase in base drag).

On many pre-war aircraft (with fabric-covered ailerons) a common means of thickening up the trailing edge to improve control response was to glue a length of cord along it (which also served to adjust aileron trim). In more recent years, some Cessna Citation and Mooney aircraft have been fitted with a strip of metal or rubber along the rudder trailing edge to eliminate a dead-band in the yaw response (a so-called ‘deadband dam’).

In supercritical aerofoil design the upper and lower surfaces close to the trailing edge are parallel, with a fairly thick ‘cut-off’ at the base. The MD-11 actually has a slightly divergent trailing edge which served to reduce the degree of aft pressure recovery still further.



An illustration of the effectiveness of fixes applied to the trailing edge is provided by the Gurney flap – a rare example of an aerodynamic device developed (empirically) for automobile racing crossing over into aircraft applications.

The Gurney Flap is a small (<5%) spoiler-like surface mounted at the trailing edge, at an angle of 60-90° to the lower surface. The flow separation over the flap tends to turn the local flow around the trailing edge, modifying the Kutta condition and hence increasing lift/circulation. The time-averaged flow looks like a pair of counter-rotating vortices in the wake of the flap – in fact the flap generates an unsteady vortex shedding flow, but the effect is the same.

Lift increments are surprisingly large for such a small device, up to a ΔC_L of the order of 0.6 for a 2D aerofoil. The resulting nose-down pitching moment corresponds closely to the pitch/lift ratio predicted by thin aerofoil theory for small flap chord. Experimental data suggests that the aerodynamic centre moves rearward with flap deployment, increasing pitch stability significantly.

The (base) drag penalty is of the order of twice the frontal area of the flap, although in some 3D cases this can be offset by a (so far unexplained) improvement in induced drag,

so that overall L/D ratio is enhanced. The drag increase can be alleviated by reducing the flap frontal area, by:

- reducing flap height – optimum height scales with local boundary layer depth, so is dependent on Re
- angling the flap aft – a 60° angle seems to work as well as the same flap at 90°
- partitioning the flap – for example a triangular serration halves the frontal area but appears to have little impact on lift increment

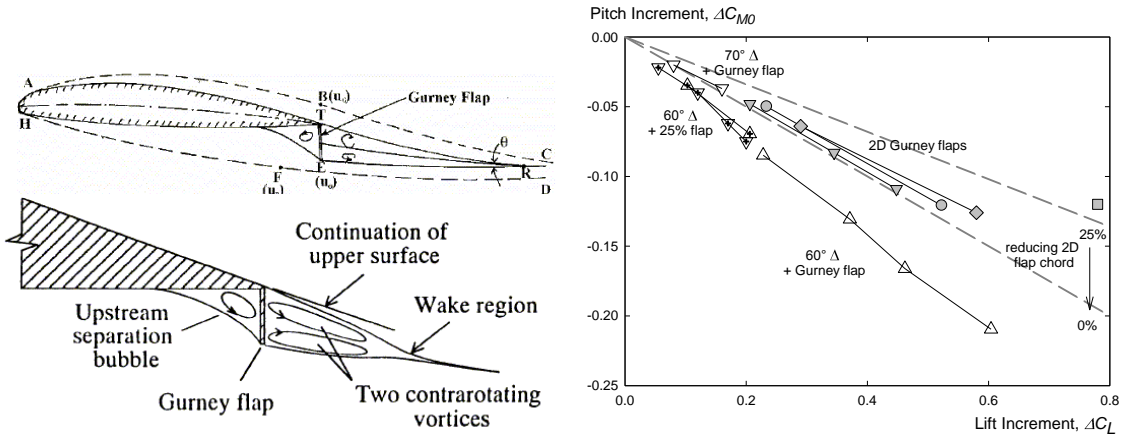


Figure 50: Gurney Flap flow and performance

Gurney Flaps are in common use on F1 car wings, where the drag increment is not important but the lift increase is. In aeronautical applications, Gurney flaps are used on helicopter tails as trim devices – but where they are starting to become of interest is as additional control surfaces on airliner wings (the flaps are small, and so can be easily actuated). US work is looking at an array of flap-like surfaces (MiTEs) along a wing trailing edge actuated at high-speed to control wing aeroelastic response (ie buffeting or gust response). In Europe the Airbus AWIATOR project worked on distributed Gurney flaps (TEDs) on an airliner wing as means of control of the spanwise lift distribution and hence optimising drag in different flight regimes.

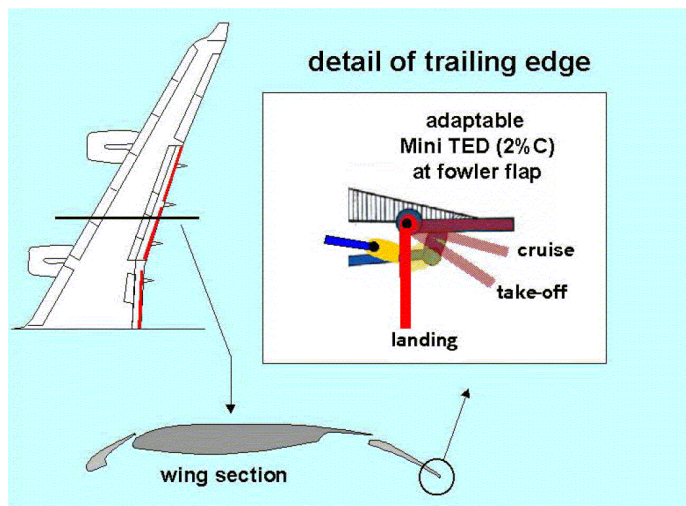


Figure 51: AWIATOR Gurney Flap installation

1.5 2D Aerofoil Section Design

1.5.1 Aerofoil geometry

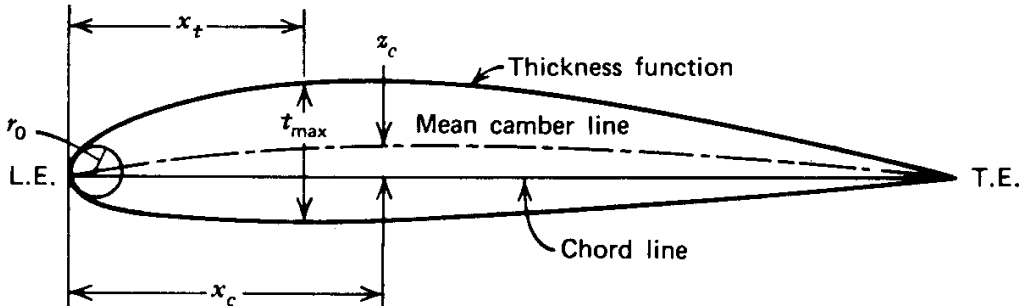


Figure 52: Basic aerofoil geometry

1.5.2 Historical

Previous to the early years of the 20th century development of aerofoil sections was almost entirely empirical. Most early workers (from Cayley onwards) used flat plate sections combined with very low aspect ratios – presumably for structural reasons – so their lack of success does not seem surprising!

The importance of camber appears to have first been recognised in the late 19th century, with Phillips in the UK building the first wind tunnel to test very highly cambered sharp-edged sections and Lilienthal in Germany using a whirling arm rig to test bird-like cambered sections. The Wright brothers were greatly influenced by Lilienthal and used similar thin, highly-cambered sections for their aircraft.

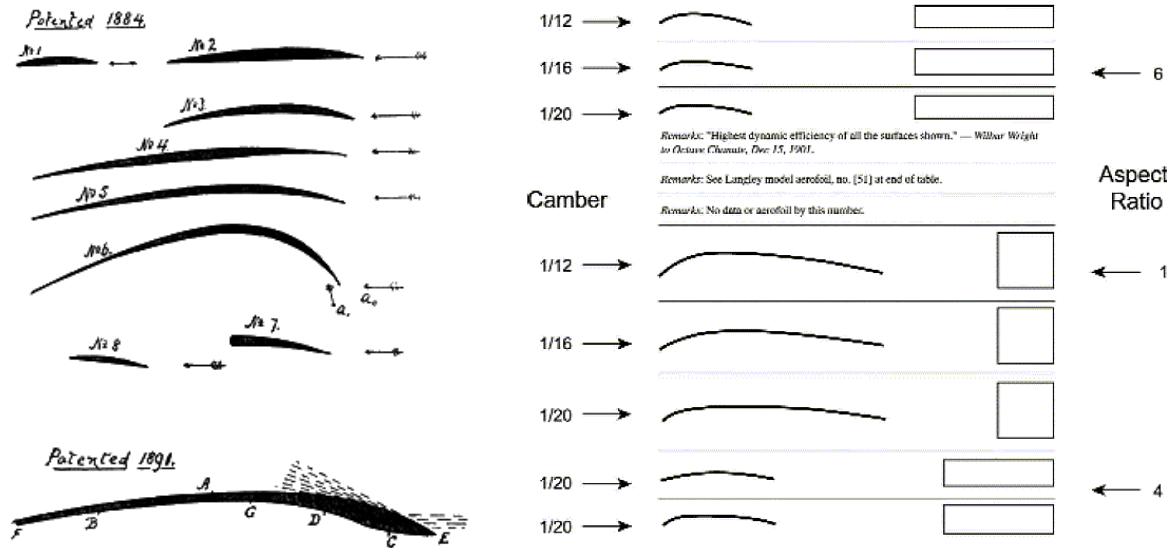


Figure 53: Examples of Phillips and Wright aerofoil sections

The mistaken idea at that time that aerofoil sections had to be thin appears to stem from the very low Reynolds Numbers achieved in wind tunnel testing (and to some extent in flight!). At these conditions very thin sections perform better (at least in terms of lift) than

thick sections due to the nature of the flow at pre-stall incidences – limited leading edge separation vs extensive (laminar) trailing edge separation.

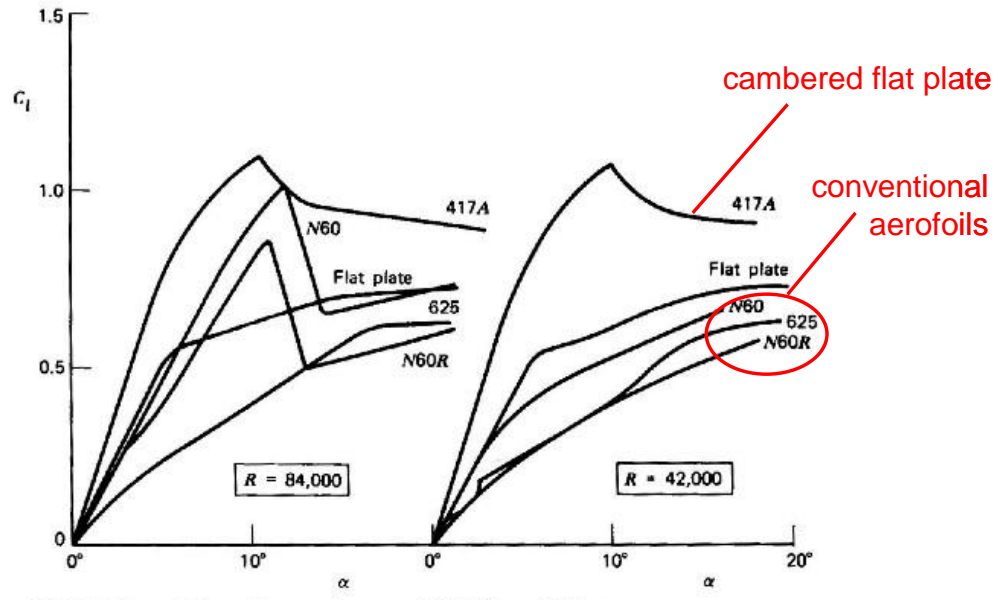


Figure 54: Superior performance of flat plate aerofoils at low Reynolds number

Having selected a thin section, a high degree of camber then improves cruise performance by limiting the extent of leading edge separation with the leading edge pointing into the flow at the cruise incidence.

The 1st World War saw the appearance of thicker aerofoils, based on a better understanding of the flow physics, better wind tunnel facilities and the need for high performance (improved structure = less external bracing = low drag).

Practical section design continued to be rather ad-hoc, with the exception of the Gottingen series of aerofoils from Germany. Beginning with simple Joukowsky aerofoils in 1912 a large parametric study was undertaken which led to the thick aerofoil sections characteristic of later WW1 German fighter aircraft.

[NB Joukowsky sections (ie those given by a conformal transformation of the flow round a circle) were attractive because of the existence of an analytical solution for the flow around them – however the cusped trailing edge made them rather inefficient in practice. More complex transformations were later developed (eg the Theodorsen transformation) that gave finite trailing edge angles, and have been used in Eppler's well-known design code 'Profil' – possibly no other practical application.]

Post-war, a number of similar aerofoil sections had emerged as being reasonably efficient – the Clark Y and the Gottingen 398 amongst them. These aerofoils had thicknesses of the order of 12-14%, cambers of the order of 3-5% and a lower surface that was (nearly) flat over an appreciable distance. The latter feature was of some practical significance, giving a simple reference line for incidence and permitting wings to be built-up on a flat surface (making the Clark Y a popular shape with model builders to this day!) ... unfortunately,

the angular offset of the lower surface from the true chord line has also led to generations of confusion about twist and (under)camber.

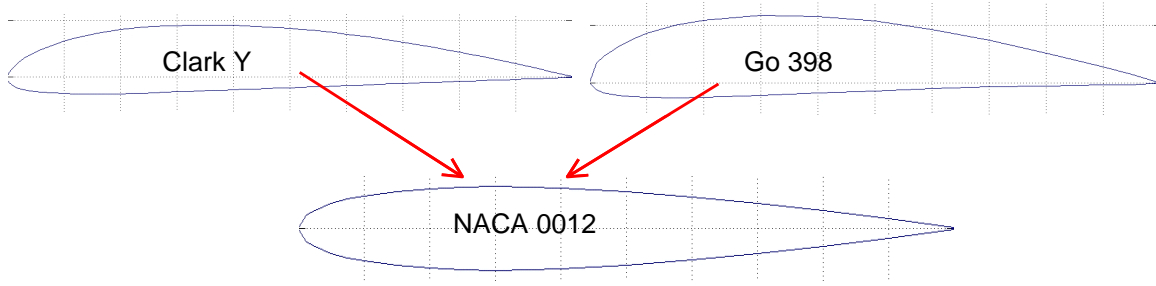


Figure 55: Derivation of NACA 4- and 5-digit profile from Clark Y and Go 398

1.5.3 NACA 4 and 5-digit aerofoils

By this stage thin aerofoil theory (see your 2nd and 3rd year Aerodynamics notes) had made it possible to select the shape of the chord line (ie degree of camber and position of maximum camber) on the basis of some desired aerodynamic performance. Since thin aerofoil theory says nothing about section thickness, and the most successful aerofoils of the day were found to have very similar thickness distributions, NACA in the 1920's took an average (!) of these thickness distributions and applied this to a parabolic mean (or camber) line to give the famous **NACA 4-Digit** series of aerofoils. The basic thickness distribution has its maximum thickness at 30% chord and a leading edge radius $r_t = 1.1019t^2$.

The mean line for these 4-digit aerofoils in fact consisted of two parabolic arcs joined at the point of maximum camber (implying a break in the surface curvature at this point – corresponding to a local discontinuity in theoretical pressure distributions!).

The numerical designation of these aerofoils indicated the geometry – the 1st digit giving the camber (maximum offset of the mean line) as a percentage of the chord, the 2nd digit the position of maximum offset in tenths of the chord, and the 3rd and 4th the maximum thickness as a percentage of the chord. Thus for example the still common NACA 2412 (eg Cessna 152 and 172) has 2% camber at 0.4c from the leading edge and is 12% thick.

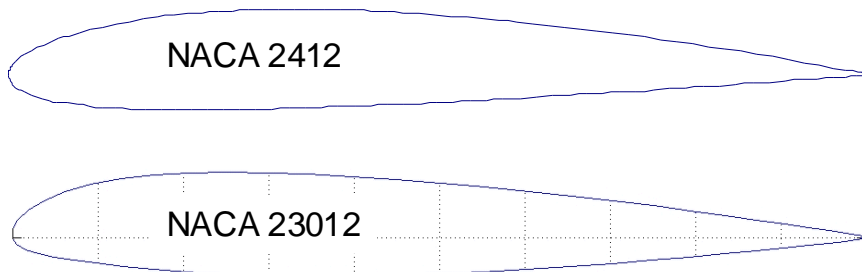


Figure 56: Two typical 12% thick cambered 4- and 5-digit aerofoils

Some 4-digit aerofoils had thinner (sharper) and blunter nose sections, denoted by a *T* or *B* suffix. Reflex camber lines (to reduce zero-lift pitching moment) were also developed, denoted by numbers of the type $2R_112$ or $2R_212$ where the subscripts 1 and 2 indicate

small positive and negative moments respectively. The 1st, 3rd and 4th digits denote the degree of camber and thickness as before.

NACA undertook a very comprehensive parametric wind tunnel test programme on these (and later) aerofoil designs and made the performance data freely available – resulting in the almost universal application of them in aircraft design in the inter-war years. Cambered 4-digit aerofoils such as the 2412 and 4412 have relatively high maximum lift and docile stalling behaviour. Combined with gradual changes in drag and pitching moment with lift, these characteristics have made the 4-digit aerofoils popular for light training aircraft which are required to fly in a wide range of conditions.

Symmetric (and rather thinner) 4-digit sections (eg NACA 0008) are still to be found on many aircraft empennages, particularly the fin where the performance at very low incidence (= sideslip) is similar to more sophisticated aerofoils – an example of industry inertia more than anything else.

The 4-digit aerofoils were soon followed by the **NACA 5-Digit** series. The same basic thickness distribution was used, but coupled with a more sophisticated definition of the mean line as a combination of a cubic curve at the front blended into a straight line at the rear, with no break in curvature.

In particular, each 5-digit aerofoil had a *design lift coefficient*, at which value the slope of the mean line at the leading edge is equal to the flow direction just ahead of the nose – in other words the aerofoil nose is pointing into the flow in an attempt to reduce form drag at the cruise incidence. Maximum camber for 5-digit aerofoils is rather further forward than for the 4-digit aerofoils, in an attempt to improve maximum lift. This was successful, but at the expense of poorer stall behaviour that is also rather sensitive to scale effects. As a result, for wings where high-lift performance is a requisite a 5-digit root aerofoil is often combined with a 4-digit aerofoil at the tip.

Once again the numerical designation of these aerofoils indicated the geometry, but in a rather more complicated way. The 1st digit is 2/3 of the design lift coefficient in tenths (and also the approximate camber as a percentage of chord). The 2nd and 3rd digits indicate the position of maximum camber – but at half this number in terms of percentage of the chord! Finally, the 4th and 5th digits simply give the maximum thickness as a percentage of the chord. Thus for example the very popular NACA 23012 has a design lift coefficient of 0.3 (= 3/2 x 2/10), has its maximum camber at 0.15c from the leading edge (= 30/2) and is 12% thick. *Don't ask why they did it this way...!*

The most important modifications to both the 4- and 5-digit series aerofoils were a set of systematic variations of the thickness distribution, designated by two further digits after a dash, where the 1st digit denotes a change to the nose radius of curvature which varies with the square of this integer¹⁶ and the 2nd digit the position of maximum thickness in tenths. So for example the NACA 0012-34 is a 12% thick symmetrical aerofoil with a reduced (sharper) nose radius and maximum thickness at 40% chord. Note that if the second digit is 3 the maximum thickness is at 30% (as in the standard 4-digit aerofoil) but the thickness distribution is *slightly different*.

¹⁶ ($r_t = 1.1019(tI/6)^2$ with $I = 0 - 8$. Therefore, $I = 0$ for a pointed LE, 3 for $\frac{1}{4}$ of the baseline radius, 6 for the baseline radius. For $I > 8$ the variation is arbitrary.)

1.5.4 NACA 1 and 6 series aerofoils

Starting in 1939, NACA began producing a series of aerofoil sections designed specifically for low drag – attempting to maintain laminar flow over the forward section of the aerofoil by retaining a favourable longitudinal pressure gradient for as long as possible. Although very successful in wind tunnel tests, real-life surface conditions (roughness, dust, insect contamination, icing) precluded any significant laminar flow in flight; nevertheless, these aerofoils performed well, with good high-speed (critical Mach number) characteristics.

The **1-series** aerofoils were designed with a thickness distribution intended to give a low velocity maximum (suction peak) at a relatively far aft position in order to maintain a favourable pressure gradient over the forward half of the aerofoil. Maximum thickness is therefore rather further aft than for the empirically designed 4- and 5-digit aerofoils. The corresponding camber line was designed to produce a constant pressure difference Δp across the aerofoil (equivalent to a constant chordwise vorticity distribution $\gamma(x)$ – see your 2nd year Aerodynamics notes), again to avoid high velocity regions.

This combination of thickness distribution and camber line makes the 1-series aerofoils popular for both marine and aircraft propellers – in the former case because of the avoidance of *cavitation* (formation of bubbles in low pressure regions leading to excessive vibration and blade erosion when the bubbles burst), and in the latter case because of the avoidance of shock wave formation in high speed regions.

1-series aerofoil geometry is defined by five digits, as for example the NACA 16-012. The 1st digit denotes the series and the 2nd the location of the minimum pressure at zero lift in tenths of chord (ie the thickness distribution). After the dash, the 3rd digit gives the design lift coefficient in tenths (ie the maximum camber) and the 4th and 5th the thickness as before. Only '16-' designations were reported in the literature, so these aerofoils are often referred to as the *16-series*.

The **6-series** aerofoils followed on from the 1-series (the design methods used for the 2- to 5-series aerofoils not having proven terribly successful!) and have been very popular despite their lack of laminar flow in practice. Having said this, the 6-series aerofoils could sustain laminar flow over a limited range of lift coefficients, particularly at lower speeds with good surface conditions (eg well-maintained, clean high-performance glider wings) – resulting in the so-called ‘laminar drag bucket’. Avoidance of high local velocities also gives these aerofoils a high critical Mach number, but maximum lift is generally lower than equivalent 4- and 5-digit aerofoils due to lower leading edge radii. Stall behaviour tends to be worse.

The 6-series aerofoils were synthesised from thickness distributions with the maximum velocity points ranging from 30% to 60% of the chord (corresponding to maximum thicknesses from 35% to 45% of chord). Note the cusped nature of the trailing edge region (giving concave surface curvature here). A range of camber lines give piece-wise linear variations in incremental pressure differential Δp , ranging from a constant distribution ($a = 1$) to a linear reduction from leading-edge to trailing edge ($a = 0$). Intermediate values of a correspond to the chordwise break-point between constant Δp over the forward part of the aerofoil and linear reduction over the rear.

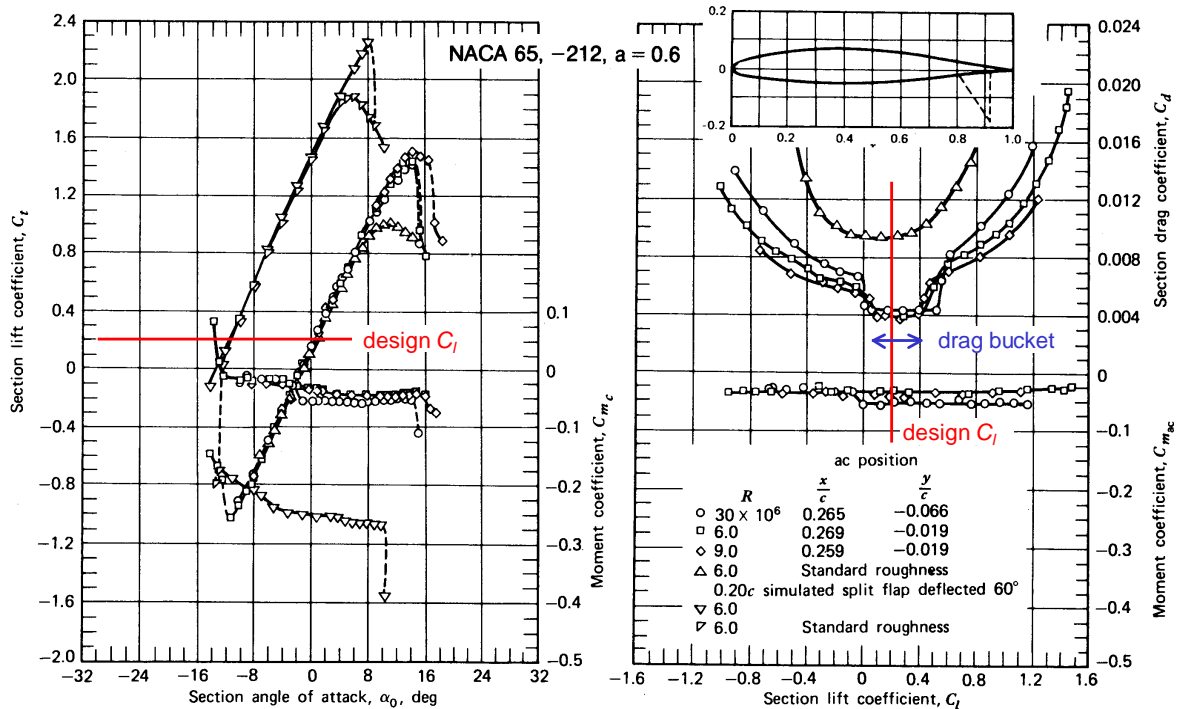


Figure 57: Typical 6-series aerofoil characteristics, showing drag bucket at design lift

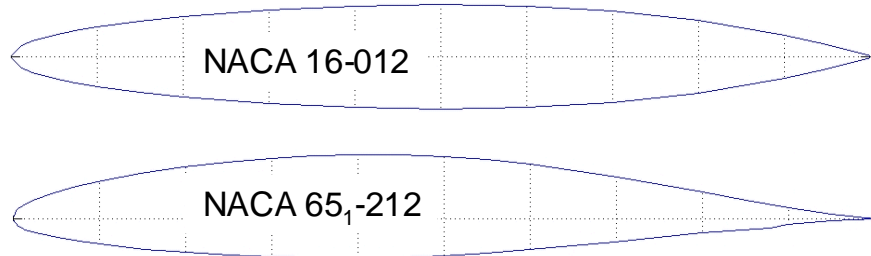


Figure 58: Two typical 12% thick 1- and 6-series laminar flow aerofoils

Basic 6-series geometry is defined by six digits, but with a number of additional parameters denoting various modifications. Taking for example the NACA 65₁-212 $a = 0.6$, the 1st digit denotes the series and the 2nd the position of maximum velocity at zero lift in tenths of the chord (as for the 1-series aerofoils). The subscript denotes the C_L range (in tenths) above and below the design lift coefficient for which laminar flow is maintained. After the dash, the 4th digit gives the design lift coefficient in tenths (ie a function of the maximum camber) and the 5th and 6th the thickness as before. Finally, the camber line form is given by the value of a (assumed to be 1 if not specified, equivalent to the 16-series camber line).

Thus in this case the NACA 65₁-212 is 12% thick, has its maximum velocity at 50% of the chord, has a design C_L of 0.2 with laminar flow maintained over a ± 0.1 range about this point. The camber line gives a (theoretical) pressure increment that is constant ahead of 60% chord.



Figure 59: Modified trailing edge on later 6-series aerofoils

Some modified 6-series aerofoils have the dash replaced by an ‘A’, denoting that the cusped trailing edge has been replaced by essentially straight upper and lower surfaces from about 80% chord – making trailing edge flap integration rather easier. The 64A series were particularly popular for 3rd generation jet fighters (eg F-15) – and are still often used as a starting point in wing design.

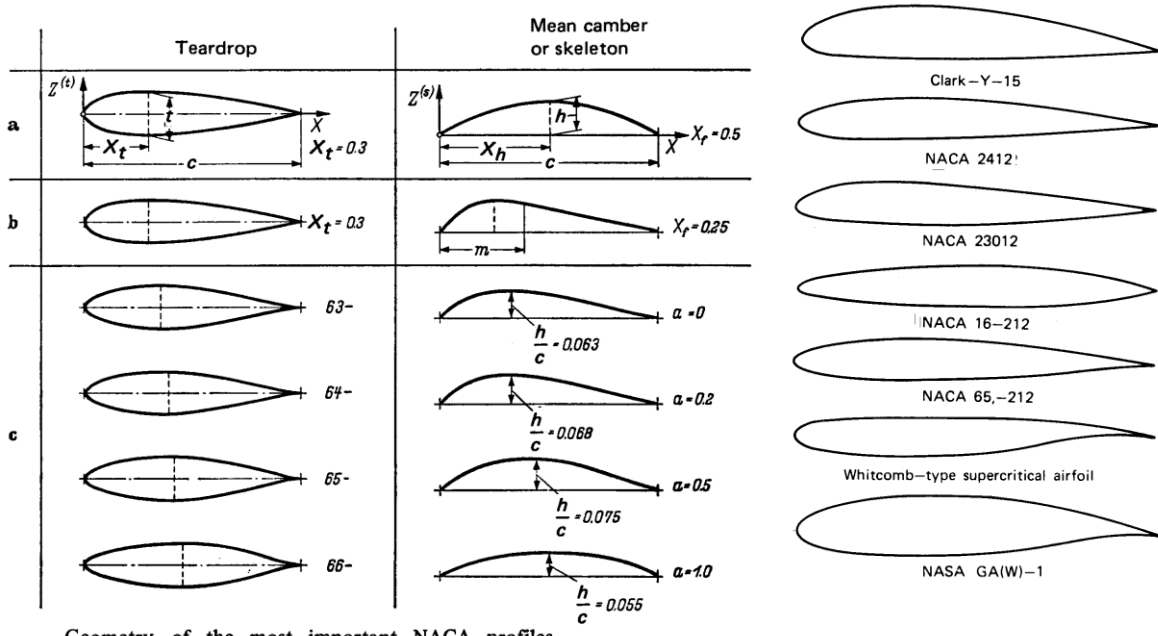
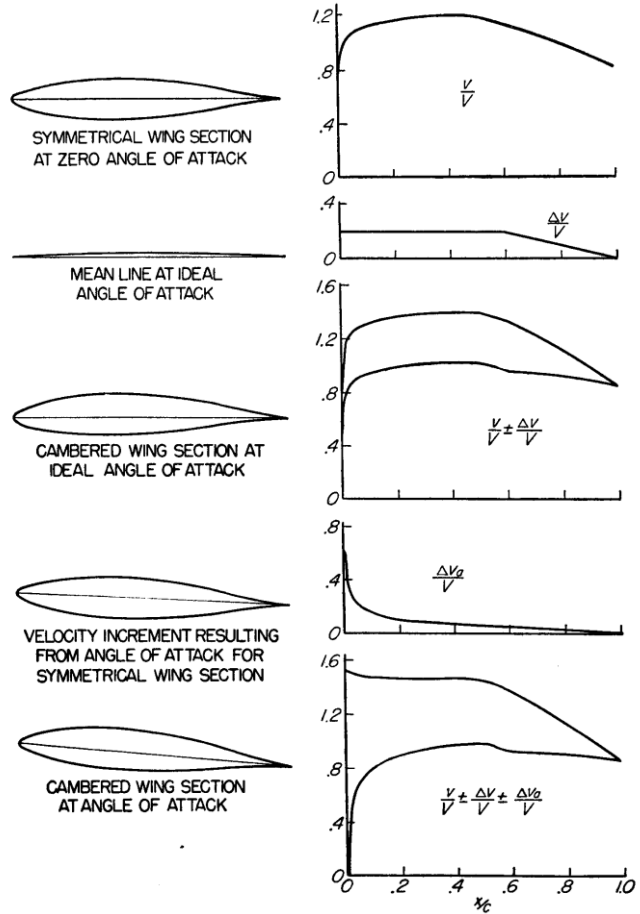


Figure 60: NACA aerofoil profiles compared

1.5.5 Pressure distributions on NACA aerofoils

The theoretical (inviscid) pressure distributions over these aerofoils can then be built up from three components:

- a (symmetric) chordwise velocity due to *the thickness distribution* (usually given as w/V – the German practice, or $(v/V)^2$ – the NACA convention). This fixed velocity can readily be calculated using a source distribution along the centreline to model the section thickness.
- a pressure difference ΔC_p between upper and lower surfaces at the *design lift coefficient* due to the *camber line shape* – can be calculated using thin aerofoil theory. This corresponds to a fixed velocity increment $\pm \Delta v/V$ (recall that camber does not affect lift-curve-slope).
- a pressure difference ΔC_p between upper and lower surfaces due to varying the incidence from the design value – this additional lift can again be calculated using thin aerofoil theory (see 2nd year *Aerodynamics notes*), and corresponds to a varying velocity increment $\pm \Delta v_a/V$.



Recall your 2nd year thin aerofoil theory – the pressure difference between upper and lower surface $\Delta C_p(x)$ is directly related to the vorticity distribution $\gamma(x)$, which in turn is related to the chordwise velocity increment $\Delta v(x)$ – assuming the increment on the upper surface is equal to the decrement on the lower surface

$$\Delta C_p = 2 \frac{\gamma}{V_\infty} = 2 \frac{v_{upper} - v_{lower}}{V_\infty} = 4 \frac{\Delta v}{V_\infty}$$

Adding the two velocity increments $\pm \Delta v/V$ (for camber) and $\pm \Delta v_a/V$ (for incidence) to the basic thickness velocity distribution v/V and squaring gives the theoretical¹⁷ pressure distribution in inviscid flow, as illustrated below.

For the **4- and 5-digit** aerofoils, the basic velocity distribution has a peak rather too close to the leading edge, giving an adverse pressure gradient over most of the aft portion of the profile. For the best combination of high C_{lmax} and low pitching moment C_{m0} a forward position for maximum camber is desirable; however, the parabolic-arc camber line of the 4-digit series gives a poor incremental pressure distribution in this case – a ‘peaky’ shape

¹⁷ This technique has got some ‘loose ends’ (not all the steps are perfectly justified theoretically) but it produces extremely accurate results for practical applications and is also very fast to implement.

with a high adverse pressure gradient just aft of the maximum camber being conducive to early separation. The compound camber lines of the 5-digit series (combining a straight line and a 3rd order parabola with no curvature discontinuity) give a much smoother distribution for the same maximum camber location.

Note that the incremental velocity/pressure distribution at the design point goes to zero at the leading edge as well as at the trailing edge. The latter is the result of applying the Kutta condition that the flow leaves the trailing edge smoothly – the former comes from applying a similar constraint to the leading edge flow so that it flows smoothly onto the wing (ie the nose is pointing into the local flow).

The incidence dependent velocity/pressure increment is given by basic thin aerofoil theory¹⁸.

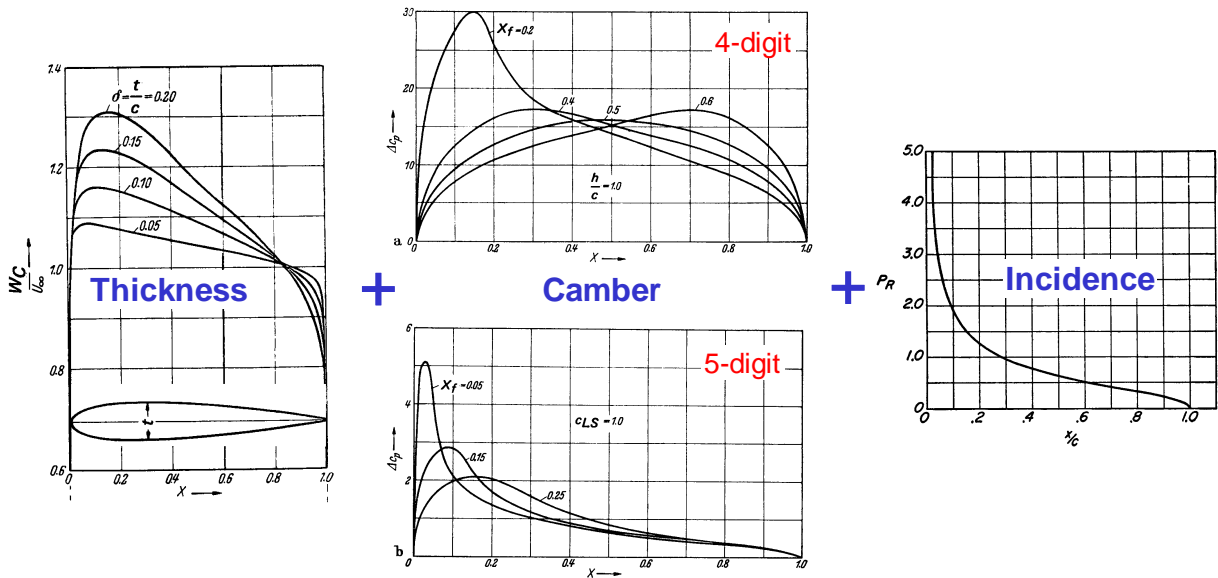


Figure 61: Pressure distribution build-up for 4- and 5-digit aerofoils

Although 2D aerofoil flows are not now designed in this manner, it is still useful to consider this three-part split when analysing or modifying aerofoil pressure distributions, particularly when looking at the impact of viscous effects.

For example, Fig. 62 compares experimental pressures for the cambered NACA 4412 aerofoil with an inviscid panel code solution at an incidence of 1.9° (well above the design incidence for this camber line). Overall, the agreement is excellent except near the trailing edge where the inviscid pressure recovery (corresponding to a stagnation point at the trailing edge) is not achieved. This is typical viscous flow behaviour, with the merging boundary layers at the trailing edge giving velocities at the edge of the BL close to freestream, so that the static pressure at the surface is also close to freestream (ie $C_{pTE} \approx 0$ rather than = 1).

¹⁸ $\Delta C_p = 2 \frac{\gamma \theta}{V_\infty} = 4\Delta\alpha \frac{1 + \cos\theta}{\sin\theta}$ with the mapping $\frac{x}{c} = \frac{1}{2} (1 - \cos\theta)$

The previous discussion suggests that this impacts primarily on the thickness contribution v/V , since all the basic Kutta condition (for the camber and incidence contributions) requires is that the upper and lower surface velocities at the trailing edge are equal (but not necessarily zero). One would therefore expect little effect on the lift curve-slope (as is the case), but a significant increase in form drag due to the fore-and-aft asymmetry in pressure distribution. Note however, that the rate of boundary layer growth depends on the lift level (as the adverse pressure gradients increase), so that the form drag will increase with lift (and camber).

There is a small reduction in lift distributed over most of the lower surface, probably due to a reduction in effective camber as the upper surface boundary layer grows more rapidly than the lower surface boundary layer (displacement thickness effect).

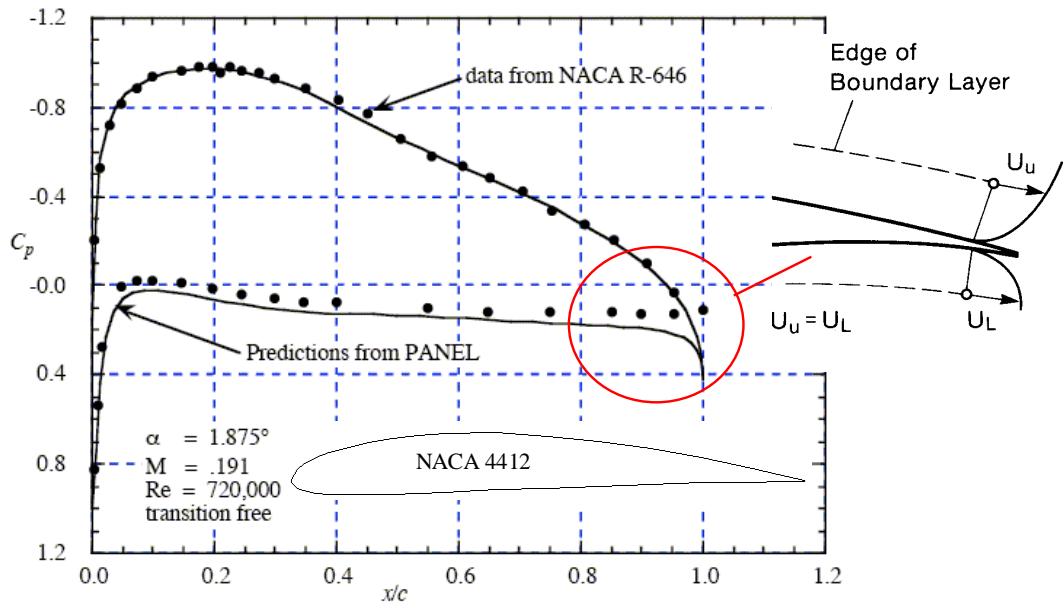


Figure 62: Theoretical and experimental pressure distributions for the NACA 4412

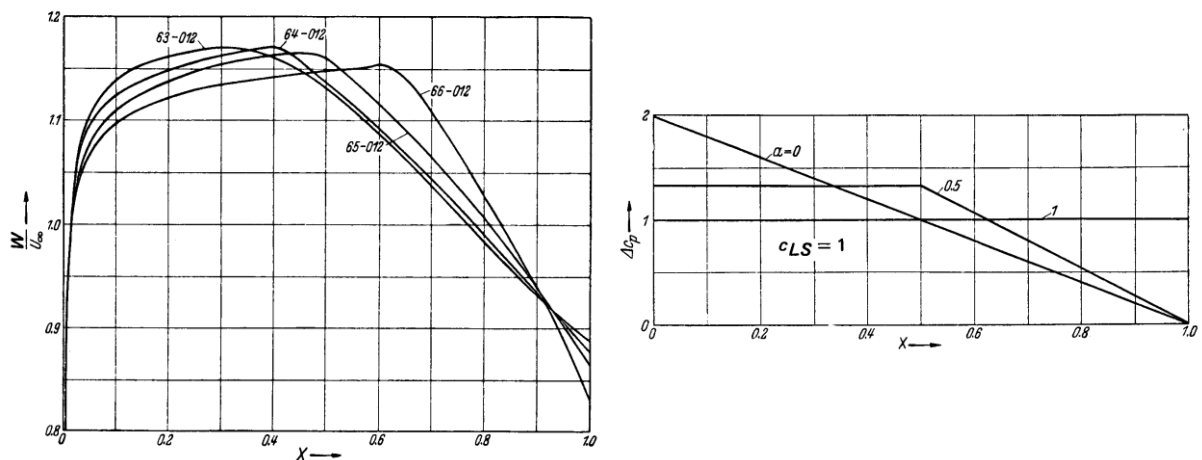


Figure 63: Typical thickness and camber contributions for 6-series aerofoils

The basic thickness contributions to the surface velocity distribution for the various **6-series** profiles shown above illustrates how different these aerofoils are from the 4- and 5-

digit profiles. The velocity peak is much further aft, with a long run of favourable pressure gradient intended to preserve laminar flow for as long as possible.

For these 6-series aerofoils the simple thin aerofoil theory for the incidence-dependent contribution was found to be inadequate – instead Abbott presents pressures for symmetric sections at zero incidence and at \pm the intended limits of the drag bucket calculated using a more accurate potential flow method. The incidence contribution $\pm \Delta v_a/V$ can then be determined using linear interpolation.

For example, the 64₂-015 profile shown below has a favourable pressure gradient at zero lift up to its velocity maximum at 40% chord. At the limit of its design envelope however (with $C_l = 0.22$) the velocity profile on the upper surface has become almost flat – so no significant region of laminar flow would be expected.

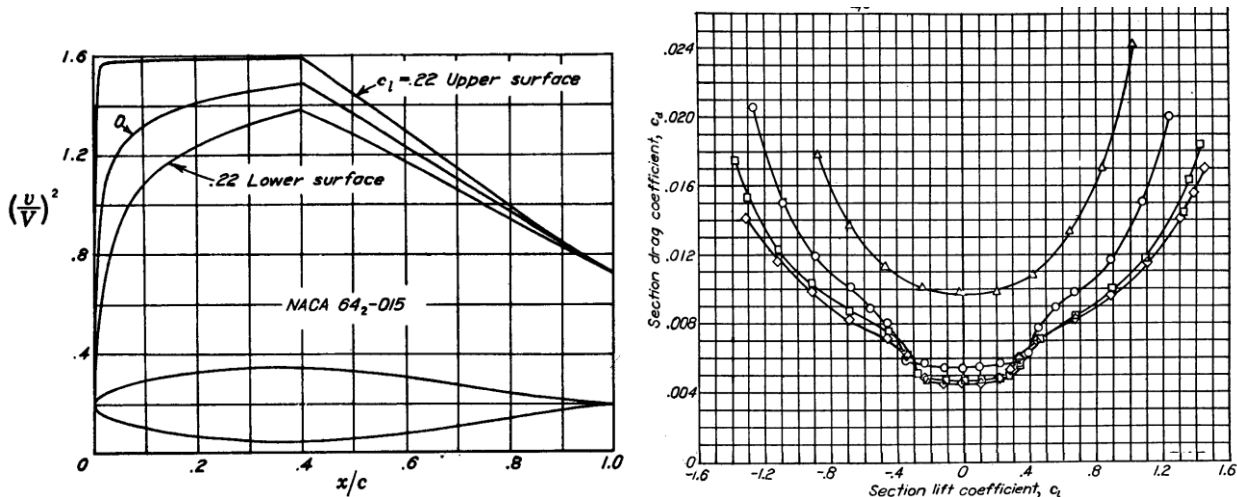


Figure 64: Theoretical surface velocity distribution at the edge of the drag bucket

The pressure increment due to camber also shown above appears to display a similar design goal. The loading is finite at the leading edge at the design lift coefficient, corresponding to a smooth on-flow (nose pointing into the local flow) for this ‘non-thin’ profile. Velocity increment $\pm \Delta v/V$ is constant over the front portion of the wing, therefore not affecting the designed favourable pressure gradient. Section data given in Abbott appears to be restricted to either $a = 1$ camber line (constant loading) or $a = 0.5/0.6$ (loading constant on forward half only) – the only effect seems to be a small reduction in nose-down pitching moment for the latter case.

Family	Advantages	Disadvantages	Applications
4-Digit	<ul style="list-style-type: none"> 1. Good stall characteristics 2. Small centre of pressure movement across large speed range 3. Roughness has little effect 	<ul style="list-style-type: none"> 1. Low maximum lift coefficient 2. Relatively high drag 3. High pitching moment 	<ul style="list-style-type: none"> 1. General aviation 2. Horizontal tails Symmetrical: 3. Supersonic jets 4. Helicopter blades 5. Shrouds 6. Missile/rocket fins
5-Digit	<ul style="list-style-type: none"> 1. Higher maximum lift coefficient 2. Low pitching moment 3. Roughness has little effect 	<ul style="list-style-type: none"> 1. Poor stall behaviour 2. Relatively high drag 	<ul style="list-style-type: none"> 1. General aviation 2. Piston-powered bombers, transports 3. Commuters 4. Business jets
16-Series	<ul style="list-style-type: none"> 1. Avoids low pressure peaks 2. Low drag at high speed 	<ul style="list-style-type: none"> 1. Relatively low lift 	<ul style="list-style-type: none"> 1. Aircraft propellers 2. Ship propellers
6-Series	<ul style="list-style-type: none"> 1. High maximum lift coefficient 2. Very low drag over a small range of operating conditions 3. Optimised for high speed 	<ul style="list-style-type: none"> 1. High drag outside of the optimum operating range 2. High pitching moment 3. Poor stall behaviour 4. Very susceptible to roughness 	<ul style="list-style-type: none"> 1. Piston-powered fighters 2. Business jets 3. Jet trainers 4. Supersonic jets
7-Series	<ul style="list-style-type: none"> 1. Very low drag over a small range of operating conditions 2. Low pitching moment 	<ul style="list-style-type: none"> 1. Reduced maximum lift coefficient 2. High drag outside of the optimum range of operating conditions 3. Poor stall behaviour 4. Very susceptible to roughness 	Seldom used
8-Series	Unknown	Unknown	Very seldom used

Table 1: Summary of NACA aerofoil characteristics (from www.aerospaceweb.org)

1.5.6 More recent aerofoil catalogues

For high-speed aircraft it is now rare to use ‘off-the-shelf’ aerofoil sections – instead 2D and 3D optimisation techniques are applied to tailor aerodynamic surfaces directly to the mission requirements (more later...).

For low-speed aircraft (and in particular model aircraft and UAVs), however, a number of theoretically designed aerofoil series continue to be produced.

The most well-known of these is probably the Eppler series of low-speed aerofoils designed using a panel code with a simple 2D boundary layer model ‘*Profil*’ (including an empirical prediction of the onset of laminar separation). *Profil* uses a combination of an accurate high-order panel code and conformal transformation to provide both inverse and direct design capabilities. Eppler’s aerofoils have been designed for a wide range of applications, from high-performance sailplanes to foot-launched gliders, and have been very popular. Although designed using simple theory, extensive testing at a number of universities (in particular Illinois and Stuttgart) has produced a large database of lift, drag and pitching moments at low Reynolds numbers for the most common Eppler profiles. Unfortunately, the numbering scheme appears to be sequential, rather than denoting any specific aerodynamic or geometric characteristics of the aerofoils. The Eppler code continues to be developed by Maughmer in the US, and has been used by Dan Somers at Airfoils Inc. to design many successful aerofoils for light aircraft and wind turbines, including the NASA NLF (‘natural laminar flow’) series of low-speed aerofoils.

Other popular low-speed aerofoil series for more specialised applications have been produced by Wortmann (1960s UAVs), Liebeck (high-lift designs) and Lissaman, but probably the most prolific aerofoil designer of recent times has been Selig at the University of Illinois, with his *S* and *SD* (D for Donovan) series. Selig’s inverse design method ‘*PROFOIL*’ is based on the Eppler code, with a cut-down version available on the web. Although not a parametric series as such (with each aerofoil designed for a specific application), the use of a reasonably meaningful numerical designation and the availability of extensive experimental data from a collaborative programme headed up by the University of Illinois has made these aerofoils very popular with model aircraft designers.

Many modern aerofoils are designed using ‘*X-Foil*’, a modern code developed by Mark Drela of similar capability to *Profil*, but with a more sophisticated coupled viscous-inviscid model for the boundary layer which can handle laminar separation bubbles (although the predictions become less reliable as separation becomes more widespread!). *X-Foil* has a less accurate paneling scheme than *Profil* and is much slower to run – but this has become much less of a problem now! A word of warning here: *X-Foil* is free for academic and private use, so is widely used by designers who do not appreciate its limitations ... just because a code predicts aerodynamic characteristics with separation present does not mean it gets them right!

Selig maintains an extremely useful website cataloguing many low and high-speed aerofoils, with a huge list of section coordinates, profile drawings, some aerodynamic data (mostly for his own aerofoils) and a growing list of aerofoils cross-referenced to aircraft they were used on.

Other smaller, more specialised aerofoil families exist (eg the NASA GA(W) general aviation or the ARA-D high-speed propeller sections), but none on the scale of the earlier NACA work, reflecting the modern trend to either (a) use custom-designed aerofoils or (b) play safe and stick to safe, tried-and-tested NACA/Eppler/Selig aerofoils.

1.5.7 Aerofoil design methods

The process of airfoil design requires knowledge of:

- the relation between geometry and pressure distribution, and
- the boundary layer properties

The goal of an airfoil design varies. Some airfoils are designed to produce low drag (and may not be required to generate lift at all). Some sections may need to produce low drag while producing a given amount of lift. In some cases, the drag doesn't really matter – it is maximum lift that is important. The section may be required to achieve this performance with a constraint on thickness, or pitching moment, or off-design performance, or other unusual constraints.

Methods for airfoil design can be classified into two categories: direct and inverse design.

Direct aerofoil design methods involve the specification of a section geometry and the calculation of pressures and performance. The shape is evaluated and then modified to improve the performance.

The simplest (and oldest) form of direct aerofoil design involves starting with an assumed shape (such as a NACA section), determining the characteristic of this section that is most troublesome, and fixing this problem. This process of fixing the most obvious problems is repeated until there is no major problem with the section.

The design of such aerofoils does not require a specific definition of a scalar objective function, but it does require some expertise to identify the potential problems and often considerable expertise to fix them. Adjustments to the aerofoil section are almost invariably aimed at alleviating viscous effects – for efficient airfoils viscous effects should be small at normal operating conditions – so a good knowledge of the interaction between aerofoil shape, pressure distribution and boundary layer behaviour is essential.

More sophisticated direct design methods have come into use recently, which involve the application of some form of automated optimisation process. Many stand-alone optimisation packages are now available which can be coupled with a CFD code for the solution of the aerofoil flow, so the difficulties with this approach are primarily concerned with:

- identification of an appropriate measure of performance (eg design lift coefficient),
- definition of constraints on both aerodynamic characteristics (eg pitching moment) and on aerofoil shape (eg structural limits), and
- how the aerodynamic profile is specified and modified.

Without adequate constraints direct design methods can produce apparently optimised aerofoil sections which are unusable – typically due to poor off-design performance or inadequate structural performance (spar depth, trailing edge thickness etc).

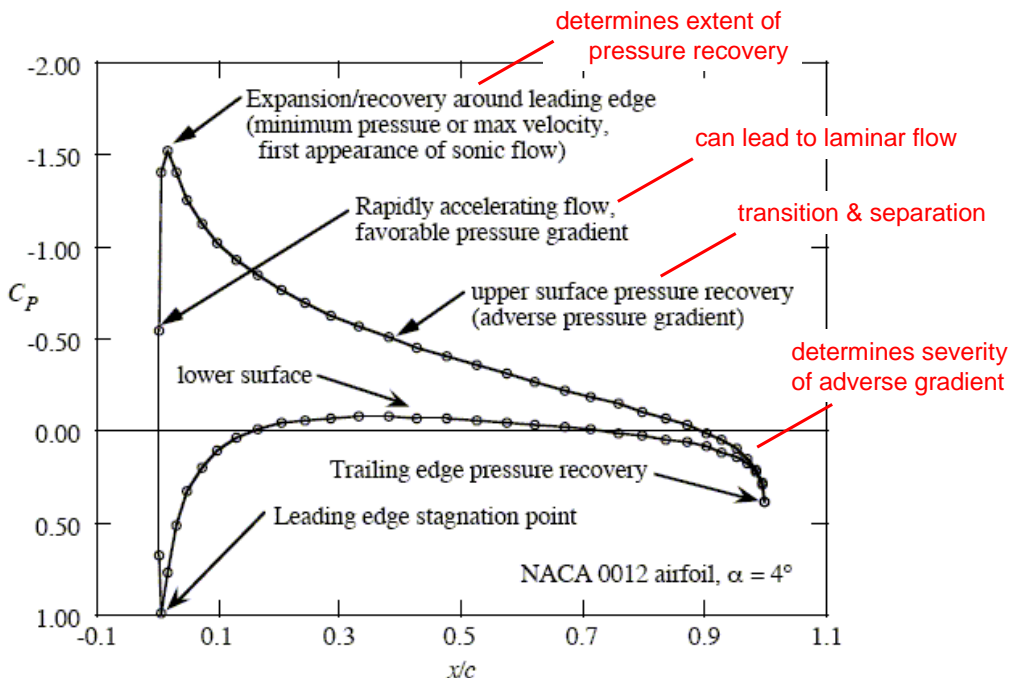


Figure 65: Areas of interest in examining aerofoil pressure distributions

Inverse aerofoil design starts with a desired pressure distribution and modifies the aerofoil shape to achieve it. This is an intermediate step between the simple direct process of modifying an existing section and the sophisticated automated optimisation design process.

Inverse design methods are relatively straightforward to implement for 2D aerofoils, from NACA applications of thin aerofoil theory through to modern panel codes with boundary layer models (eg Eppler's low-speed inverse design code, now superseded by Drela's *X-Foil* code as the current 'standard' – in the public domain for academic use). The difficulty in any of these methods is the selection of the desired pressure distribution, which will depend on the operational requirements for the section. Some of these are discussed below.

1.5.8 Laminar flow aerofoils

Laminar flow is useful for:

- reducing skin friction drag,
- increasing maximum lift, or
- reducing heat transfer.

It can be achieved without too much work at low Reynolds numbers by maintaining a smooth surface and using an airfoil with a favourable pressure gradient. At high Reynolds number some form of boundary layer flow control is generally necessary.

Design for laminar flow requires balancing two conflicting requirements:

- maintaining a favourable (negative) pressure gradient over as much of the forward part of the aerofoil as possible, and
- managing the pressure recovery from the peak suction point to the trailing edge so as to avoid separation due to the adverse pressure gradient,

which ideally should result in an aerofoil with laminar flow up to the peak suction point (reduced drag) followed by turbulent flow aft of peak suction (resistance to separation). The resulting profile drag will then lie between the theoretical values for fully laminar and fully turbulent flows (see 2nd & 3rd year Aerodynamics notes on skin friction drag).

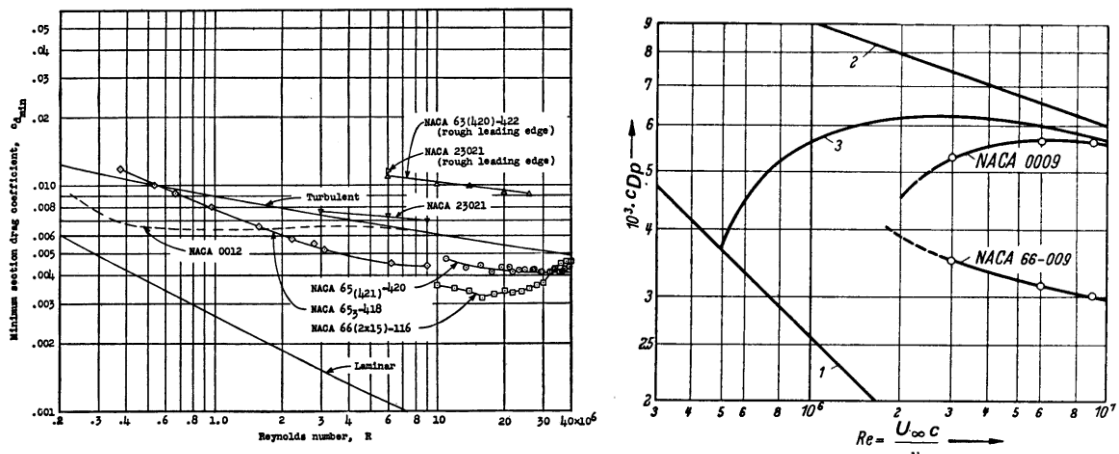
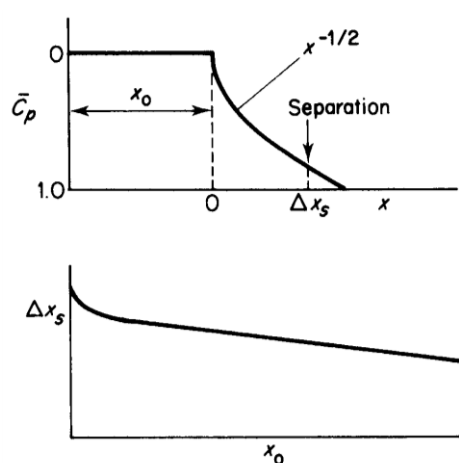


Figure 66: Profile drag of NACA laminar flow aerofoils

For a turbulent boundary layer, the minimum length of pressure recovery is achieved if the boundary layer is kept on the verge of separation – leading to the so-called ‘Stratford recovery’ with its characteristic concave pressure distribution as shown below. In Stratford’s theoretical distribution the initial pressure gradient dC_p/dx in the recovery region is infinite (!), and in the early stages $C_p \propto x^{-1/3}$. Compare this with the linear pressure recovery used on the NACA 6-series aerofoils.

This form of ‘roof-top’ pressure distribution with a Stratford recovery is also used for ‘very high lift’ aerofoil designs.



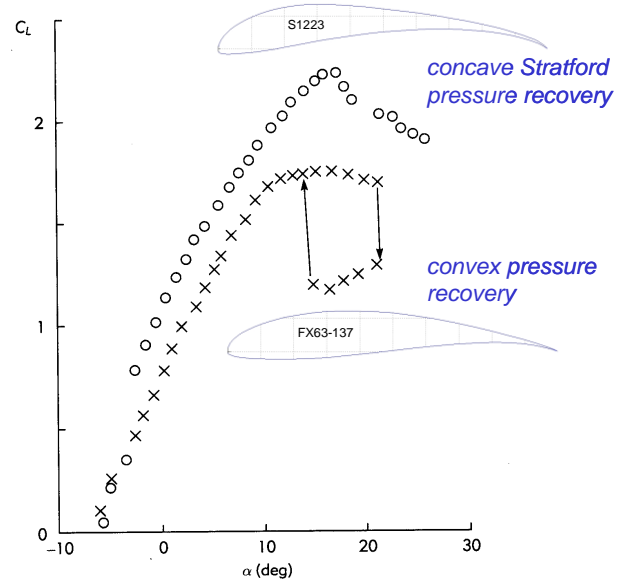
As demonstrated by the 6-series distributions presented above, the effect of increasing incidence is to counteract the favourable pressure gradient – until laminar flow breaks down at the edge of the drag bucket. Note that this breakdown has little discernable effect on lift.

A consequence of designing thickness and camber distributions to achieve this form of pressure distribution is that the resulting aerofoil sections tend to:

- be rather aft-loaded,
- have high levels of camber at the rear of the aerofoil,
- consequently have large nose-down pitching moments,
- have thin cusped trailing edges.

Laminar flow aerofoils with concave Stratford pressure recoveries tend to have high maximum lift, but rather an abrupt (trailing edge) stall as the aft region separates all at once. A linear (eg NACA 6-series) or convex (eg Wortmann FX63-137) pressure recovery reduces maximum lift, but gives a gentler stall (lift curve flattens out rather than drops at the stall).

At low Reynolds numbers these aerofoils can suffer from static lift (and pitching moment) hysteresis (separated flow condition is rather stable and persists when incidence is reduced from a stalled point).



As you may recall, laminar flow is very sensitive to disturbances – so the performance of these aerofoils can be upset by a wide variety of (often unavoidable) occurrences:

- *surface roughness* – inevitable in production aircraft (and one of the reasons why pilots of high-performance gliders and race aircraft spend so much time polishing them)
- *insect contamination* – many gliders are fitted with leading edge ‘wipers’ to remove splattered insects
- *icing* – changes the aerofoil shape, particularly near the nose. Affects the extent of laminar flow and reduces maximum lift.
- *rain* – similar impact to icing. Modern gliders can experience a significant performance reduction in rain. The highly loaded canards on the Rutan VariEze and Long-EZ led to many pilots reporting pitch trim changes due to rain, especially at landing when the loss of maximum lift could give a significant nose down pitch – not a good thing!
- *propeller wash* – turbulent swirling flow can cause local transition. In extreme cases tip vortices from highly loaded props can cause early stall (eg C-130J)



It is possible in theory to use flow control (generally pneumatic – blowing or sucking) to maintain laminar flow – but while effective in wind tunnel testing, implementation issues (air supply, pump drag, maintenance of porous surfaces etc) have prevented any really successful full-scale use¹⁹. Nevertheless, recent work on large blended-wing-body configurations has revived interest in the concept – with NASA having tested a supersonic laminar flow control wing glove on the F-16XL. Maintenance of laminar flow has a proportionately larger effect on flying-wing aircraft (after all, the aircraft is mostly wing!) – and indeed the first (unsuccessful) flight trial of a flow control system was on the Armstrong-Whitworth AW-52.



Figure 67: F-16XL and AW-52 laminar flow control research aircraft

¹⁹ The Buccaneer had blowing implemented in its wings and tail but not for maintaining laminar flow. By increasing the bound circulation, the efficiency of the wing and tail increased leading to a reduction in the required size of these surfaces.

1.5.9 Supercritical (transonic) aerofoils

The transonic airfoil design problem arises because we wish to limit shock drag losses at a given transonic speed – which effectively limits the minimum pressure coefficient (= maximum local velocity) that can be tolerated. In turn this limits the lift coefficient and the thickness ratio, since both affect the maximum velocity over the aerofoil section.

[NB it should be noted that transonic drag rise is not the same as wave drag. In 2D subsonic flow the drag rise is due almost entirely to form drag arising from shock-induced boundary layer separation – drag due to total pressure loss through the shock itself is actually rather small. Similarly, wave drag in supersonic flow is not directly related to losses through a shock, but to the energy lost to the compression and expansion wave systems trailing behind an aerofoil or wing.]

That this is so is shown by the success of Ackeret's and Busemann's linearised theories, which treat the pressure waves generated by thin aerofoils as Mach waves – under this assumption the flow is isentropic everywhere, but still generates wave drag due to lift and thickness that agrees closely with that given by a combination of oblique shock & Prandtl-Meyer expansion theory.]

The simplest approach to improving transonic performance is to delay the onset of supersonic flow as long as possible – and it turns out that the ‘roof top’ type pressure distribution typical of the 6-series laminar flow aerofoils is a pretty good way of doing this, by maintaining a constant or gradually increasing velocity distribution over the forward part of the section. However, once the critical Mach number is exceeded large regions of supersonic flow appear aft of the crest (maximum thickness point) of the aerofoil, giving a drag increment due to the high suction levels. This supersonic flow region is then terminated by a strong shock, giving a further rapid drag rise soon after M_{crit} is exceeded. Extending the roof-top region aft would raise the critical Mach number, but at the risk of early boundary layer separation in the pressure recovery region.

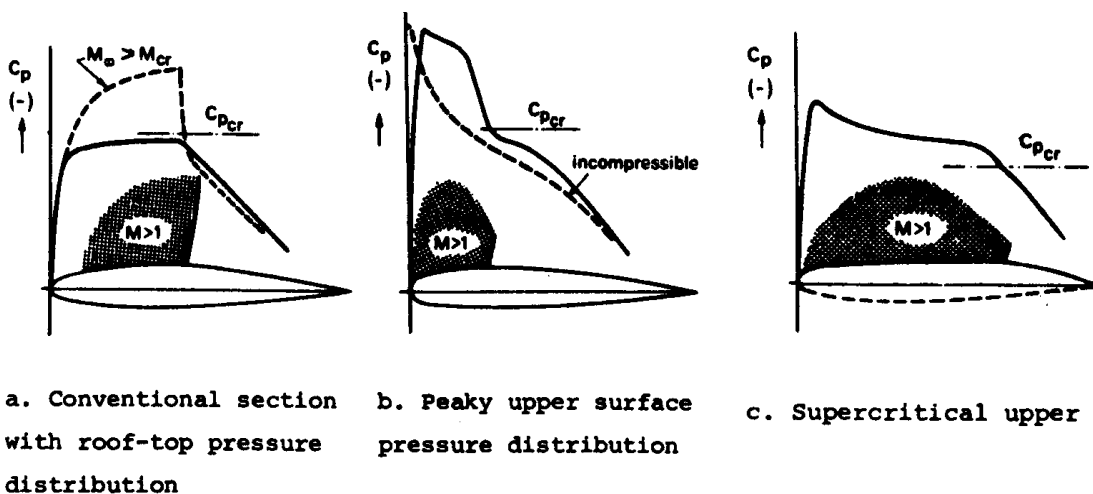


Figure 68: Transonic flows on conventional, peaky and supercritical aerofoils.

6-series aerofoils (and similar) therefore have a high critical Mach number, but then a very rapid drag rise – good for high-subsonic cruise but necessitating high sweep or low thickness for transonic and supersonic performance.

However, we **can** generally tolerate some supersonic flow over the forward part of the aerofoil without drag increase – since it is the terminating shock that causes transonic drag rise (pressure loss through the shock + shock/boundary layer interaction – see your 2nd year Aerodynamics notes), so that some sections can operate efficiently as "supercritical aerofoils". A rule of thumb is that the maximum local Mach numbers should not exceed about 1.2 to 1.3 on a well-designed supercritical aerofoil. This produces a considerable increase in available C_L compared with entirely subcritical designs.

Early supercritical sections developed in the UK (by Pearcey at NPL) made use of what is known as a 'peaky' pressure distribution to intentionally create supersonic velocities (up to $M = 1.4$) near to the leading edge, where the associated suction forces give a thrust (rather than drag) force. The nose profile is then very carefully designed to give a near-isentropic compression

(deceleration) around the leading edge followed by a weak shock. Drag rise Mach number is postponed by 0.03 to 0.05 compared to a conventional section. The ideal compression would only occur at one design point (M and α), but rate of growth of the shock off-design is slow enough to give a practical design.

'Peaky' aerofoils were quite successful, and are found on many older transport aircraft (BAC1-11, VC10, DC-9). In the limit, it is theoretically possible to design entirely shock-free aerofoils using this approach (eg Fig. 69).

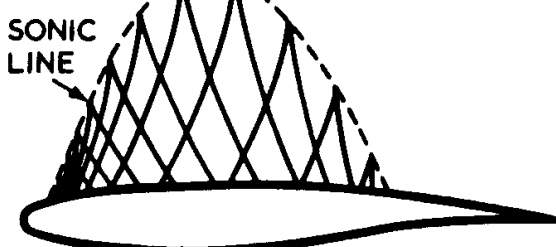
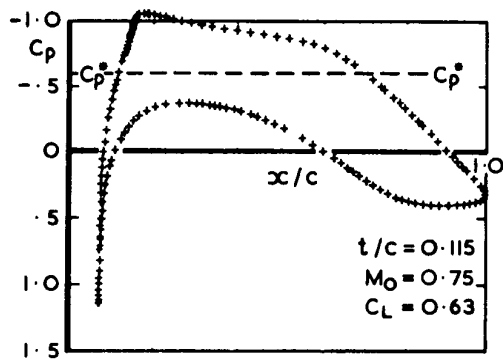
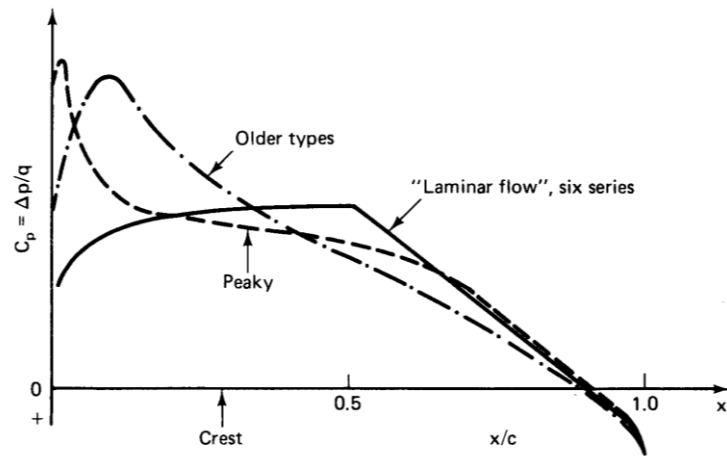


Figure 69: A shock-less lifting aerofoil design with an isentropic compression region

Following on from Pearcey's work, Whitcomb in the US (the man also responsible for the area rule concept and winglets) developed the modern **supercritical** (aft-loaded) section.

In contrast to the peaky section, these aerofoils are designed to have substantial regions of supersonic flow over much of the upper surface. This is achieved by:

- a) a forward sonic point located in a region of high curvature, near the leading edge
- b) a relatively large leading edge radius to expand the flow
- c) having very small curvature over much of the rest of the upper surface – so that the aft-facing surface has very little vertical projected area, reducing the drag penalty of the supersonic flow region
- d) cambering the aft portion of the wing to carry more load aft (particularly on the lower surface) – reducing peak local velocities and hence increasing critical Mach number
- e) using a thin trailing edge (tangential upper and lower surfaces) to reduce the adverse pressure gradient

This combination leads to significant lower surface curvature, particularly near the trailing edge.

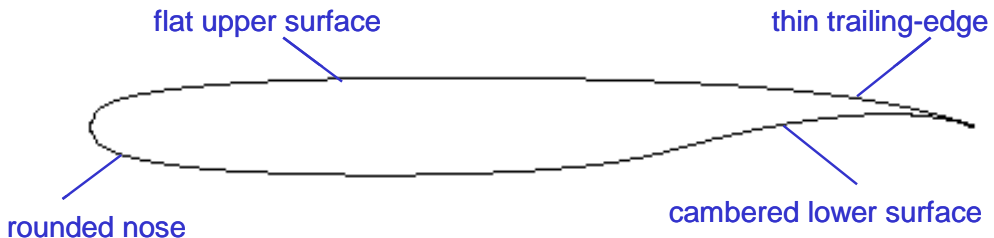


Figure 70: Design features of an early Whitcomb supercritical aerofoil section

Note the similarity of this supercritical profile to many laminar sections – hardly surprising since the need to avoid high peak suction on the upper surface is common to both design cases.

In addition to the aerodynamic performance benefits, it is evident that this section has some structural advantages – plenty of depth for spars and high internal volume fuel.

Set against these are some disadvantages:

- too much aft loading can produce large negative pitching moments with trim drag and structural weight penalties (can be alleviated in 2D by tailoring the underside of the nose region to move loading forward, or in 3D by varying camber, twist and thickness across the span)
- the adverse pressure gradient on the aft lower surface can produce separation in extreme cases
- the thin trailing edge may be difficult to manufacture, or to integrate control surfaces into (may be possible to use a blunt trailing edge)
- supercritical (and especially shock-free) designs are often very sensitive to M and C_L and may perform poorly at off-design conditions. The appearance of "drag creep" is quite common, a situation in which substantial section drag increase with Mach number occurs even at speeds below the design value.
- wing root flow separation can be a problem due to high adverse pressure gradients

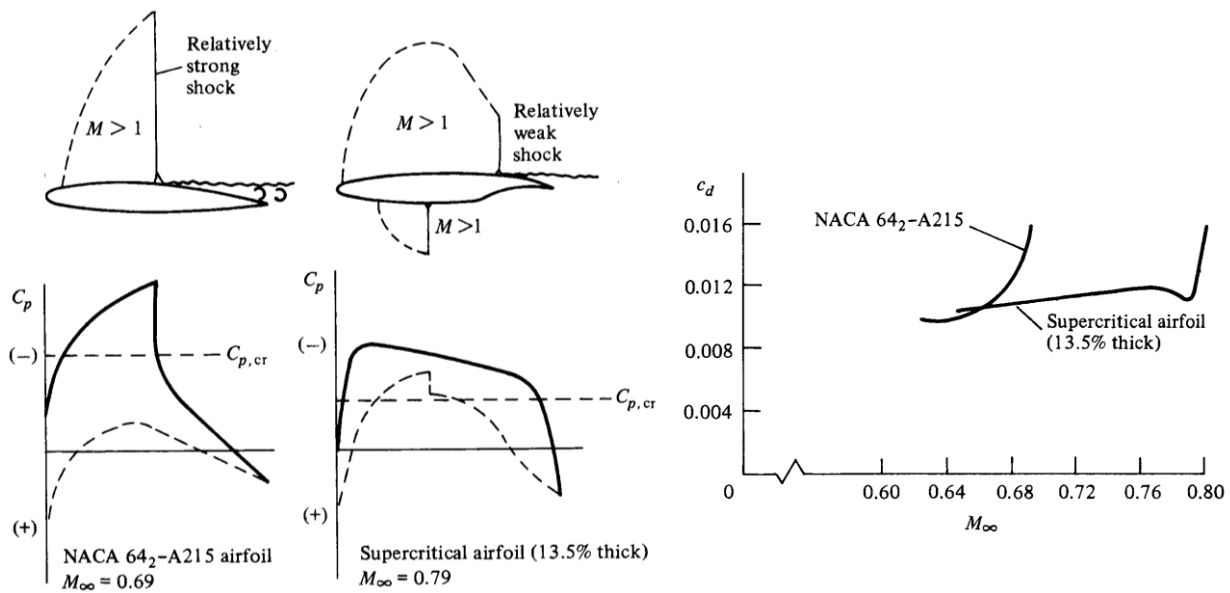


Figure 71: Effect of design for supercritical operation on drag - NASA

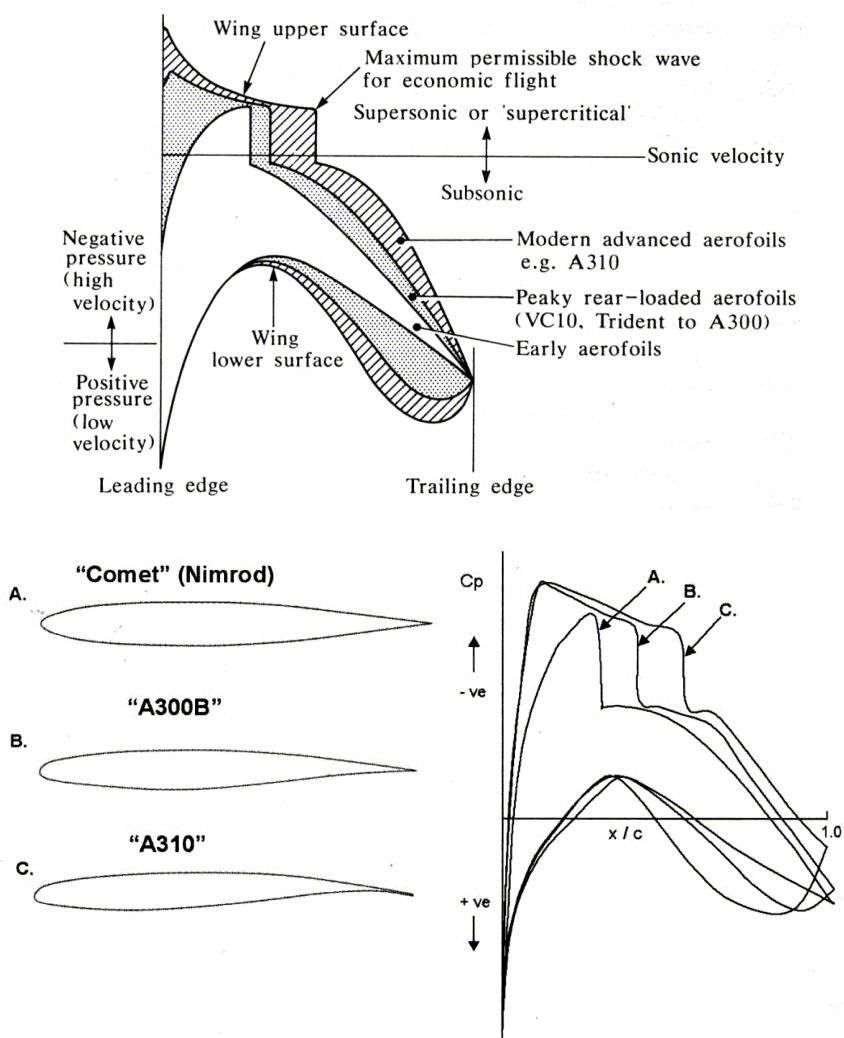


Figure 72: UK development of supercritical aerofoil sections

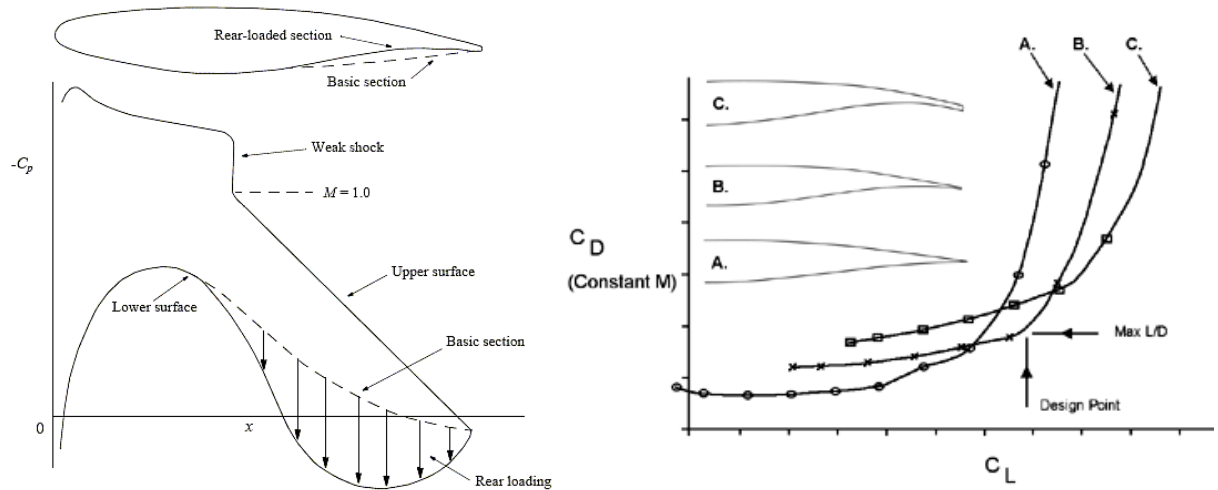


Figure 73: Effect of trailing edge shaping on aft loading & performance - Airbus

The effect of the trailing edge shape on pressure distribution and drag is illustrated in Figs 72 and 73. Increasing aft camber and reducing trailing edge thickness improves the drag rise Mach number, but also increases form drag at lower speeds.

As trailing edge angle is reduced the trailing edge pressure becomes more negative – helping to increase rear loading without increasing the upper-surface pressure gradient. However, on the minus side the adverse pressure gradient on the lower-surface is also increased, while form drag also increases due to the aft component of the upper-surface suction loading. The trailing edge pressure can be made still more negative by making the trailing edge blunt, but this must be balanced against a further increase in drag due to the base pressure. (Airbus have found a trailing edge base thickness of around 1/2% of chord to be optimum). A similar approach was taken by McDonnell-Douglas with their ‘Divergent Trailing edge’, used to isolate the upper and low surface pressures on the MD-11 (see Section 1.4.6).

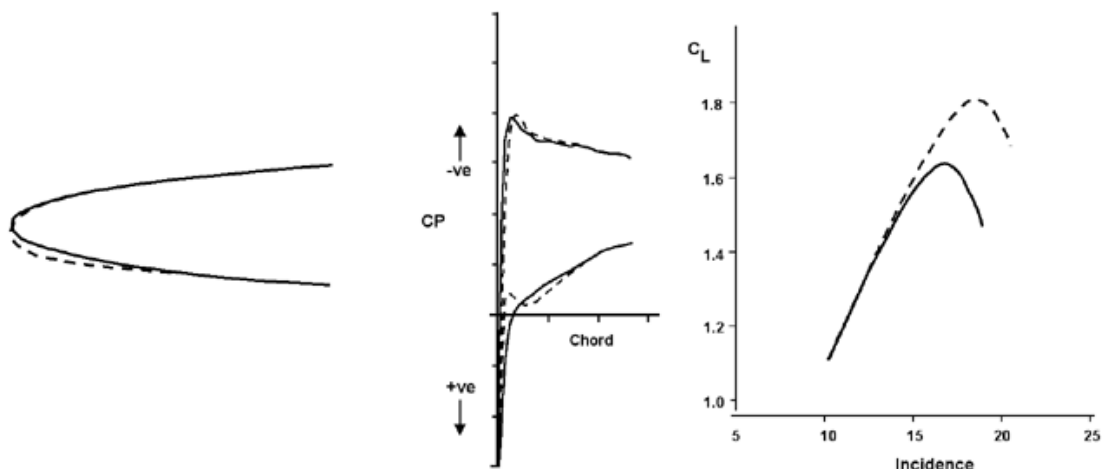


Figure 74: Effect of leading edge droop on pressure distribution and maximum lift

Off-design performance can be a problem for supercritical sections, particularly at low-speed/high-lift conditions. An alternative to complex variable geometry (eg slats) is to apply a small amount of leading edge droop to reduce the curvature from the stagnation

region to the point where the suction peak develops at high lift. This increases maximum lift by delaying stall onset (Fig. 74) but also ensures that ‘peaky’ supersonic flow still develops (albeit slightly further aft). Balanced against the increase in maximum lift is a small loss of lift at low incidence due to the change in leading edge pressure distribution (~1-2% of design C_L). The degree of droop is limited by the suction peak developed on the lower surface under the ‘chin’ of the droop, which could go supercritical at cruise conditions. The BAe146 and Airbus A400M make use of this approach to give improved high-lift performance.

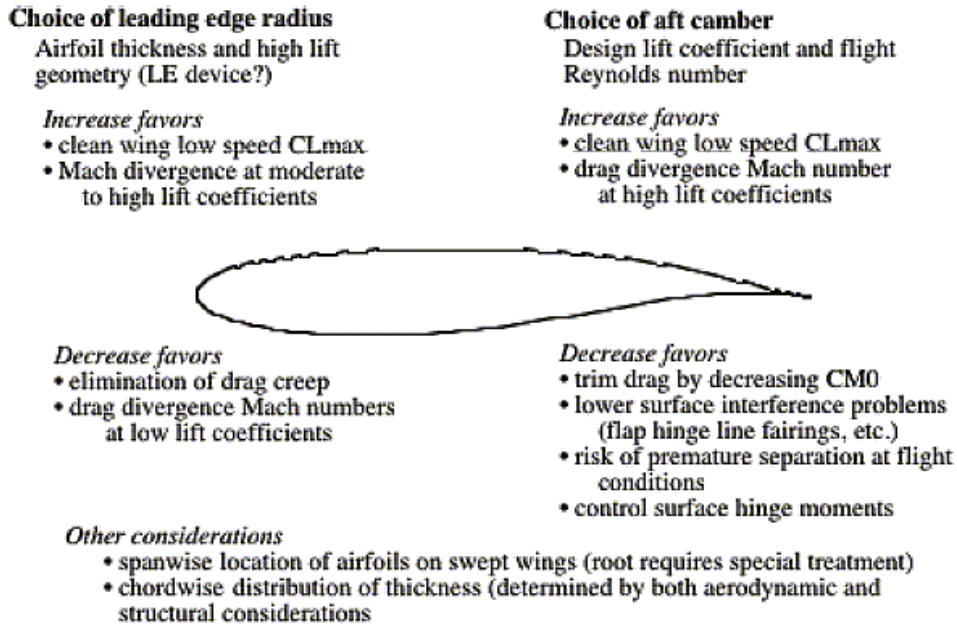


Figure 75: Some design principles for supercritical aerofoils (from Mason)

Supercritical aerofoils were also found to behave well at low-speed (with good C_{lmax}) leading to the development by NASA of the GA(W) family of aerofoils for general aviation purposes (which later became the LS and MS aerofoils) – however, these aerofoils were found to be rather sensitive to Reynolds number, and have not found wide usage.

1.5.10 Special purpose aerofoils

There are a wide range of special purpose aerofoils available – too many for the limited time available. We will just touch on a couple – low Reynolds number aerofoils and low pitching moment aerofoils.

One class of aerofoils that has recently become of more interest are **low Reynolds number** designs – once the preserve of the model aeroplane designer, these are now appearing on UAVs, MAVs and wind turbines.

The basic difficulty with low Re aerofoils is too much laminar flow! Laminar boundary layers are very much less capable of handling an adverse pressure gradient without separation, leading to flows that are rather unstable.

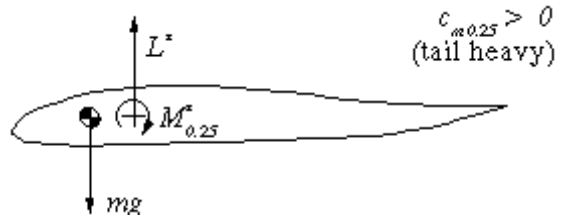
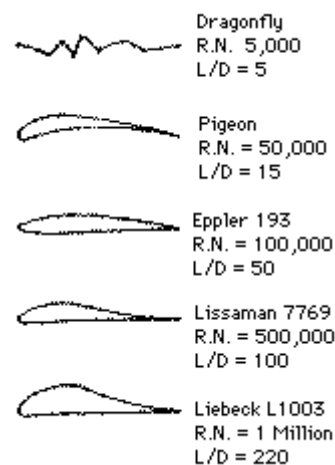
Laminar separation bubbles are common (ie separation followed by transition to turbulence and reattachment), leading to poor stall behaviour, with the potential for static hysteresis in lift and pitching moment. Asymmetric stall on 3D wings can become a real problem.

One option for ‘higher’ Re (say $\sim 5 \times 10^5$ to 10^6) is to design the pressure distribution very carefully to maintain laminar flow – even in some cases accepting laminar separation bubble formation (an *X-Foil* capability) if it does not impact too badly on performance. At intermediate Re (say 1 to 5×10^5) it is often better to deliberately design for a turbulent boundary layer. One way of doing this is to shape the nose to cause early transition (probably via a laminar separation bubble). Alternatively, transition can be forced by using some form of trip – surface roughness, trip strips, pneumatic turbulators etc. Drag may be higher, but high lift performance and aerodynamic predictability are improved.

At very low Re (say $<< 10^5$) it becomes rather difficult to generate a turbulent boundary layer – the Re being so low that the flow re-laminarises immediately after being tripped. In these conditions leading edge separation are inevitable and simple (cambered) flat plate sections become the most effective. At insect scales our simple aerofoil theory falls apart (with viscous and unsteady effects dominating) and the section shape appears to become almost irrelevant! However, recent studies have shown that this is not necessarily true. For example, in the much studied dragonfly case, the ‘valleys’ seen in the aerofoil profile help to trap vortices that increase lift (similarly to delta wing leading edge vortices).

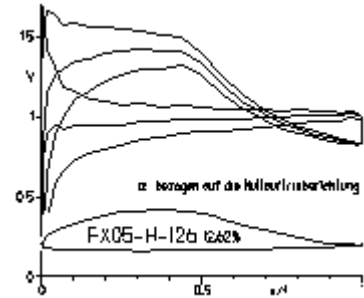
One particularly common constraint on special-purpose aerofoils is the zero-lift **pitching moment** – especially for flying wings.

Consider a rectangular flying wing in straight & level flight – for static *stability* the centre of gravity must be in front of the aerodynamic centre (ie ahead of the quarter-chord point). However, in order to *trim* at this condition we require a positive (nose-up) zero-lift pitching moment. This could be provided by a trailing edge flap, but in the interests of cruise



efficiency it is better to design the aerofoil section to have the appropriate pitching moment at the cruise lift case.

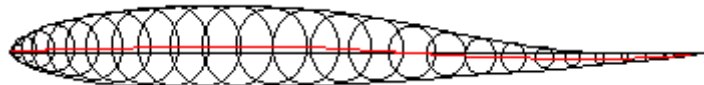
For flying wings this results in a *reflex* camber line (positive camber near the nose for good high lift performance combined with negative camber near the trailing edge) – profile drag is higher with this kind of shape, but it is more efficient than using a trailing edge flap to trim in cruise. Highly reflexed sections tend to be more sensitive to Reynolds number – because of the adverse pressure gradients due to the aft-loading on the lower surface.



A particular feature of reflexed profiles is the ‘cross-over’ between the pressure distributions on the upper and lower surfaces.

Design of these sections is a difficult compromise between:

- a) required pitching moment characteristics (negative camber aft), and
- b) adequate stall behaviour (positive camber forward).



[*NB* for a swept flying wing the same effect can be obtained rather more effectively by using twist (washout).]

Other applications where low pitching moments at high lift are important are helicopter and propeller blade sections, where excessive twist at high speed can be a major problem.

1.5.11 Aerofoil requirements

The aerofoil is in the end what generates the lift, so what makes the aeroplane fly. Its characteristics and choice are paramount in the performance of the final product. As we have seen, there is a vast variety of aerofoils for the designer to choose from and, especially today, the designer can even use a brand new custom made aerofoil. But what are the requirements for the aerofoil? Torenbeek gives a list of aerofoil requirements, mainly for civil aircraft. Most of these requirements have already been mentioned (*Sections 1.2 and 1.3*) and should appear obvious by now, but a summary wouldn't go amiss.

- The basic aerofoil must have a low profile drag coefficient for the lift coefficients used in cruise.
- For the inboard sections the aerofoil with flaps extended must not exhibit too much drag, especially during take-off and landing.
- The inboard sections should have high lift with flaps extended.
- The tip section should have a high C_{Lmax} and exhibit gradual stalling characteristics.
- The critical Mach number should be sufficiently high to avoid buffet during cruise and preferably even dive (“updated” version of Torenbeek’s actual requirement, which is clearly outdated).
- The pitching moment coefficient should be low to moderate to avoid high trim drag and torsional loads on the wing (especially at high dynamic pressures).
- The aerodynamic characteristics should not be very sensitive to manufacturing variations and environmental aspects like dust, insect contamination etc.
- The thickness ratio should be the maximum allowed (aerodynamically) to minimize weight and also maximize internal space (landing gear, fuel).

It is obvious that these requirements cannot all be met by a single aerofoil, so different sections will have to be used along the span.

1.6 3D Wing Design

1.6.1 Reminder of basic lift distribution theory

Spanwise lift distribution (and hence induced drag) is a function of aspect ratio, sweep, taper ratio and aerodynamic twist (ie geometric twist + camber). For unswept wings basic lifting line theory is useful to illustrate how planform geometry parameters affect the lift distribution.

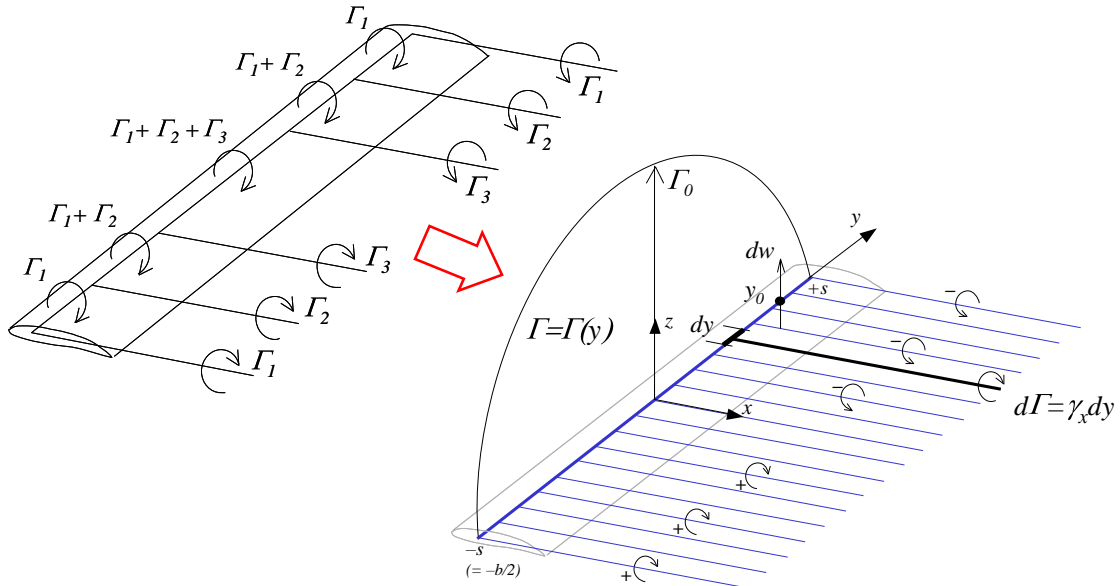
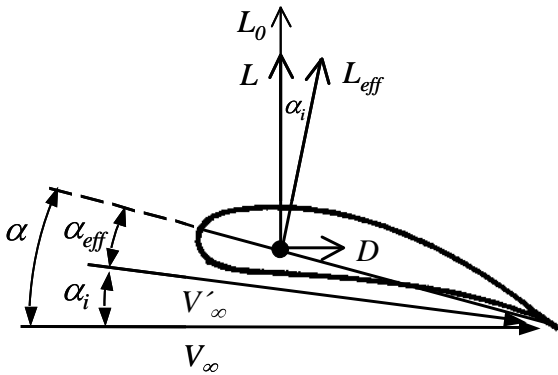


Figure 76: Lifting line representation of wing lift

First, a brief reminder of 2nd/3rd year wing theory:

Prandtl's *lifting line theories* model the lift distribution on a wing using superimposed 'horseshoe' vortices with the 'bound' central section lying along the wing quarter-chord line. In the limit this becomes a continuous circulation distribution $\Gamma(y)$ along the lifting line. The spanwise variation of circulation is balanced by the shedding of a vortex sheet of strength $\gamma_x(y) = d\Gamma(y)/dy$. This wake sheet induces a downwash velocity $w(y)$ on the wing which reduces the local effective incidence – which in turn reduces local lift *and* rotates the lift vector aft to give an (induced) drag component. The wake sheet strength and the wing lift distribution are therefore closely coupled.

In order to close the loop, the basic lifting line theory assumes that each section of the wing behaves as if it were a 2D aerofoil. The downwash velocity is determined at the quarter-chord point for each section (ie along the lifting line), and then converted into an induced incidence $\alpha_i = -w(y)/U_\infty$. The corresponding local lift is then calculated from 2D thin aerofoil theory. The advantage of this approach is that an analytical solution for the lift

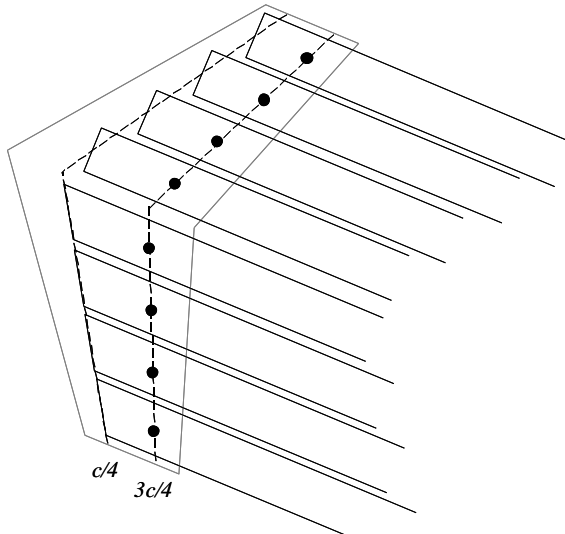


distribution is relatively straightforward.

The 2D assumption is OK for conventional straight high aspect-ratio tapered wings, but is inaccurate for:

- low-aspect ratio wings,
- low taper ratios ($\lambda \rightarrow 1$), and
- swept wings

where 3D effects are significant, particularly in the tip region. The ‘low taper ratio’ case is not one that you will find mentioned specifically in most text books – but the outboard shift in the lift distribution accentuates the 3D flow effects near the tip. As a result the induced drag variations at low taper ratio given in several texts (and Fig. 12 above) are significantly over-predicted – for example, this figure gives δ for a rectangular wing with $AR = 10$ of ~ 0.11 , whereas the true value is closer to 0.05.



The extended lifting line theory goes someway towards a more accurate representation. In this method, the 2D aerofoil theory component is replaced by a ‘lumped vortex’ model. In other words, for each horseshoe element we select a control (or collocation) point at the three-quarter-chord point and impose the Kutta condition (no through flow) at this point. There is no rigorous theoretical justification for this choice of control point – appeal is usually made to analogy with the 2D aerofoil case.

Nevertheless, it works amazingly well – although Professor Fiddes noted that an improvement in drag prediction can be obtained by (a) clustering elements at breaks in the planform (ie centreline and tip) using sine or cosine distributions, and (b) shifting the control point progressively outboard for horseshoe elements near the tip.

The offset of the control points makes an analytical solution tricky – so recourse is usually to a numerical solution, which is fairly straightforward and computationally trivial. A further refinement adds additional horseshoe vortex elements in the chordwise direction to give a vortex lattice method – which in the limit becomes 3D lifting surface theory.

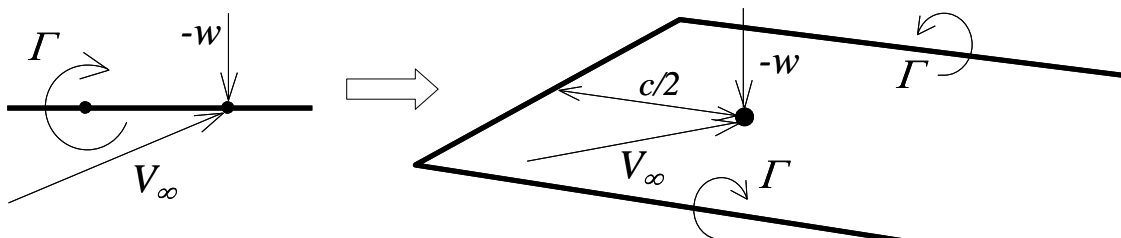


Figure 77: 3D equivalent of the ‘lumped vortex’ aerofoil model

Although the basic lifting line theory is not terribly accurate, it is still useful for demonstrating the effect of aspect ratio and taper ratio – and how to select a twist distribution for optimum cruise performance.

1.6.2 Minimum drag of non-planar wings

The Stanford ‘Aircraft Design’ website presents a very neat exposition of the wing design requirements for minimum induced drag. For a planar wing, the minimum induced drag is achieved with an elliptical spanwise loading, which in turn implies a constant induced downwash velocity over the span. Kroo generalises this design requirement to non-planar wings using the ‘method of restricted variations’.

Consider a planar wing with an arbitrary (small amplitude) variation in the circulation distribution at two points represented by $\delta\Gamma_1$ and $\delta\Gamma_2$. If this variation does *not* change the overall (total) lift L then

$$\begin{aligned}\delta L &= \rho U_\infty \delta\Gamma_1 + \rho U_\infty \delta\Gamma_2 = 0 \\ \rightarrow \delta\Gamma_1 &= -\delta\Gamma_2\end{aligned}$$

If the induced drag was a minimum for the initial circulation/lift distribution, then a small change in the distribution will give a 2nd order (negligible) change in drag (ie $dD/d\Gamma \sim 0$). Denoting the local downwash velocity *in the Trefftz plane* by w_T then from the Kutta theorem and the lift equation above

$$\begin{aligned}\delta D &= \frac{\rho}{2} w_{T1} \delta\Gamma_1 + \frac{\rho}{2} w_{T2} \delta\Gamma_2 \approx 0 \\ \rightarrow w_{T1} &= w_{T2} = \text{constant}\end{aligned}$$

That is, the downwash behind a planar wing with minimum drag is constant.

[NB the Trefftz plane is a perpendicular (y - z) plane far downstream of the wing, where the wake is parallel to the freestream velocity and only the v and w velocity perturbations are significant. The lift and drag can then be determined from a spanwise integration across the wake – the result is numerically more reliable than an integration of the surface loads, particularly for induced drag in a vortex lattice method (VLM). You will recall from 2nd/3rd year aerodynamics that the downwash velocity w_T far downstream in the wake is twice that induced at the wing w_i (as the trailing vortices become effectively infinite in extent) – hence the factor of $1/2$ in the drag equation above.]

The fact that the drag of a lifting system depends only on the distribution of circulation shed into the downstream wake leads to some very useful results in classical aerodynamics, in particular *Munk's stagger theorem*. This states that the total induced drag of a system of lifting surfaces is not changed when the elements are moved in the streamwise direction (as long as the distribution of circulation is held constant by adjusting the surface incidences). Thus for biplanes it is the vertical gap and not any longitudinal stagger which determines the induced drag – so that tandem wing aircraft are in fact equivalent to biplanes.]

The same approach can be applied to a non-planar wing, with local dihedral angle θ . Now we need to take into account the corresponding lateral inclination of the lift vector, and for the drag calculation the induced velocity *normal to the wake* in the Trefftz plane V_n (ie the ‘normalwash’). The condition for constant lift is then

$$\begin{aligned}\delta L &= \rho U_\infty \delta\Gamma_1 \cos\theta_1 + \rho U_\infty \delta\Gamma_2 \cos\theta_2 = 0 \\ \rightarrow \delta\Gamma_1 \cos\theta_1 &= -\delta\Gamma_2 \cos\theta_2\end{aligned}$$

and for minimum drag

$$\begin{aligned}\delta D &= \frac{\rho}{2} V_{n1} \delta\Gamma_1 + \frac{\rho}{2} V_{n2} \delta\Gamma_2 \approx 0 \\ \rightarrow \frac{V_{n1}}{\cos\theta_1} &= \frac{V_{n2}}{\cos\theta_2} = \text{constant}\end{aligned}$$

or more generally

$$V_n = k \cos\theta$$

In other words, the normalwash is proportional to the cosine of the local dihedral angle → thus for example the (side)wash on an optimally loaded vertical winglet is zero (exactly as mentioned in *Section 1.4.5*). With this design goal we can then solve for the required circulation distribution.

[As discussed in *Section 1.4.5* above, this implies that the winglet thrust associated with the wing flow is actually cancelled out by the winglet’s own self-induced drag. What is then left is the effect of the winglet flow on the wing – and with optimum design the winglet flow reduces the average downwash on the wing for a given lift level, which in turn reduces the overall lift-dependent drag.]

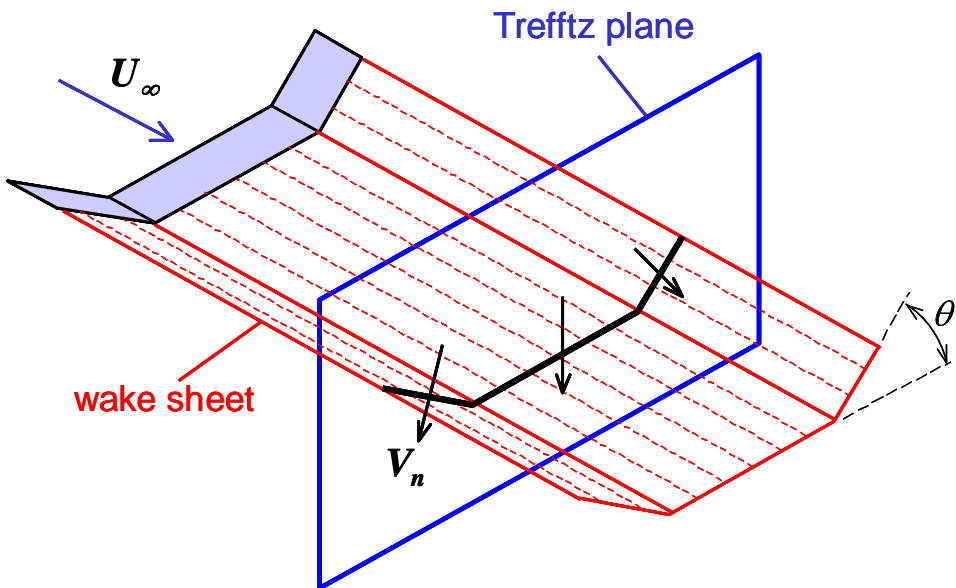


Figure 78: Trefftz plane analysis of induced drag on a non-planar wing

In general, non-planar wings have lower induced drag levels than planar wings of the same span, although the degree of improvement is dependent on the geometry – some typical examples from Kroo are shown below, designed using an optimisation process with a height/span ratio of 0.2. (Note that the advantages of non-planar wings only become really significant when span is limited by other factors.)

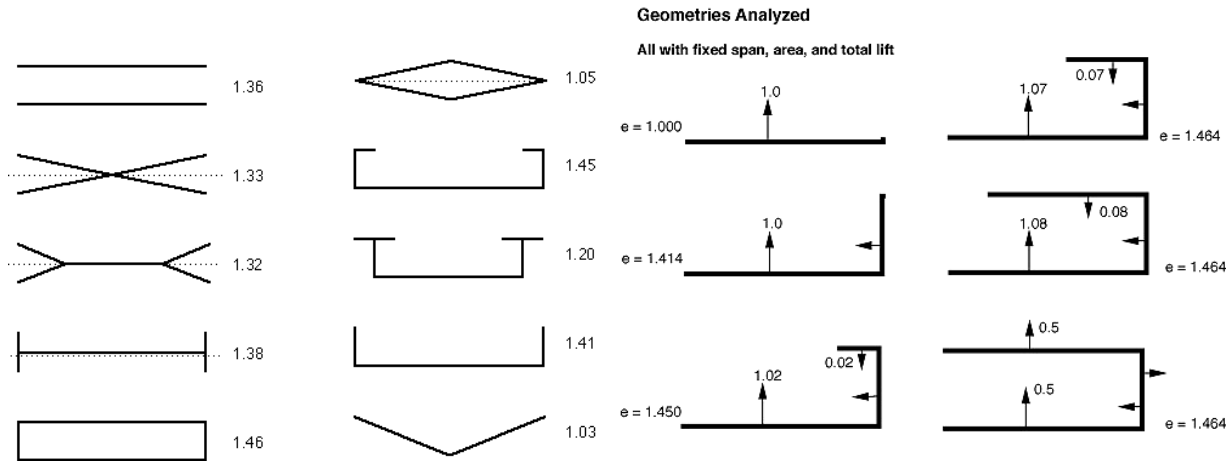


Figure 79: Span efficiency e ($\equiv I/k$) for non-planar wings

Each wing has the same projected span and total lift, and has been designed for minimum drag. Interestingly, the popular diamond wing ($e = 1.05$) shows little improvement over the basic planar wing (although if the wings are displaced longitudinally there may be some further gains to be made). The box wing is the most efficient (structurally as well as aerodynamically, with $e = 1.46$), but only by a small margin over the basic winglet ($e = 1.41$) and the C-wing ($e = 1.45$). In view of its lower wetted area, the C-wing may give lower overall drag. The C-wing load distributions are rather unexpected, with the upper stub wing loaded downwards.

Increasing the height/span ratio greatly increases the potential saving in induced drag.

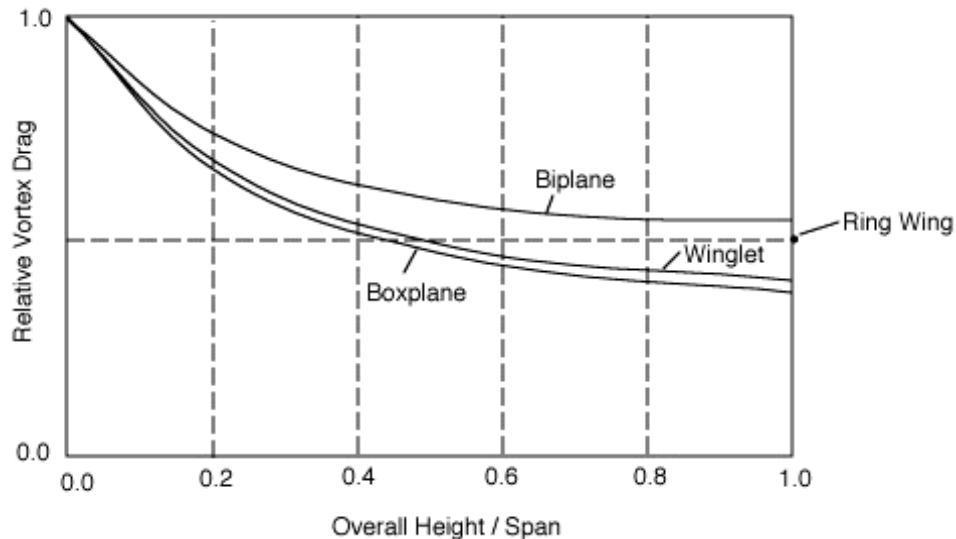


Figure 80: Effect of vertical extent on induced drag of non-planar wings

The analysis above suggests that it is the non-planar shape of the wake not the wing as such that gives the drag reduction. An alternative approach to drag reduction might therefore be to use a highly curved trailing edge to generate a curved wake from a planar wing at incidence (Fig. 81). However, a complex twist or chord distribution would be required to achieve the corresponding optimum load distribution.

This concept was rather popular some years ago, leading to designs for crescent-shaped (or lunate) wings reminiscent of many fish tail planforms (Fig. 82). However, the potential gains were found to be small (~1% for reasonable aspect ratios) and never definitively confirmed in practice.

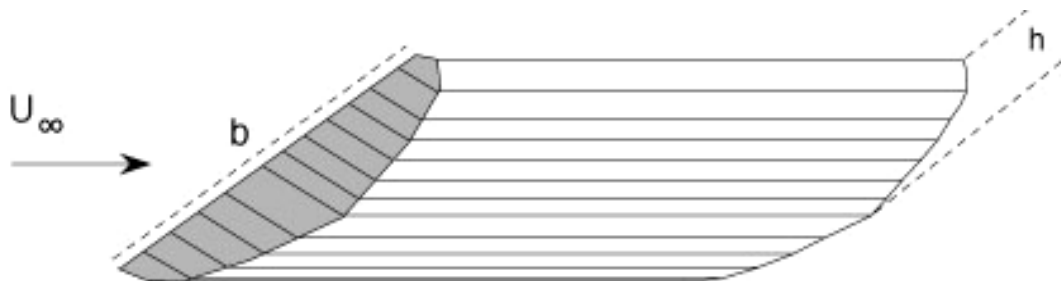


Figure 81: Non-planar wake from a planar wing

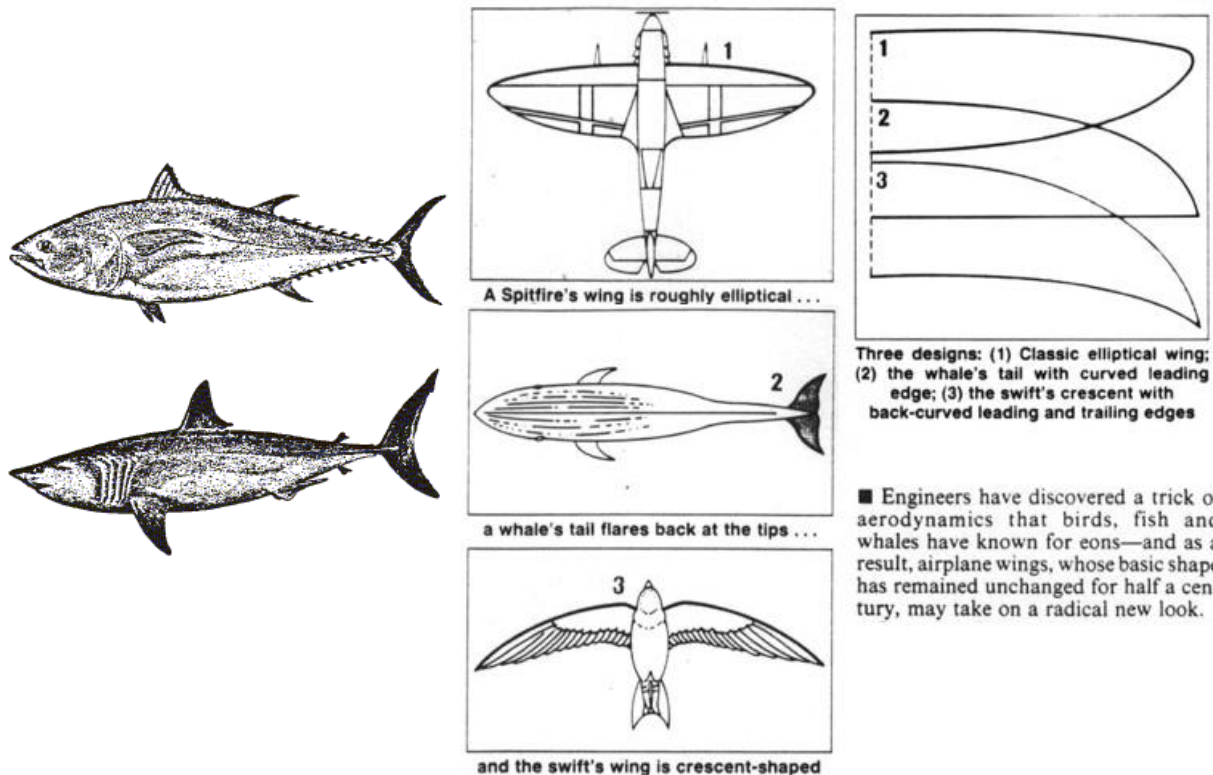


Figure 82: Crescent/lunate wings in nature

1.6.3 3D wing design – direct method

In many respects, 3D wing optimisation has followed the development of 2D aerofoil optimisation – from direct methods (start with a given geometry based on simple design tools, then modify it) to the increasingly popular application of inverse methods.

The **direct** method requires an understanding of how wing surface shape affects the flow topology – and ESDU datasheets 97017 and 90008 give a good introduction to the various interactions for a transonic wing (probably the most difficult design case), with an emphasis on use of surface curvature to match a number of design points.

For a swept wing with a reasonable aspect ratio much of the flow is 2D and hence design rules for 2D supercritical aerofoils (see *Section 1.5.9*) can be applied to the 3D wing – eg a roof-top pressure distribution over the forward section.

For an untapered wing the equivalent 2D flow is that of an infinite yawed wing, and can be related to the 3D flow by a number of (relatively) simple geometric transformations (see your 2nd year Aerodynamics notes).

The equivalent *freestream* Mach Number is the familiar component normal to the leading edge

$$M_{2D} = M_\infty \cos \Lambda$$

where Λ is the sweep angle. (Note that ESDU 90008 uses a double-star subscript to denote the equivalent 2D flow, ie M^{**} rather than M_{2D}).

Since for an infinite wing there can be no pressure gradients parallel to the leading edge, the pressure *perturbations* ($p - p_\infty$) are the same in the 2D and 3D cases. The *local* pressure coefficients (and hence also overall section lift coefficient) therefore become

$$C_p = C_{p2D} \cos^2 \Lambda \quad \text{and} \quad C_L = C_{L2D} \cos^2 \Lambda$$

The corresponding geometric transformations are

$$\frac{t}{c} = \left(\frac{t}{c} \right)_{2D} \cos \Lambda \quad \text{and} \quad \alpha = \alpha_{2D} \cos \Lambda$$

The combination of pressure and thickness scaling gives the *pressure* and *wave* drag transformations (for inviscid flow) as

$$C_{D_P} = C_{D_{P2D}} \cos^3 \Lambda \quad \text{and} \quad C_{D_W} = C_{D_{W2D}} \cos^3 \Lambda$$

Thus the flow on a swept wing may be compared with the flow on an equivalent aerofoil which is:

- at a lower free-stream Mach number,

- thicker, and
- at a higher lift coefficient.

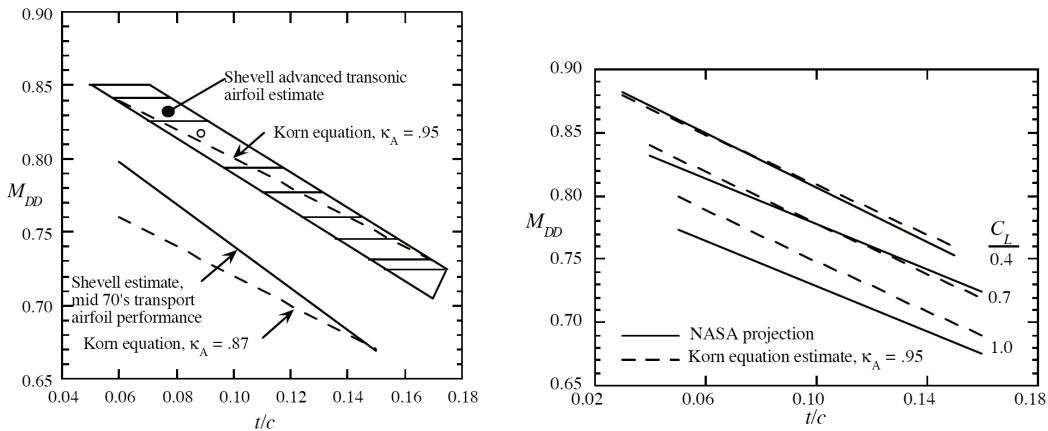
The beneficial effect of sweep is due to the fact that the first of these three factors generally easily outweighs the adverse effects of the last two. In particular, the appearance of shock waves, and their consequent adverse effects on the development of drag and separation, is progressively delayed as the sweep angle is increased.

[NB These scaling transformations can also be seen in the empirical Korn equation used to relate drag rise Mach number to wing sweep, lift and thickness for transport aircraft.

$$M_{cruise} = 0.05 \cos \Lambda_{c/2} + \frac{0.123 C_L}{\cos^2 \Lambda_{c/2}} + \frac{C_D / c_{20\%}}{\cos \Lambda_{c/2}} \approx 0.9$$

It can be seen that each parameter has actually been transformed to its 2D equivalent, and then linearly combined to approximate their effect on the critical Mach number.

The validity of the Korn equation is illustrated by two figures below (from Mason), showing the variation of drag rise Mach number with thickness and lift coefficient. With the appropriate ‘technology factor’ applied, the thickness and lift effects are well matched – apart from an overly optimistic prediction at high lift.]



[NB Skin friction drag C_{DF} can also be scaled from 2D data on the basis of the usual boundary layer scaling laws, so that to a first approximation the boundary layer drag becomes

$$C_{D_{BL}} = C_{D_P} \cos^3 \Lambda + C_{D_F} \cos^n \Lambda$$

where $n = 1/2$ for fully laminar flows and $1/5$ or $1/6$ for fully turbulent flows.]

For isentropic, adiabatic flow the local 2D Mach Number M_N can be obtained from the pressure coefficient distribution using ‘compressible Bernoulli’. Recall from your 2nd year notes that

$$q = \frac{1}{2} \rho_\infty V_\infty^2 = \frac{1}{2} p_\infty \gamma M_\infty^2 \quad \text{and} \quad p_0 = p \left(1 + \frac{\gamma-1}{2} M^2 \right)^{\frac{\gamma}{\gamma-1}}$$

then equate total pressure p_0 and substitute for local pressure coefficient C_{p2D} to give (with a little algebraic manipulation)

$$M_N^2 = \frac{2}{\gamma-1} \left\{ \frac{1 + \frac{1}{2} (\gamma-1) M_{2D}^2}{(\gamma + \frac{1}{2} \gamma M_{2D}^2 C_{p2D})^{\frac{\gamma-1}{\gamma}}} - 1 \right\} = \frac{2}{\gamma-1} \left\{ \frac{1 + \frac{1}{2} (\gamma-1) M_\infty^2 \cos^2 \Lambda}{(\gamma + \frac{1}{2} \gamma M_\infty^2 C_p)^{\frac{\gamma-1}{\gamma}}} - 1 \right\}$$

With a bit more manipulation, the critical pressure coefficient C_p^* (ie the pressure coefficient corresponding to a local 2D Mach number M_N of 1) becomes

$$\frac{1}{2} \gamma M_\infty^2 C_p^* = \left(\frac{2}{\gamma+1} + \frac{\gamma-1}{\gamma+1} M_\infty^2 \cos^2 \Lambda \right)^{\frac{\gamma}{\gamma-1}} - 1$$

so that for a given free-stream Mach number the critical pressure coefficient in 3D flow becomes more negative as wing sweep increases.

However, if the wing tapers significantly (as most do), then the geometric sweep angle varies (reduces) from leading edge to trailing edge, so that the critical pressure (for supersonic flow) also reduces – leading to a ‘sloping roof-top’ pressure distribution in 3D (Fig. 83). This in turn gives a design isobar distribution where the isobars follow constant-percentage-chord lines.

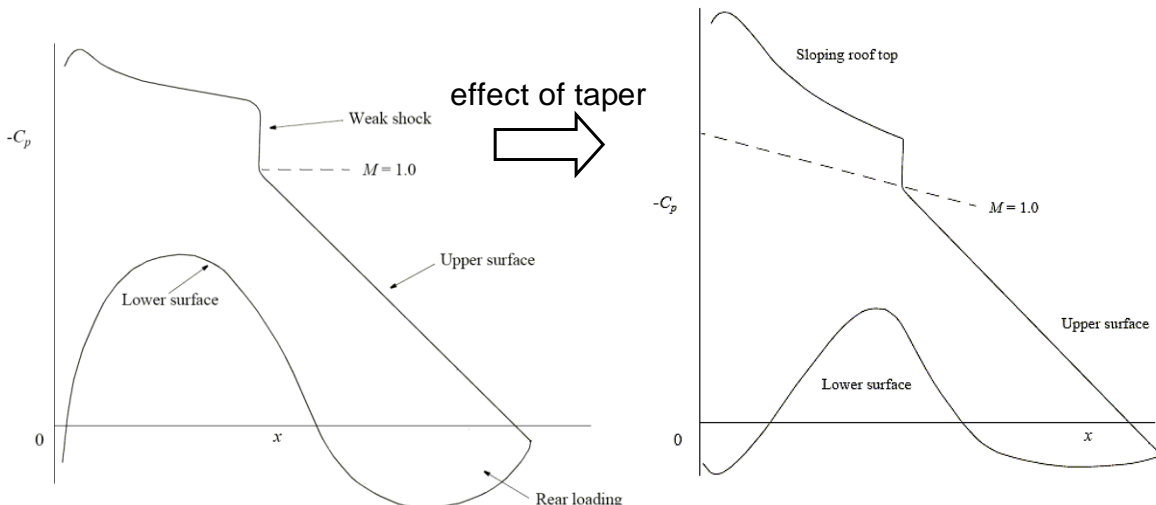


Figure 83: Effect of taper on desired pressure distributions in transonic flow (from ESDU 97017)

The corresponding pressure transformation (as used in the UK) was derived by Lock (NPL Aero Report 1028) and is based on a *mean* sweep angle $\bar{\Lambda}$ and *local* geometric sweep angle Λ_x

$$\tan \Lambda_x = \tan \Lambda_{LE} - \frac{4}{AR} \left(\frac{1-\lambda}{1+\lambda} \right) \frac{x}{c}$$

The required pressure transformation is then derived from a generalised equivalence principle:

that two supercritical flows are identical if the Mach number of the component of the flow normal to an isobar at a given fraction of the chord is the same in the two cases.

In other words, the effect of taper can be accounted for by equating the local 2D and 3D normal Mach numbers, using the equation just derived above for M_N^2 as a function of sweep angle and pressure coefficient.

Taking the pressure coefficient at the chordwise location corresponding to the mean sweep angle as a reference, yet more algebraic manipulation yields

$$C_p = \frac{2\gamma - 1}{\gamma M_\infty^2} + f C_{p_{2D}} \cos^2 \bar{\Lambda}$$

where

$$f = \left(\frac{1 + \frac{1}{2}(\gamma - 1)M_\infty^2 \cos^2 \Lambda_x}{1 + \frac{1}{2}(\gamma - 1)M_\infty^2 \cos^2 \bar{\Lambda}} \right)^{\frac{\gamma}{\gamma - 1}}$$

For a local sweep greater than the mean (ie towards the leading edge) $f < 1$, and vice versa for the trailing edge region, leading to a 3D pressure distribution tending to slope downwards as shown in Fig. 83. As a starting point for a direct design iteration, the corresponding local geometric transformation for a tapered wing has been found empirically to be

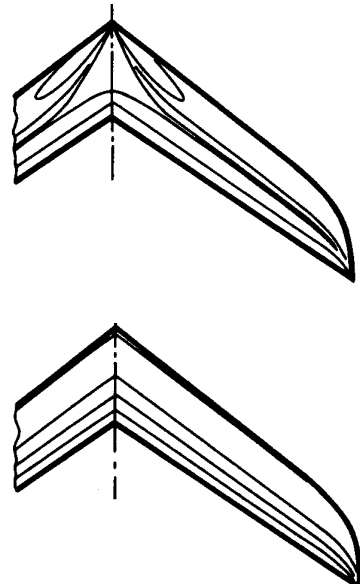
$$\frac{t}{c} = \left(\frac{t}{c} \right)_{2D} \frac{\cos^{n+1} \bar{\Lambda}}{\cos^n \Lambda_x}$$

where n lies between 2 and 3.

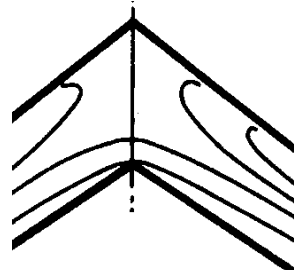
This ‘equivalent 2D’ approach corresponds to designing for a pressure distribution with straight spanwise isobars (see *Section 1.3.5* above), and is not suitable for:

- the root region, where it can lead to complex inner-wing and wing/fuselage shaping, and
- low aspect ratio wings, where the transonic flow becomes highly 3D and a complex shock system forms (see sketches below from ESDU 97107 & 90008)

In both cases, detail design to suppress local flow deviations from the ideal can result in a grossly distorted surface shape. Instead, the designer needs to look at the wing flow as a whole, for example increasing local isobar sweep at the root to give a shock-free region over the inner wing. Clearly this is a much more difficult process, and can lead to difficulties with off-design performance.



Care also needs to be taken if the trailing edge sweep angle changes rapidly (for example in the inboard region of a modern airliner wing, or on the complex wing planforms typical of stealth aircraft) since this can lead to high adverse local pressure gradients. This effect can be visualised as a ‘bunching-up’ of the isobars near the trailing edge ‘crank’ (see sketch). The resulting pressure gradient can lead to early shock formation or flow separation, and needs to be alleviated by local aerofoil section shaping in a similar manner to the wing/root junction flow (see *Section 1.3.5*).



For low aspect ratios shock-free flow is generally unachievable, and instead the designer will aim to shift the intersection of leading edge and trailing edge shocks outboard (Fig. 84), since this is the region where separation will begin. In order to prevent rapid spread of separation (and hence a danger of heavy buffet and wing drop) the region outboard of the shock intersection should be designed for moderate spanwise and chordwise pressure gradients and a gentle suction peak.

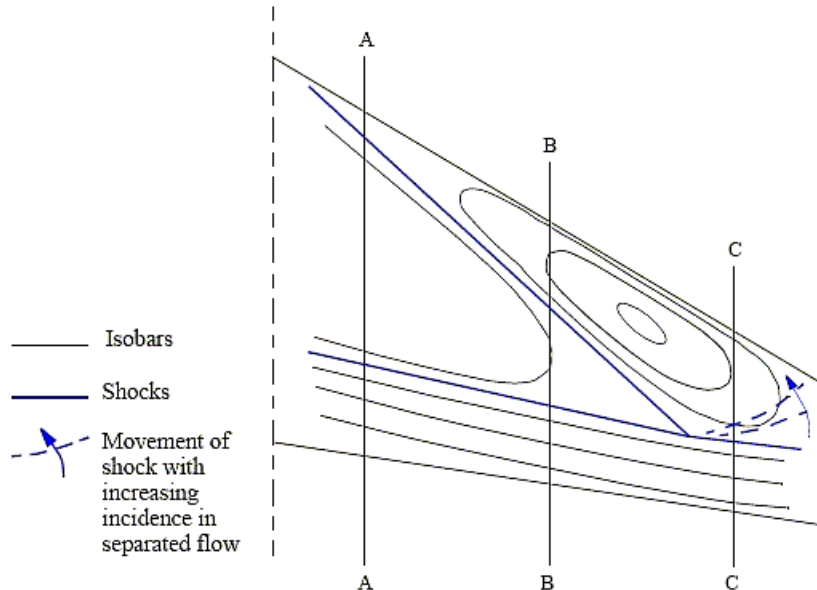


Figure 84: Typical λ shock formation on a low aspect ratio wing (from ESDU 97017)

The potential complexity of transonic flow development over low aspect ratio wings is illustrated by Fig. 85 below from ESDU 90008, for a 53.5° swept combat aircraft wing (Mach number = 0.6 to 1.4, incidence = 0° to 15°).

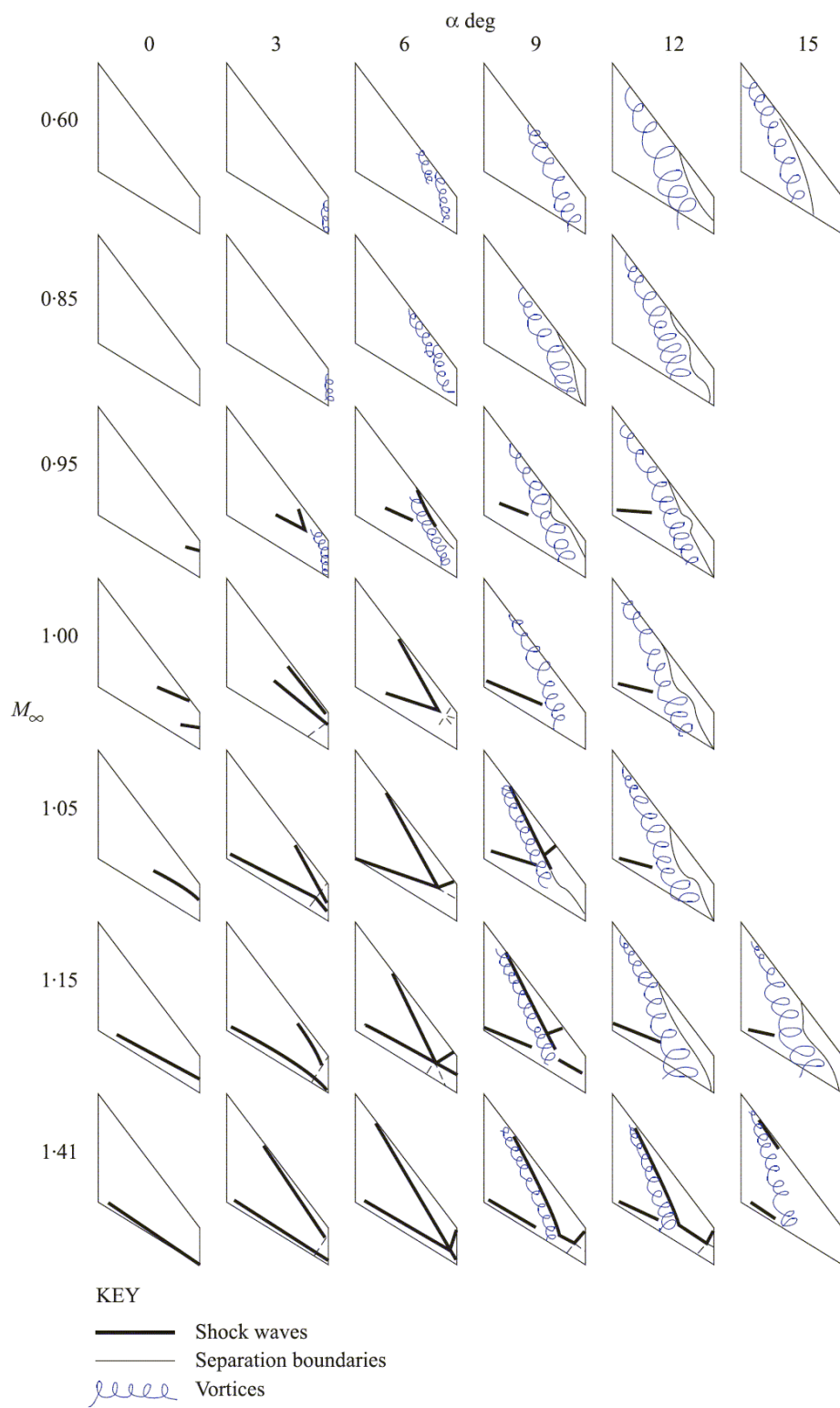


Figure 85: Transonic flow features on a typical combat aircraft wing [ESDU 90008]

1.6.4 3D wing design – inverse & optimisation methods

Having defined a baseline planform (sweep, span, taper ratio), the **inverse** design approach requires a design goal for the optimisation. At its most basic level this might be a desired span load distribution, from which the required twist may be computed – for which a simple vortex lattice method may be sufficient. A more sophisticated approach is to specify the section pressure coefficient distribution at a number of stations, from which the local thickness and camber distributions can be computed. The choice of flow code is important. A panel code or vortex lattice method is relatively simple to reformulate as an inverse design method (being basically linear), but will not accurately represent viscous effects – nevertheless, the speed with which a solution is obtained means that these methods are still in widespread use for preliminary design work.

Full CFD methods can be used in an inverse design, but since these cannot generally be inverted then an iterative approach is necessary – which in turn will require the definition of a starting geometry. The more appropriate this is to the final geometry then the quicker the code will converge.

It is also preferable if the code allows the user to define which areas of the wing are to be changed and which are to remain fixed. This not only allows the wing to be designed in a controlled manner (from inboard to outboard, say) but also can be useful in exploring sensitivities of the flow to particular features of the geometry. However, it is important to examine the derived curvature distribution carefully to ensure that a sensible shape has been achieved, in particular the leading edge region – indeed, it may be necessary to fix the leading edge radius to maintain control over this highly sensitive area. Further checks are required on the wing thickness (both overall and near wing spars, trailing edge, etc). to meet the structural requirements.

Clearly, some considerable skill and experience is required to set-up these design goals in the first place.

The clearest benefit offered by inverse methods is the speed with which a design can be achieved, giving a cost/time saving and/or the ability to explore a number of different pressure distribution designs. Other benefits come from the inverse method indicating, directly or indirectly, that particular combinations of pressure and geometric constraints are incompatible, saving otherwise-wasted design effort. As an extreme example, if the inverse method points to a negative wing thickness then the complete target pressure distribution does not represent a realistic flow and changes must be made, at least to part of it.

More recently, work has focussed on direct numerical multivariable optimisation (MVO) of the wing shape to achieve a desired performance goal – which with the introduction of structural modelling/constraints has now become multidisciplinary optimisation (MDO).

Rather than specifying a target load or pressure distribution as in an inverse method, optimisation methods use mathematical techniques coupled with a CFD code to minimise an objective function (often the drag coefficient, but could be specific geometric parameters) which can involve several design points. Early methods used simple flow codes because of the sheer number of calls to the optimisation routine – but recent

developments in hardware and numerical algorithms have allowed more sophisticated Euler and Navier-Stokes codes to be used. Checks on optimisation results are similar to inverse methods, except for the addition of the pressure distribution (not often prescribed). This is particularly true if the flow code used is too simple, in which case running the final geometry through a more advanced flow code may be necessary.

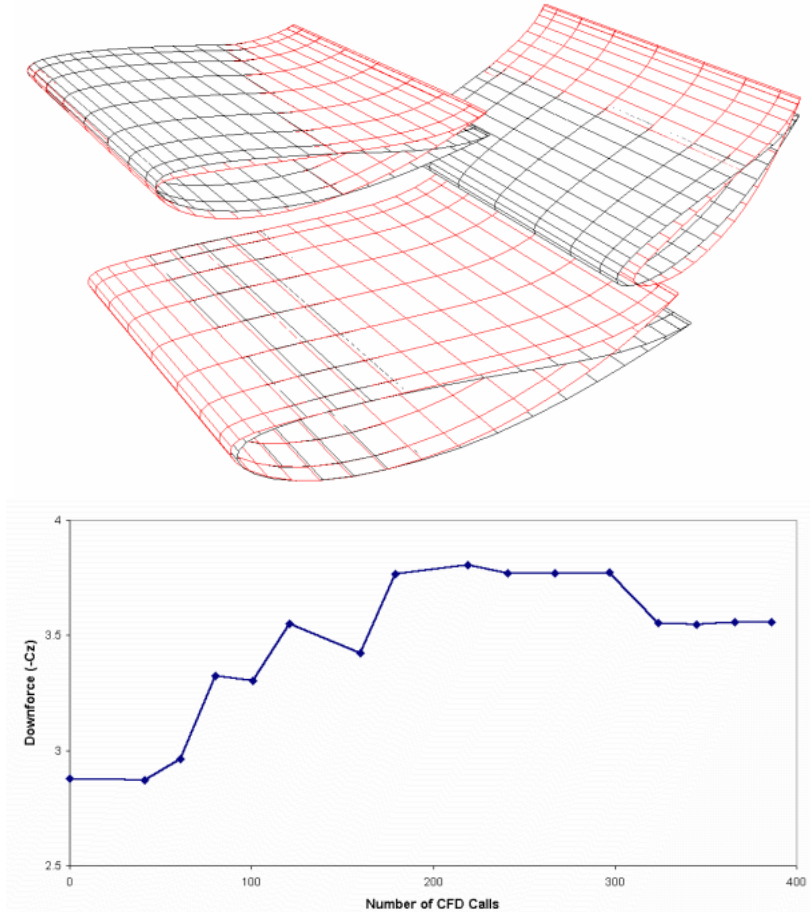


Figure 86: F1 car wing optimised in 3D for maximum downforce using NEWPAN + CODAS (black = initial geometry, red = optimised)

Benefits of optimisation codes are, potentially, far greater than for inverse methods, particularly for multi-point designs. Again, the benefits accrue principally in the saving of design time and the ability to consider a large spectrum of flow conditions.

Conceptually, implementation of an MVO optimisation can be achieved by coupling a CFD solver with a (non-linear) optimiser – for example QinetiQ use the SAUNA code in conjunction with the generic CODAS optimisation package. One problem is how to define the shape and its constraints, since the more degrees-of-freedom the greater the computational overhead (and the greater the chance of coming up with an unrealistic shape!). Early efforts defined a combination of fixed and moveable spline points on the surface, while other workers have used a membrane analogy to define how a surface can be deformed (ie by maintaining a constant imaginary tension). This is an area of intense current research, and the technical literature abounds with different approaches to both the geometry/constraint representation and the optimisation process.

Finally, it should be noted that multi-disciplinary optimisation is not new. For planar wings, many researchers (beginning with Prandtl ... again!) have obtained analytical or numerical solutions for minimum drag with (structural) constraints on wing span, root bending moment, weight and thickness. An early example of a more sophisticated coupling of wing structure and aerodynamics was G.T.R. Hill's 'aero-isoclinic' wing – a swept wing planform with the flexibility tailored to prevent any change in twist (washout) as lift is increased. This was achieved on the Shorts SB4 tailless research aircraft (1953) by locating the flexural axis well aft in the wing and suitably proportioning the torsion-resisting portions. The SB4 also had rotating wing-tip controls – a favourite concept of Shorts' then chief designer.



Figure 87: Shorts SB4 Sherpa with aero-isoclinic wing